Reconstruction of ancient environments using stable isotope analysis of archaeological charcoal from Sibudu Cave, KwaZulu-Natal

Volume II

Grant Hall

A thesis submitted to the Faculty of Science, University of the Witwatersrand, Johannesburg, in fulfilment of the requirements for the degree of Doctor of Philosophy

Johannesburg, 2010

DECLARATION

I declare that this thesis is my own unaided work. By thesis, it is understood to mean my contribution, as described in Chapter One, for submission for the degree of Doctor of Philosophy at the University of the Witwatersrand. The thesis has not been submitted before for any degree or examination at any other University.

____

Grant Hall

________________ day of ____________________ 2010.

ABSTRACT

The stable carbon isotopic analysis of archaeological charcoal has the potential to provide an archive of environmental change during the Middle Stone Age occupation of Sibudu Cave, KwaZulu-Natal, South Africa. A wide array of evidence from the site suggests that profound environmental and cultural changes took place in the region through the past 75ka. The aim of this project is to develop a methodology to obtain such isotopic evidence and to test the validity of this evidence through comparison with additional proxy environmental data from the site.

Analogue data from modern tree species, *Mimusops caffra*, *Podocarpus latifolius* and *P. falcatus* provide an absolute annual chronological isotopic record of environmental response to prevailing climatic conditions. High precision radiocarbon dating of growth rings demonstrates that these species produce annual growth rings. Wholewood samples provide an accurate record of climatic conditions. Direct comparison of $\delta^{13}C$ value of *M. caffra* from northern KwaZulu-Natal with the historic climatic record, shows a strong inter-annual response to rainfall variability. Signal processing approaches allow the rainfall response to be separated from long-term anthropogenic influences.

The $\delta^{13}C$ values of *P. latifolius* trunk cores and corresponding branch samples, from KwaZulu-Natal, preserve the same environmental record, correlating with humidity and temperature data from the region. It is thus possible to obtain a record of past climatic conditions from the growth rings of branches. A *P. falcatus* disc from the Baviaans Kloof (Eastern Cape) provides a $\delta^{13}C$ time series for a moisture-restricted environment, responding to annual rainfall variation and provides a contrasting analogue to the KwaZulu-Natal trees.

Branch samples from *P. latifolius*, representative of the size class of wood fuel likely utilised by MSA inhabitants of Sibudu Cave, were combusted under oxidising and reducing conditions. Their respective $\delta^{13}C$ values are more negative with respect to the source material, but reflect the same response to prevailing climatic conditions. An experiment determined the range of isotopic variability in products released during various stages of combustion. The results indicate that combustion

temperature has a significant effect on the carbon isotope signature of the various products released during combustion, but the isotopic composition of the remaining wood tissue remains relatively constant, preserving seasonal and inter-annual isotopic trends. These modern analyses indicate that it is possible to obtain an isotopic record of past climatic conditions from archaeological charcoal.

The isotopic variability of archaeological *Podocarpus* and *Celtis* charcoal, from the MSA layers of Sibudu Cave reflect past environments. During the Howiesons Poort (65ka-62ka) the $\delta^{13}C$ charcoal data indicate a cool, humid forested environment predominated. $\delta^{13}C$ data from the post-Howiesons Poort (~58ka) and late MSA (~48ka) occupations show that conditions shifted to a dry, open grassland/woodland mosaic community with remnants of riverine forest. These interpretations were validated through comparison with additional faunal, botanical and sedimentological proxy data from Sibudu.

The environmental record from Sibudu Cave and palaeoenvironmental proxy data from seven South African MSA sites provide evidence for the local manifestation of large scale climate events between 70ka and 50ka. During Marine Isotope Stage (MIS) 4 it appears that southern Africa experienced conditions similar to those during the Last Glacial Maximum. At Sibudu the environment changed from a predominantly forested community to more open grass/wood land mosaic. Such environmental change is thought to be due to a weakening of the Agulhas Current and eastward shift of the Agulhas Retroflection resulting in lower sea surface temperatures and a corresponding decrease in humidity and rainfall. Adverse environmental conditions ultimately led to Sibudu being abandoned from about 37ka until approximately 1000 BP.

ACKNOWLEDGEMENTS

Primarily I would like to thank three influential people without whom this thesis would not have been possible, Professor Lyn Wadley for all her support, advice and enthusiasm for the project and for allowing the chance to spend time working on my thesis at Moletadikgwa in the Waterberg, as well as a number of stimulating excavation seasons at Sibudu Cave; Professor Mary Scholes for all her pertinent advice, guidance and for getting me to China (and back again) and Dr. Stephan Woodborne for the enormous amount of time he spent working with and training me in the operation of the mass spectrometer, as well as improving my writing skills. All proof reading and editorial work was carried out by all three of my supervisors and is gratefully acknowledged.

During the initial stages of the project advice and ideas were provided by my research proposal committee, Dr. Lucy Allott, Dr. Amanda Esterhuysen and Christine Steininger. Robyn Pickering also gave me some great suggestions which helped to led me into the world of stable isotopes and climate change.

A number of individuals provided me with assistance in obtaining all the suitable sample material needed for the project. Firstly I would like to thank Dr. Lucy Allott for permission to use a number of her charcoal samples for stable carbon isotope analysis and for her help in understanding the basics of charcoal analysis and identification. Christine Sievers was a phenomenal source of information with regards finding ideal sampling locations, getting in contact with the right people and providing a roof over my head when I was down in KwaZulu-Natal on a number of collecting trips. Phoebe and Alastair Carnegie were extremely accommodating in getting me access to a number of sites (Hawaan Forest and Admiralty Beach) which provided me with a wealth of material. A big thank-you to Lance Rassmussen from the Ethikweni Municipality for granting me permission sample a number of *Podocarpus* specimens in Seaton Park and also giving me a hand with a chainsaw (no one was injured…promise). Thanks goes to Dr. Ed February and Klaudia Schactschneider from the Botany Department at the University of Cape Town for allowing me the use of an increment borer for core samples. Geoff Nicholls kindly permitted the use of the photograph in figure 2.1. Glenda Swart of the South African

Weather Service was instrumental in providing me with all the necessary climatic data that I requested.

I would like to thank Zenobia Jacobs for permission to use the currently available Optically Stimulated Luminescence dates for Sibudu Cave. Marc Pienaar assisted me with a number of complex statistical analyses and associated figures for one of the papers presented in the thesis. A final thank you goes to all the members of the ACACIA team (Lucy Allott, Andrew Herries, Marlize Lombard, Wayne Glenny, Ina Plug, Jamie Clark, Chet Cain, Paolo Villa, Sally Reynolds and others) who have worked at Sibudu Cave producing a wealth of data which has been of invaluable use to my research.

Support and encouragement for my endeavours from outside the academic forum was provided in ample amounts by my Mother and two very good friends, Arnaud and Natasha who helped to keep me focused (most of the time). Thanks guys!

Financial assistance is gratefully acknowledged from the National Research Foundation (NRF) for providing a grant holder's bursary awarded by Professor Wadley, the Palaeoanthropological Scientific Trust (PAST) provided grants from 2005 to 2007 (a big thank you to Andrea Leenen for her help) and the University of the Witwatersrand for a post-graduate merit award in 2005. The Council for Scientific and Industrial Research (CSIR) in Pretoria provided funding in 2009 allowing me to complete my thesis. Funding for the conference trip to Beijing, China in November 2006 was provided by the School of Animal, Plant and Environmental Sciences (APES) through Professor Scholes.

VOLUME II CONTENTS

INTRODUCTION

This volume contains all figures and tables that relate to Chapters 2 to 7, as well as supplementary information contained in Appendices A, B and C. The rationale for a second volume is to allow the reader easier access to the relevant figures and tables for each chapter.

FIGURES

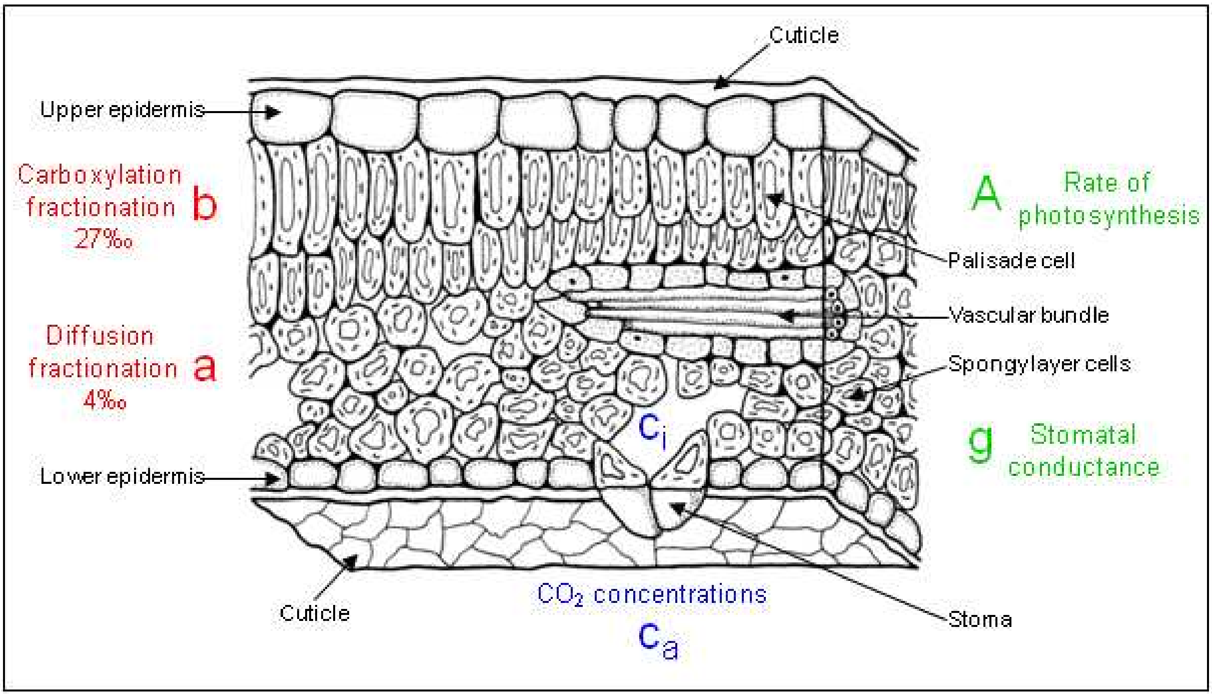

Figure 2.1. Cross-section of a leaf showing the main controls of carbon isotope fractionation (Adapted from McCarroll and Loader, 2004).

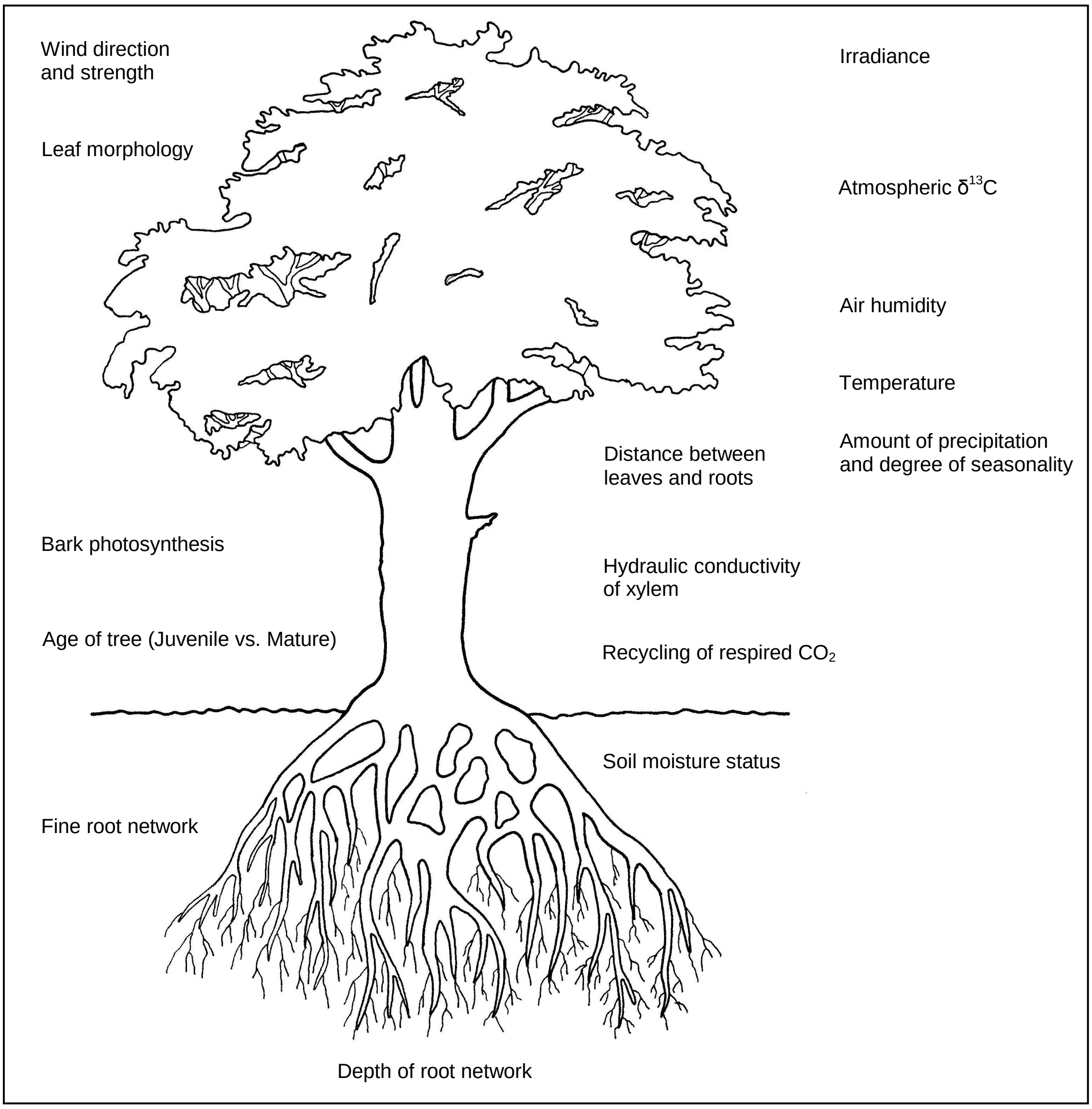

Figure 2.2. Environmental factors that have an influence on the stable carbon isotope composition of trees (Adapted from McCarroll and Loader, 2004).

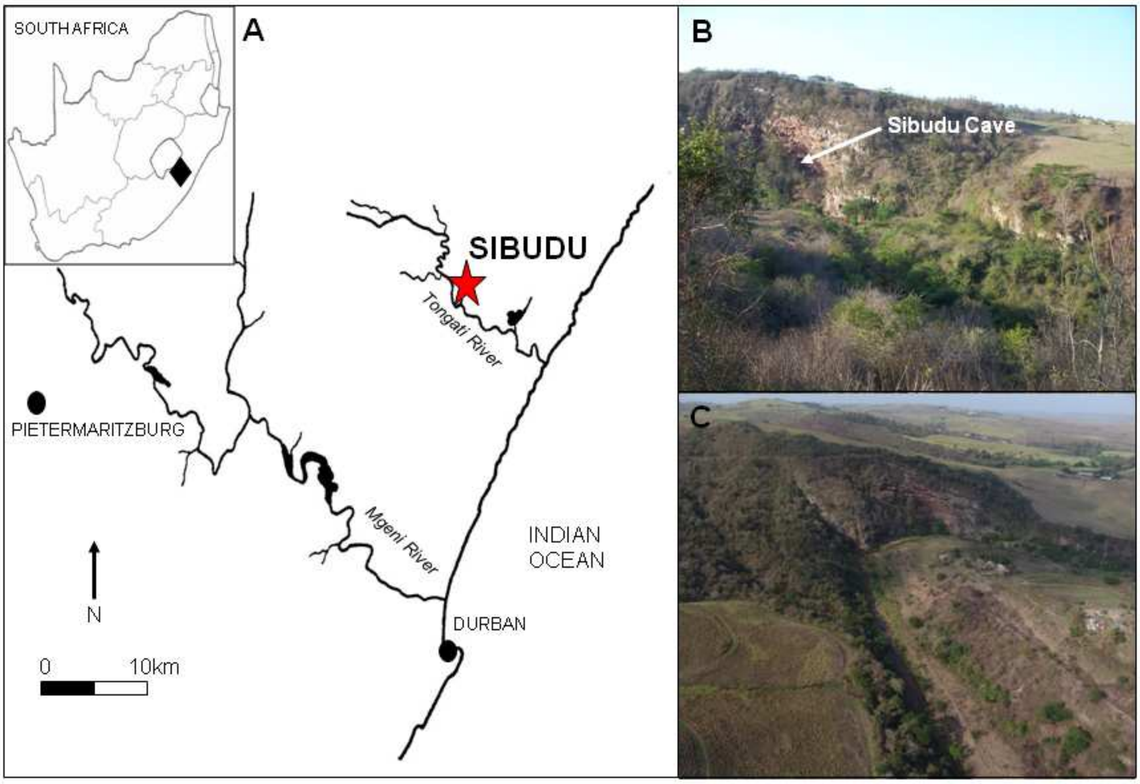

Figure 3.1. A: Location of Sibudu Cave. B: The upper right photograph shows the location of the site from a south-western viewpoint. C: The lower right aerial photograph shows the location of the site with respect to the Tongati River (Photograph courtesy of G. Nichols).

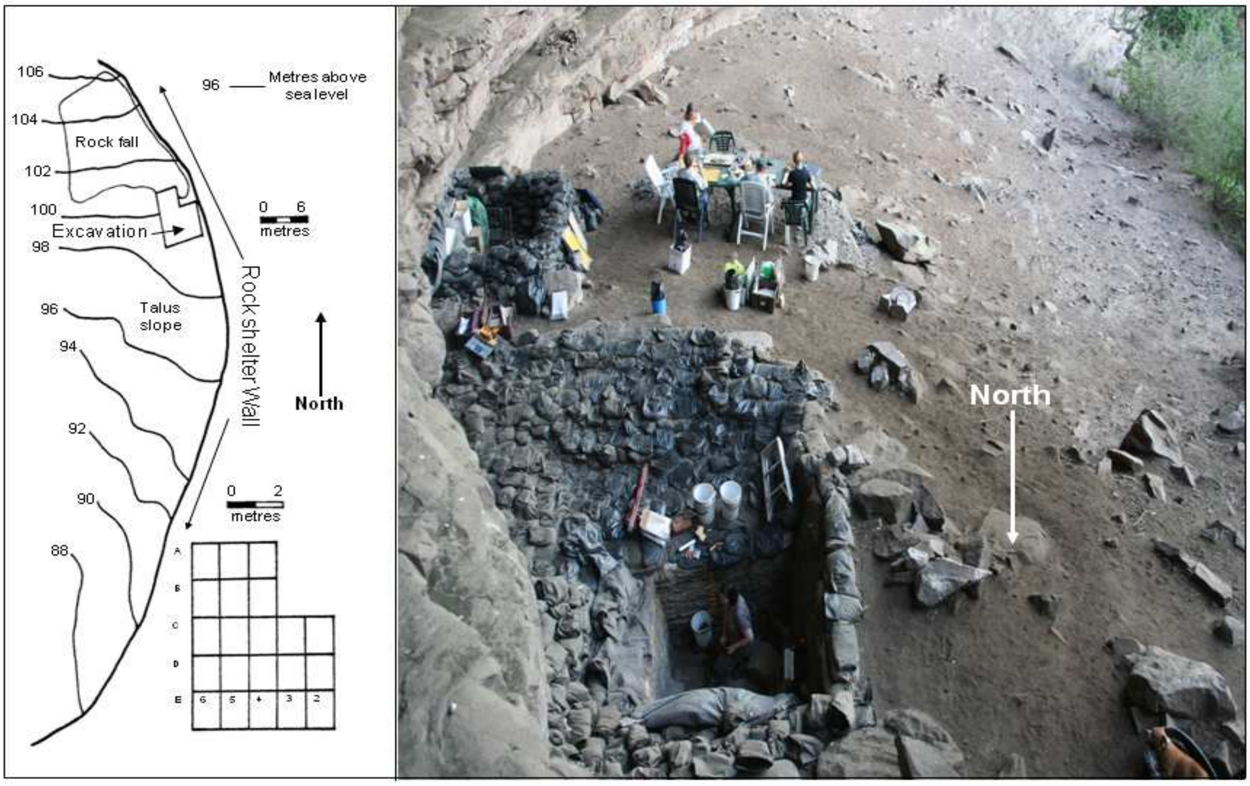

Figure 3.2. Site plan of Sibudu Cave. The right-hand photograph shows the extent of the excavation in March 2007.

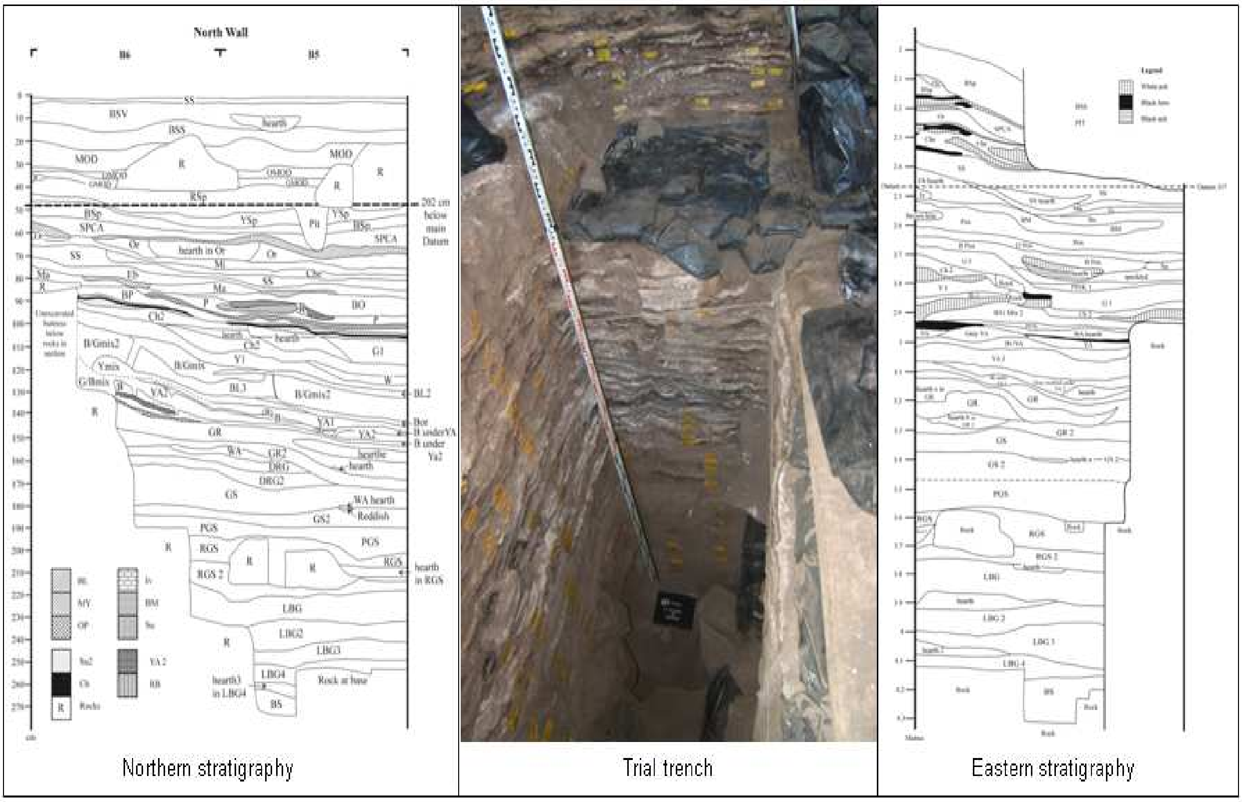

Figure 3.3. Stratigraphic drawings of the north (left) and east (right) faces of the trial trench with a photograph of the trial trench in the centre. The depth of the excavation is four metres.

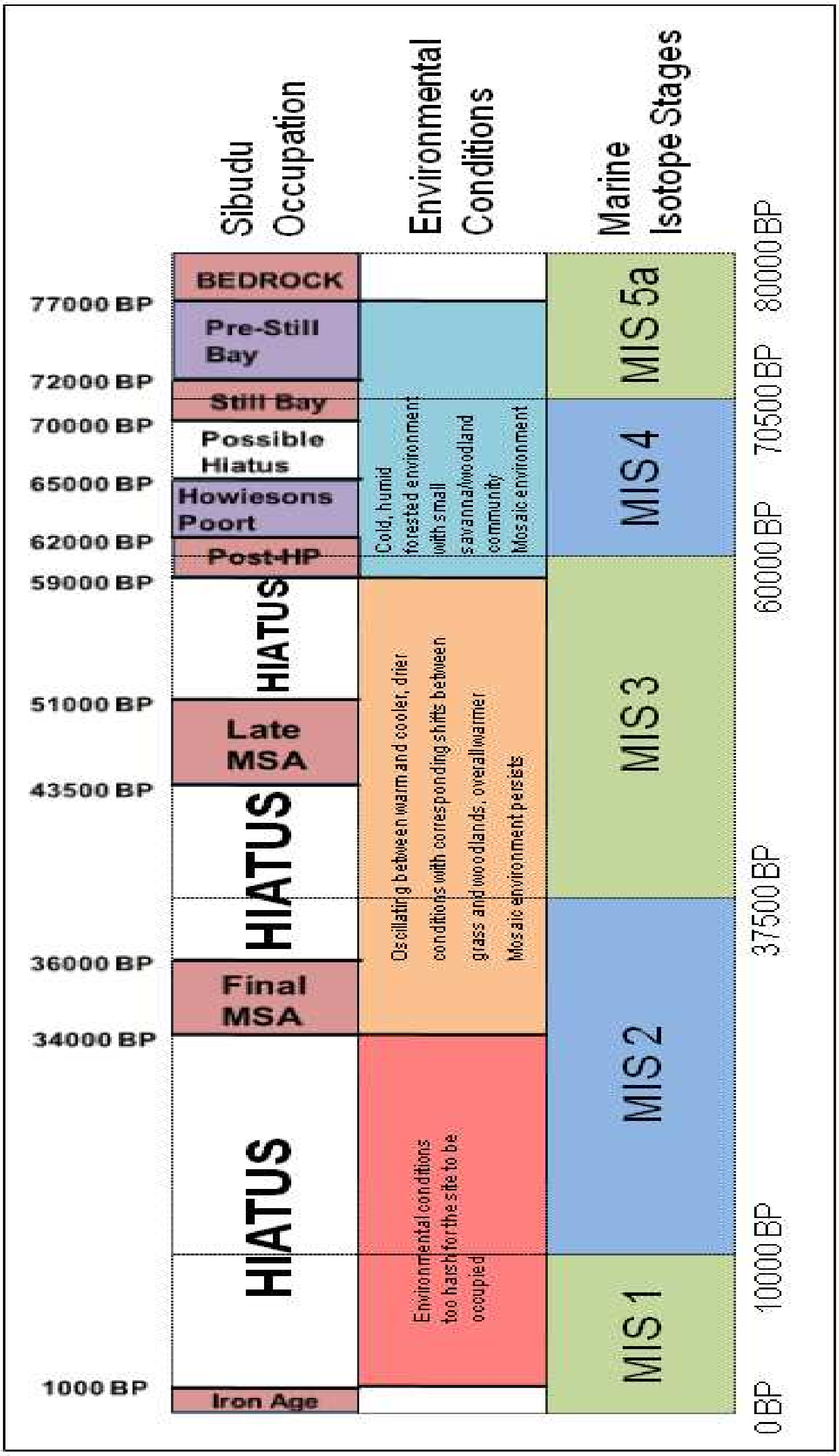

Figure 3.4. Summary of the Sibudu occupation periods, formal and informal lithic assemblages and palaeoenvironmental conditions in relation to Marine Isotope Stages 5a to 1. OSL dates are from Jacobs, 2004; Jacobs and Roberts, 2008; Jacobs *et al.*, 2008a, 2008b)

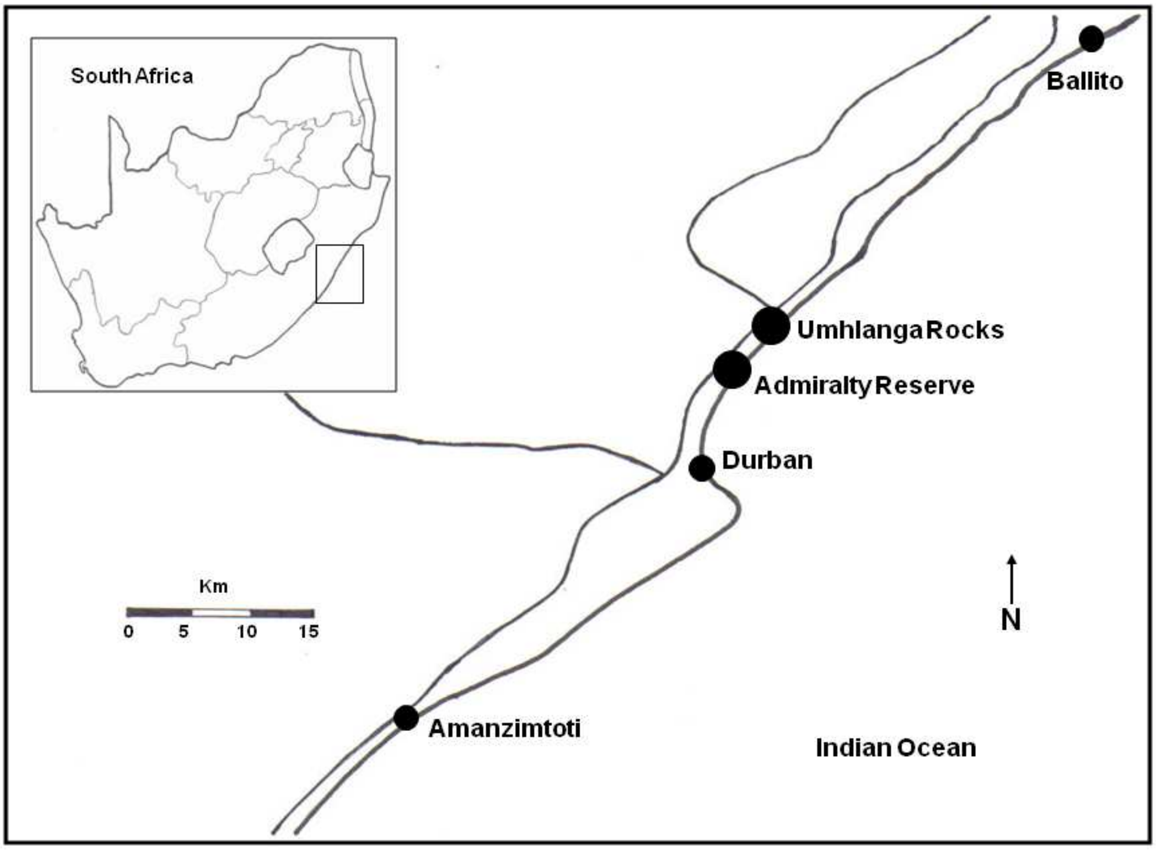

Figure 4.1. Map showing the location of the Umhlanga Rocks and Admiralty Reserve sample sites located to the north of Durban, KwaZulu-Natal, South Africa.

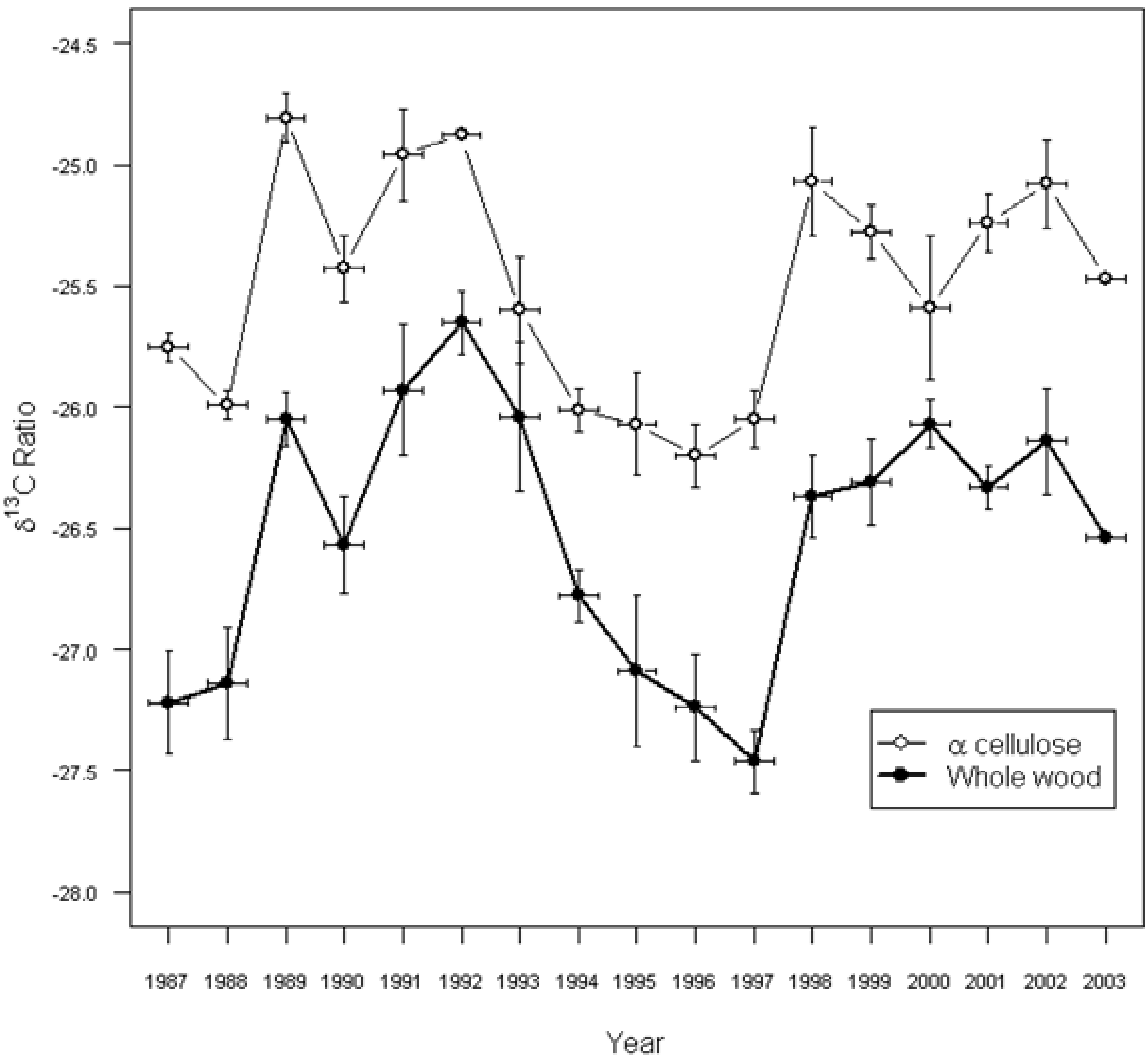

Figure 4.2. $\delta^{13}C$ annualised time series of α-cellulose and wholewood from Umhlanga 1. Variations in ring width influence the number of years sampled by each drilling. To compensate for this, the age values are depicted as a constant range (6 months) which is shown by an X-error bar. Y-error bars represent the standard deviation.

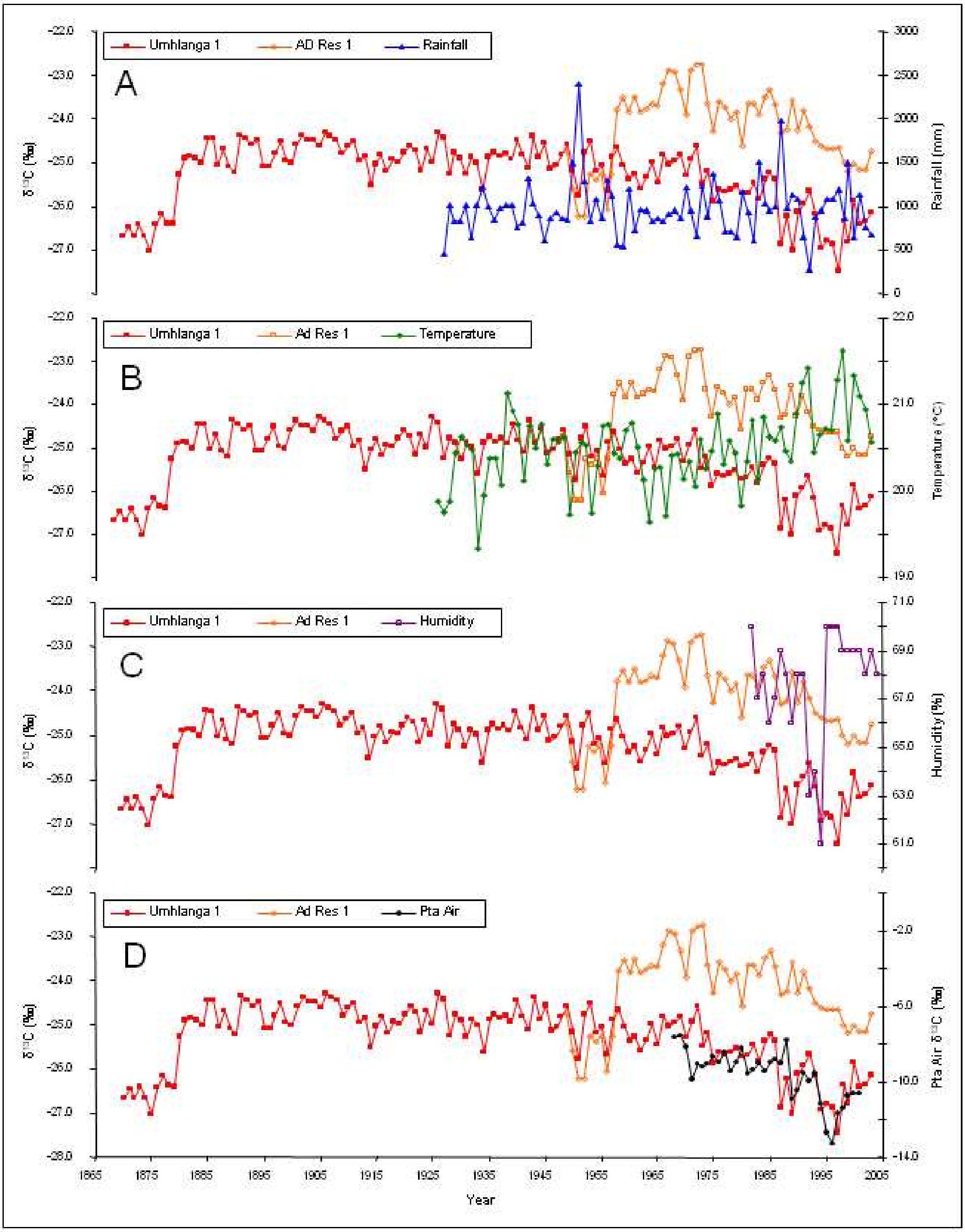

Figure 4.3. A: Annualised δ ^{13}C values from Umhlanga 1 and Admiralty Reserve 1 (Ad Res 1) are compared with local annualised rainfall. More negative δ ^{13}C values are associated with periods of high rainfall (e.g. 1987). **B:** Annualised δ ^{13}C values from Umhlanga 1 and Admiralty Reserve 1 are compared with local temperature. Isotopic values become more negative from the mid -1980's when overall temperature

shows an increase due to anthropogenic influences. **C:** Annualised $\delta\ ^{13}C$ values from Umhlanga 1 and Admiralty Reserve 1 (Ad Res 1) are compared with local humidity. During periods of low humidity, isotope values are less negative. **D:** Annualised $\delta\ ^{13}C$ values from Umhlanga 1 and Admiralty Reserve 1 are compared with $\delta\ ^{13}C$ values of Pretoria air. The isotopic variability of the tree corresponds to the overall pattern of isotopic variability seen in Pretoria air, reflecting the anthropogenic influence on atmospheric CO_2 concentrations.

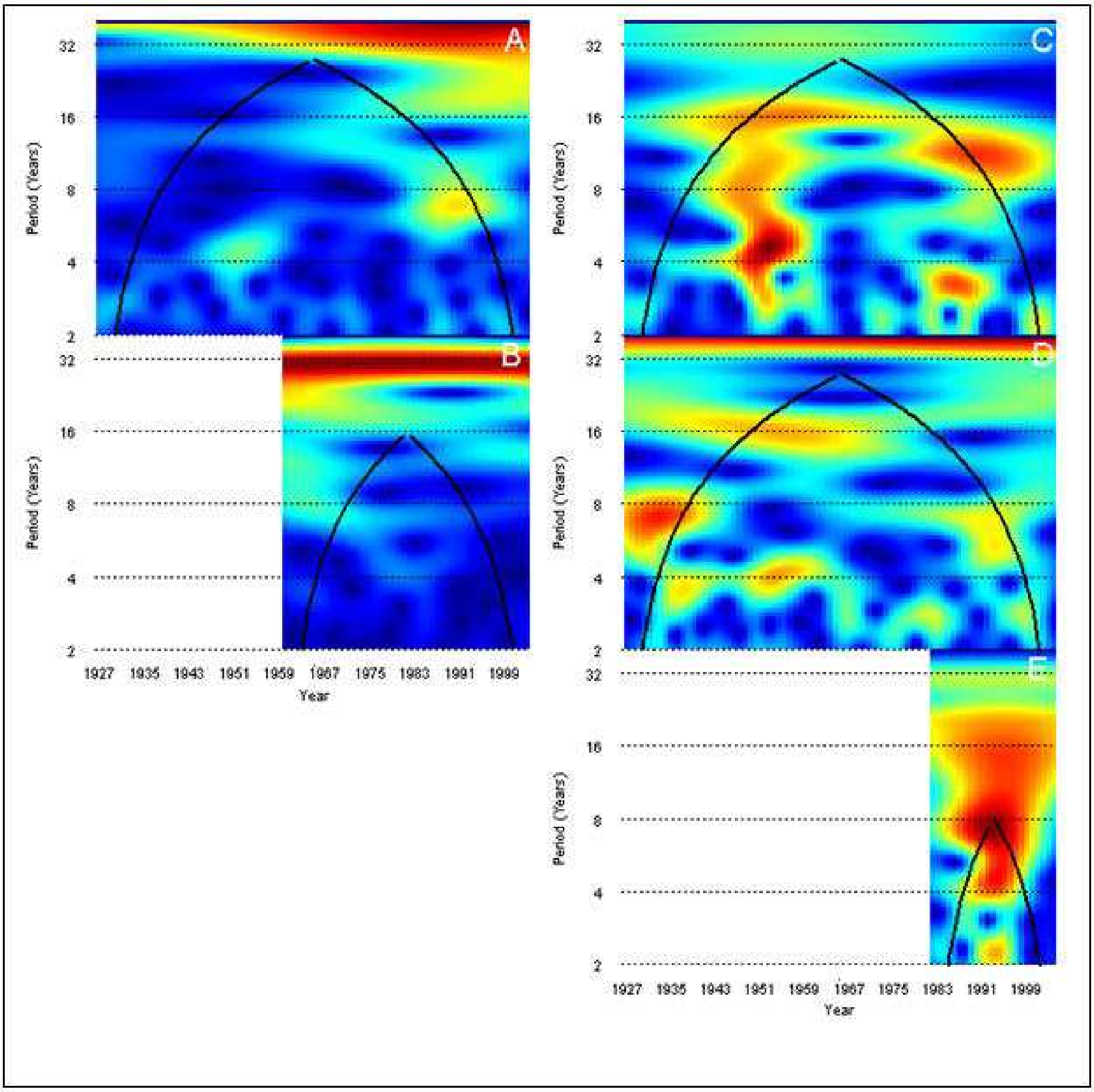

Figure 4.4. The CWT power spectra of $\delta^{13}C$ data sets for Umhlanga 1 (A) and Admiralty Reserve 1 (B) are presented on the left. The CWT power spectra for local rainfall (C), mean temperature (D) and humidity (E) are presented on the right. A cone of influence is applied to the power spectrum due to errors that occur at the beginning and end of the transform.

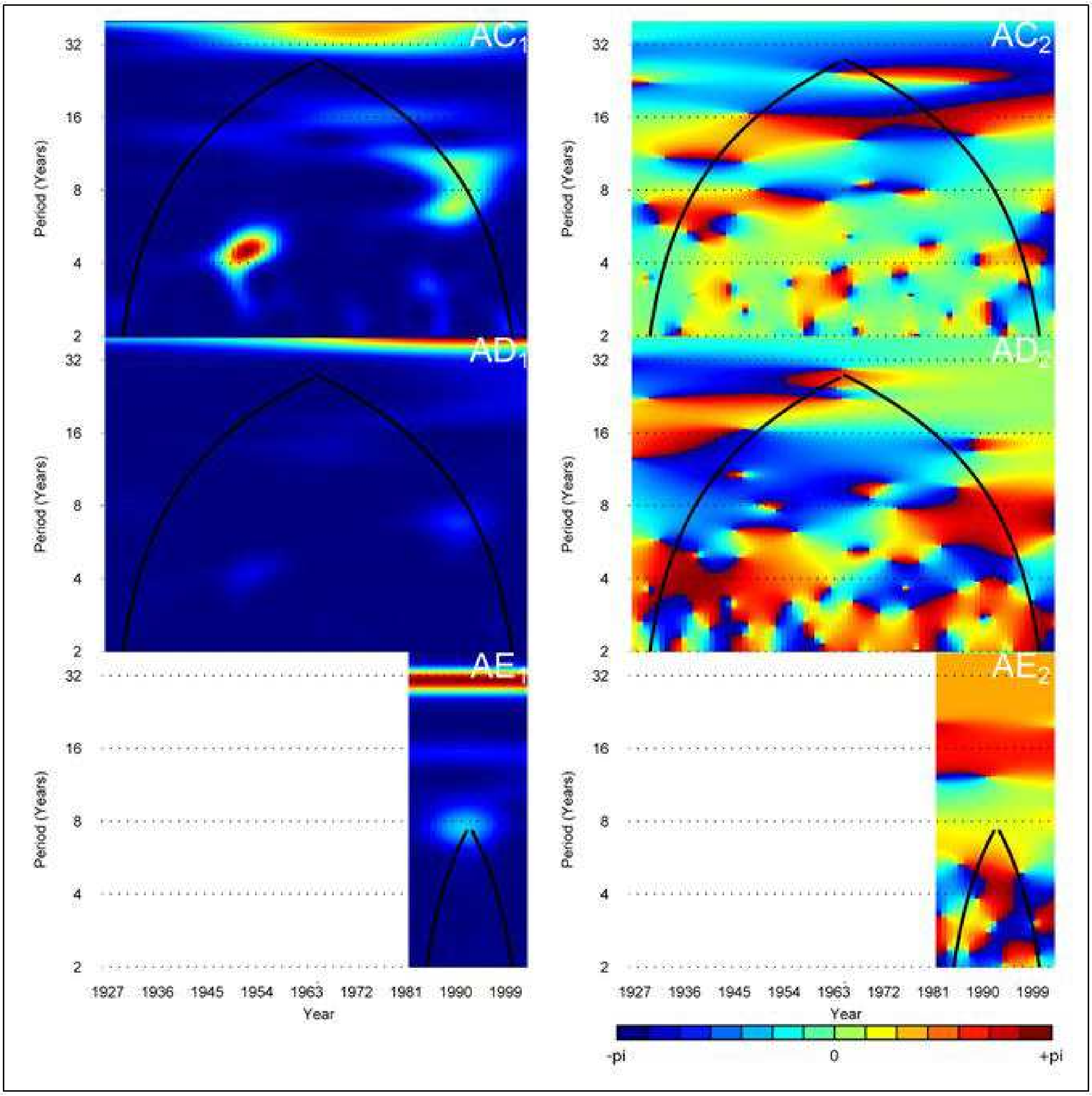

Figure 4.5. The cross CWT power spectra of $\delta^{13}C$ values for Umhlanga 1 and climatic data are presented on the left. AC_1 shows the cross with rainfall, AD_1 temperature and AE_1 humidity. Corresponding phase plots are presented on the right, rainfall AC_2, temperature AD_2 and humidity AE_2. A cone of influence is applied to the power spectrum and phase plot due to errors that occur at the beginning and end of the transform.

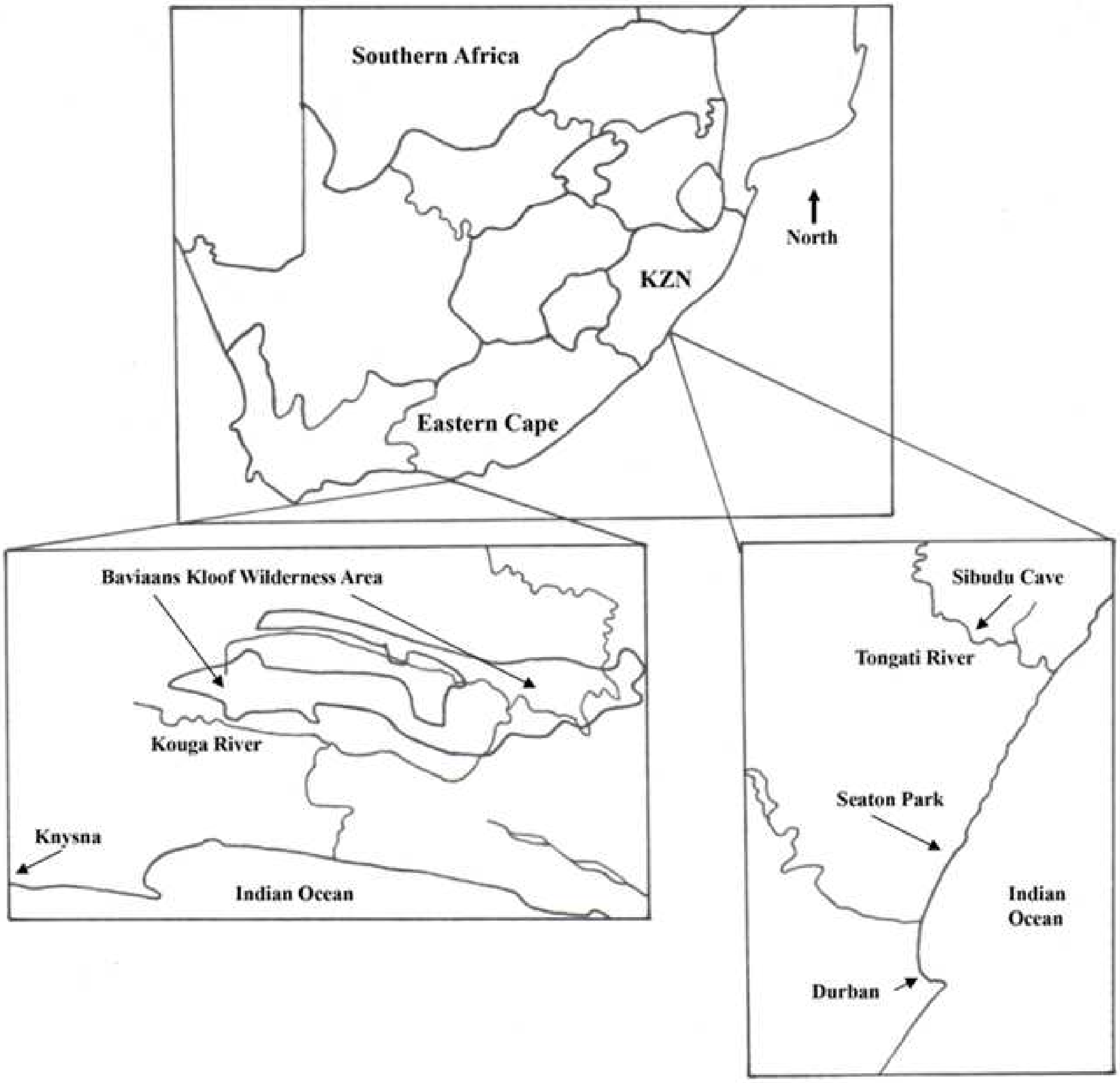

Figure 5.1. Map of southern Africa indicating the locations of Seaton Park and the Middle Stone Age site of Sibudu Cave, KwaZulu-Natal and the Baviaans Kloof Wilderness Area, Eastern Cape. Archaeological material used in this study originates from Sibudu Cave. The modern *Podocarpus* samples were collected from Seaton Park and the Baviaans Kloof.

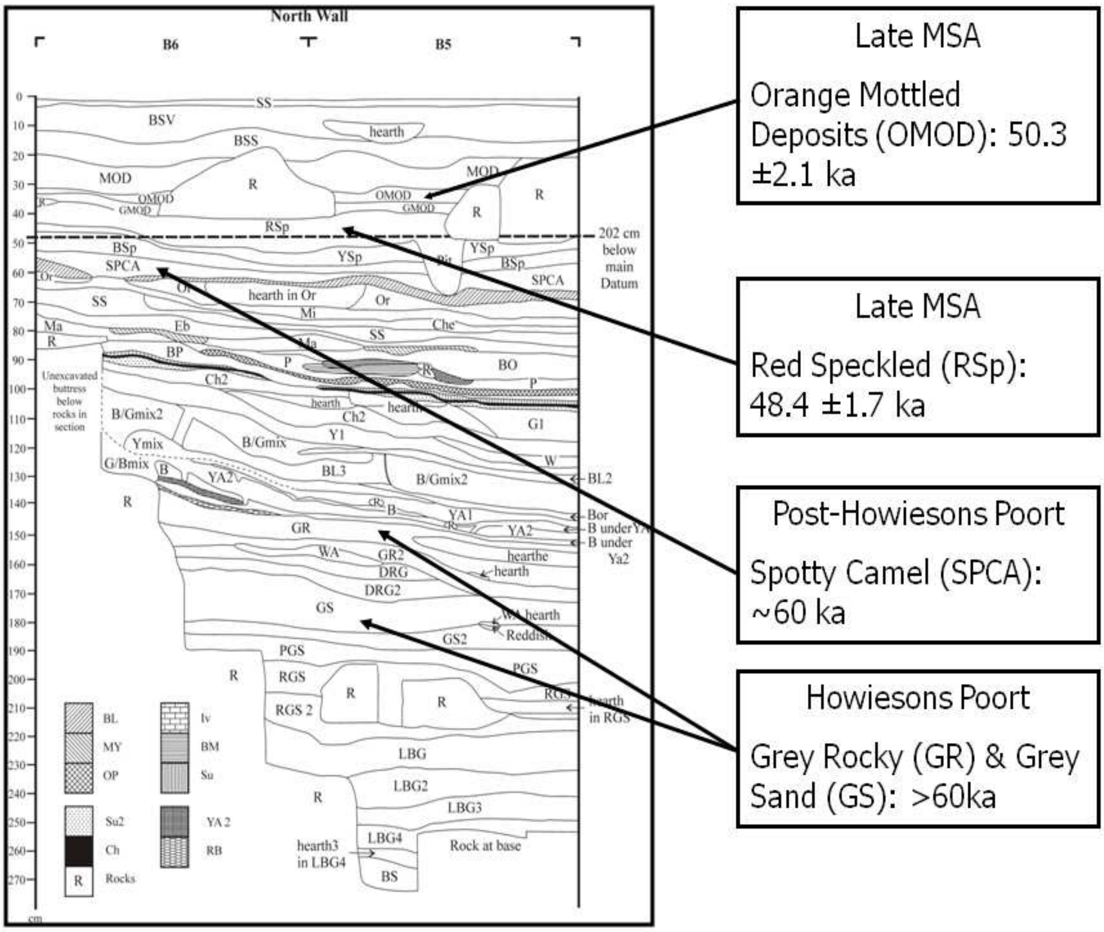

Figure 5.2. Stratigraphy of the trial trench in the northern grid from Sibudu Cave. The layers and ages (Jacobs *et al*. 2008a) from where charcoal samples for this study were collected are indicated.

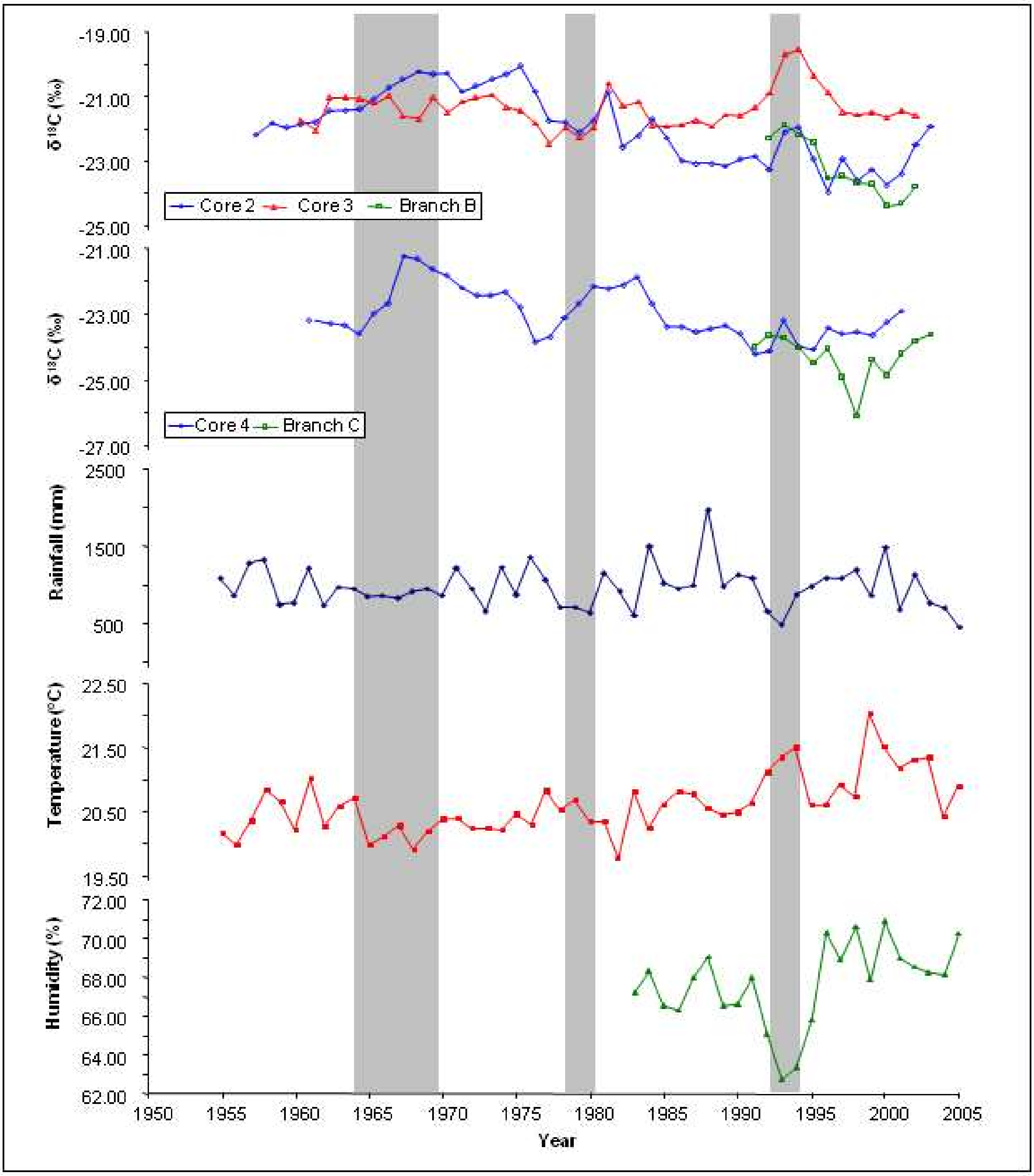

Figure 5.3. Modern δ^{13}C values from two *Podocarpus latifolius* specimens from Seaton Park plotted with the corresponding average rainfall, temperature and humidity.

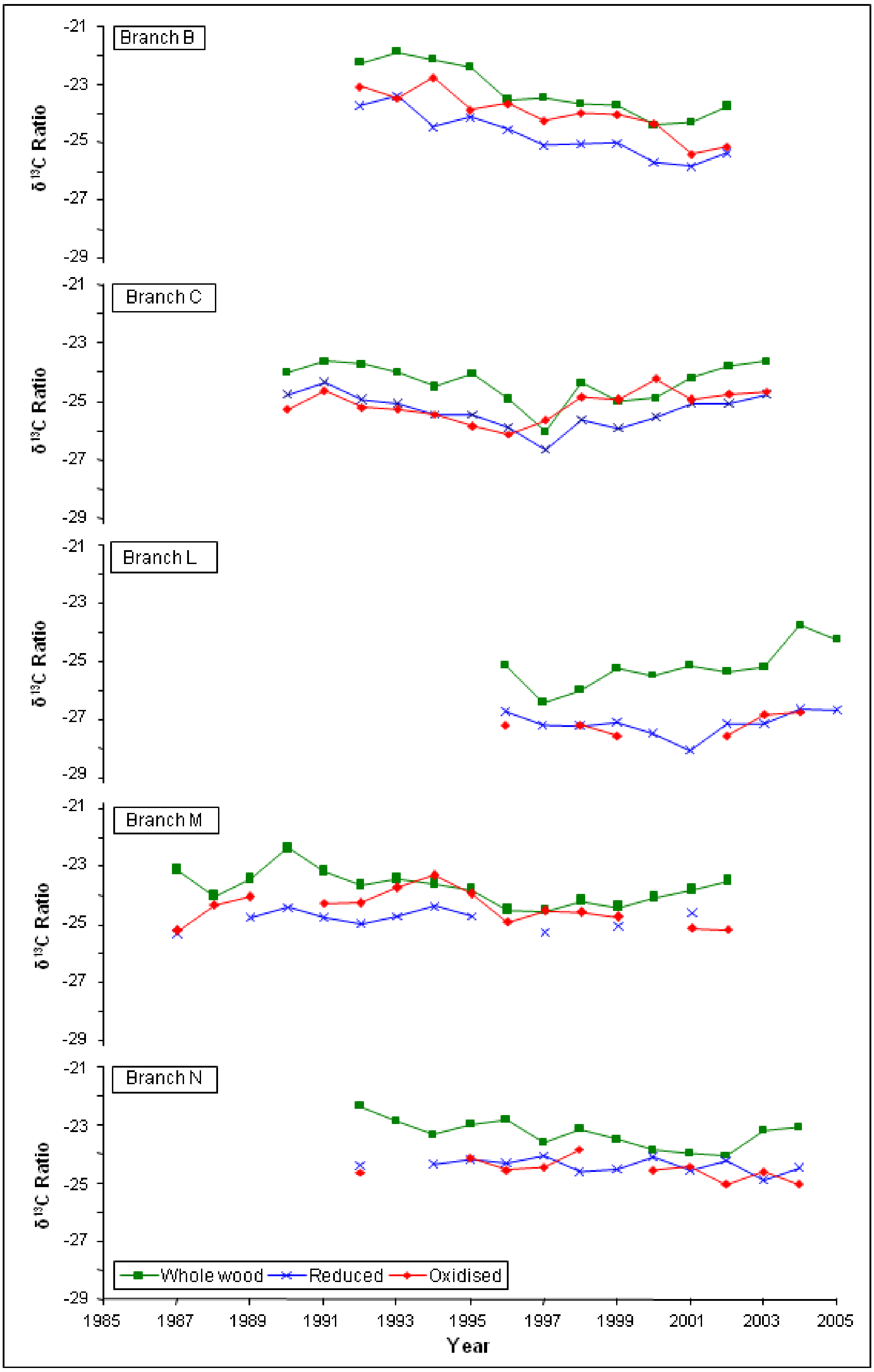

Figure 5.4. $\delta^{13}C$ values for five *P.latifolius* branch samples showing values for wholewood and charcoal produced under reducing and oxidizing conditions.

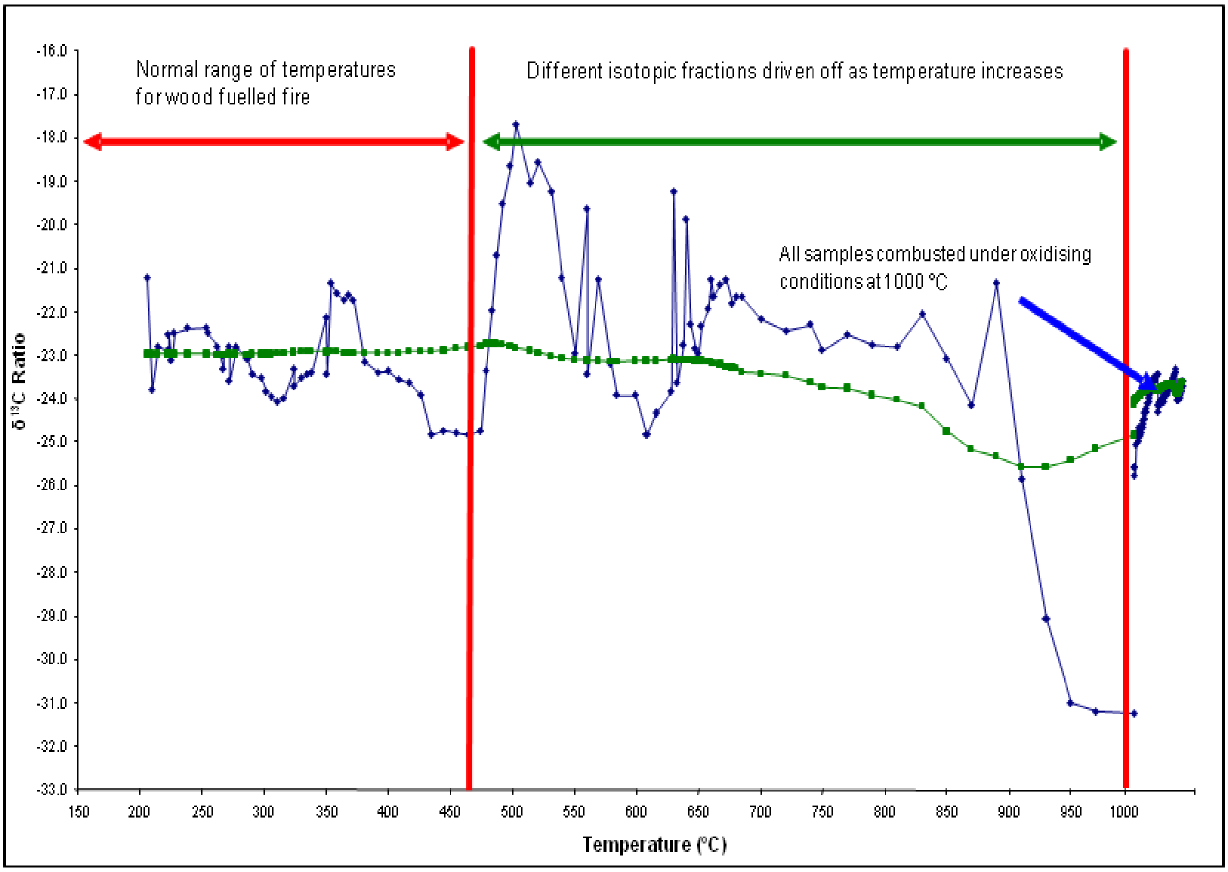

Figure 5.5. Elemental analyser experiment: In order to determine the isotopic value of the volatile compounds that are driven off during charcoal formation a small, fresh sample of *P.latifolius* was heated in an elemental analyser by pulsed heating (heating and cooling cycles with a progressive temperature increment of 5-10°C) under reducing conditions. Volatile fractions continued to be produced up to 1000°C and the isotopic values for the different fractions showed a large range of variability (colour diamonds). When no further CO_2 was produced (at 1000°C) the oxygen cycle in the elemental analyser was used and the remaining carbon was oxidised. Using the mass spectrometer peak integral, the isotopic contribution of the CO_2 pulses were integrated to approximate the isotopic value of the "remaining carbon fraction" at any point in the heating experiment (colour squares). Isotopically light volatile fractions driven off up to approximately 650°C make up a relatively small proportion of the overall carbon, but above this temperature the "remaining carbon fraction" shows progressively more negative values because of a substantial and very negative compound evolved between 900-1000°C. The isotopic values for the specific volatile compounds that are driven off during burning comprise both isotopically light and

heavy fractions, and the seemingly erratic fractionation observed during charcoal formation experiments is likely to relate to the presence of the different (unidentified) volatile compounds.

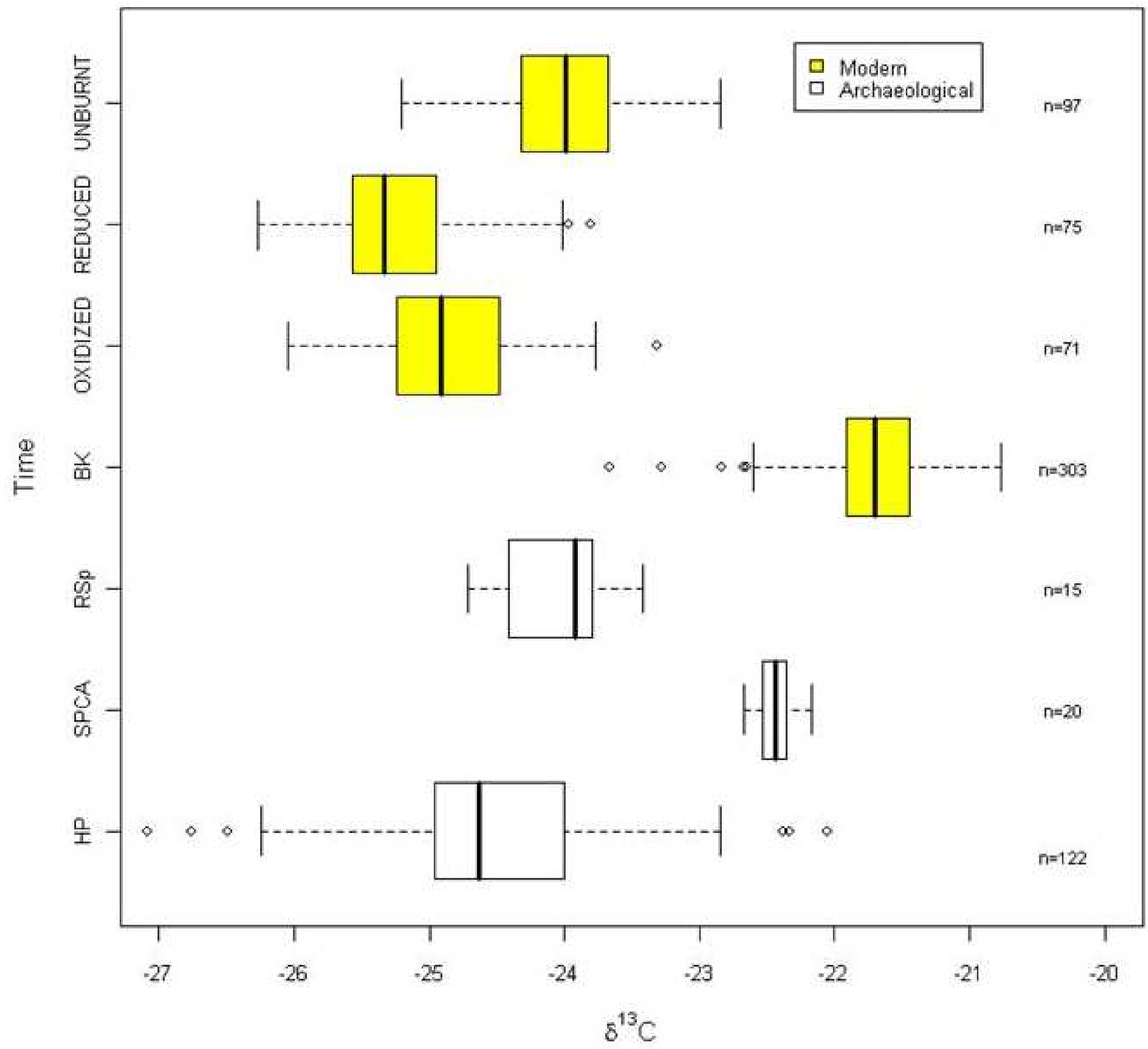

Figure 5.6. The relationship between $\delta^{13}C$ values of modern *Podocarpus latifolius* wholewood and charcoal from Seaton Park, KwaZulu-Natal and Baviaans Kloof (BK), Eastern Cape and archaeological *Podocarpus* charcoal from three MSA layers at Sibudu Cave.

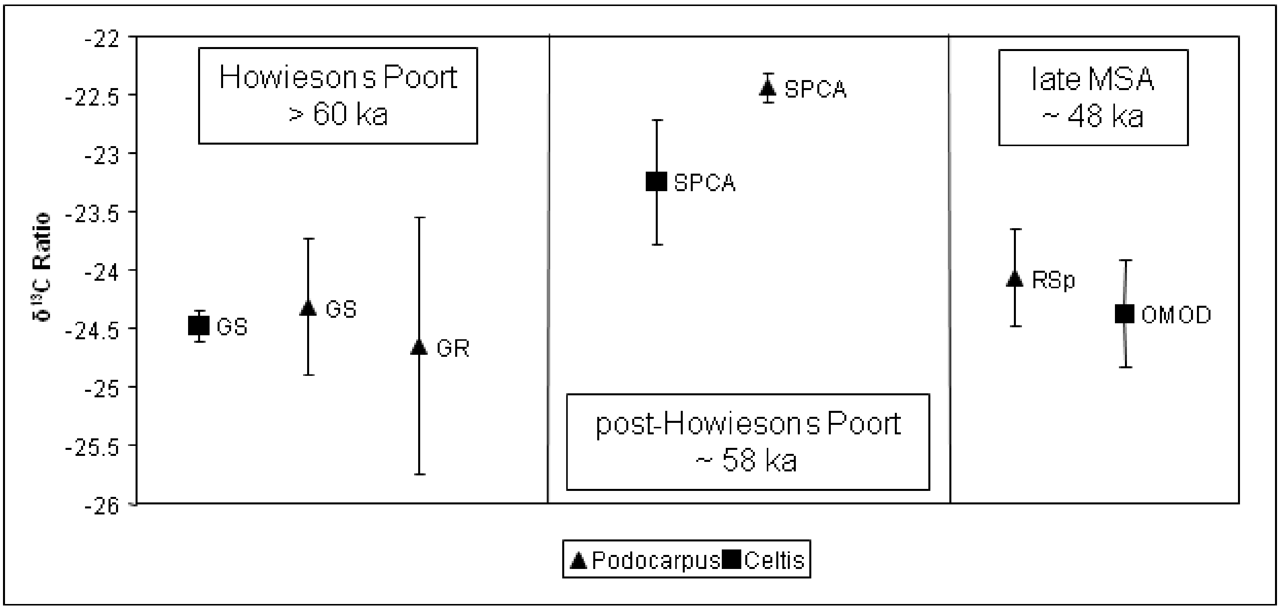

Figure 5.7. Mean carbon isotope values for *Podocarpus* and *Celtis* archaeological charcoal showing changes in carbon isotope values over time. Error bars represent the standard deviation for each sample set.

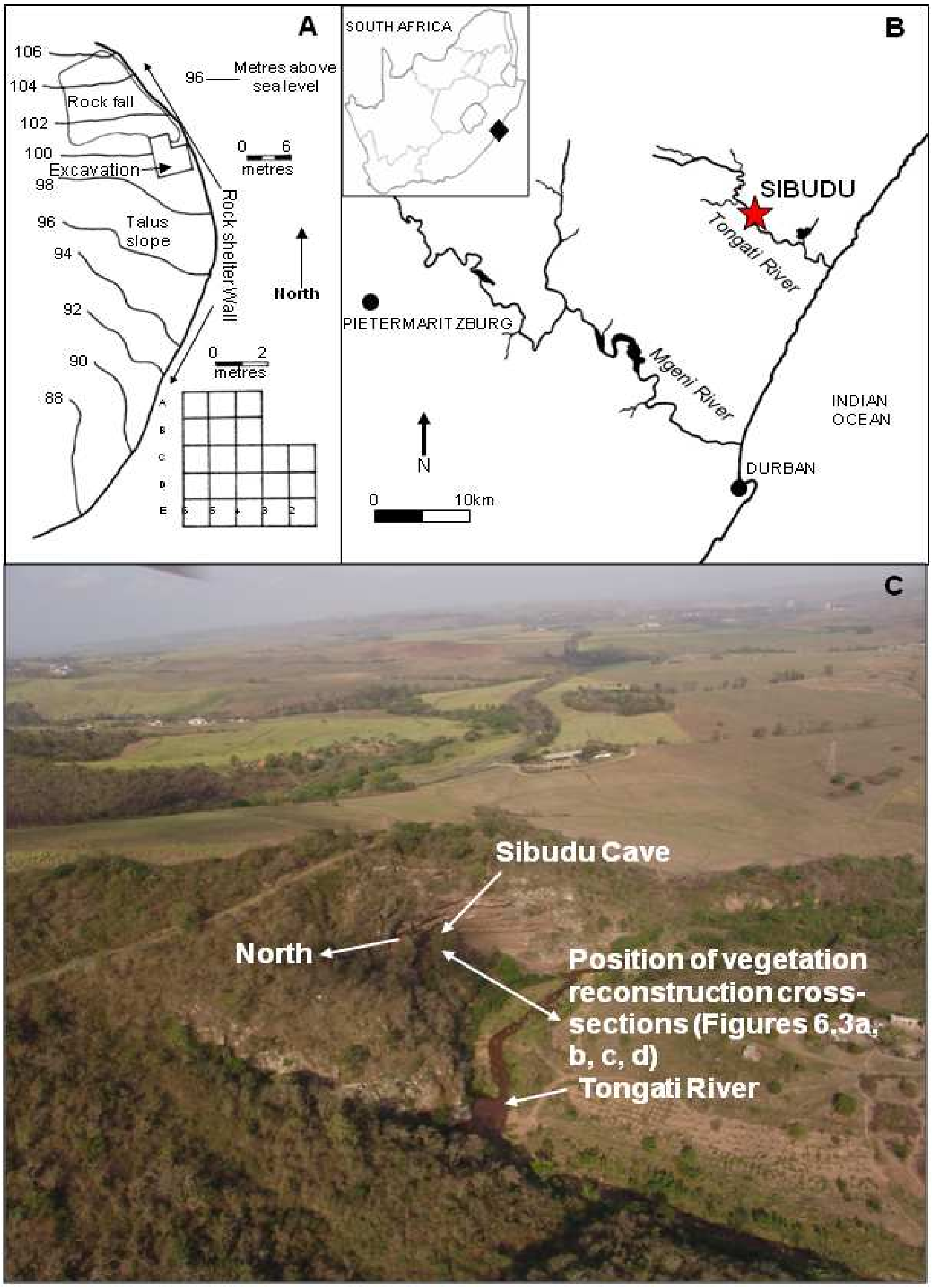

Figure 6.1. A: Plan of Sibudu Cave. B: Location of Sibudu Cave. C: Aerial photograph of the Sibudu modern environment showing the location of the shelter, the Tongati River and orientation of the past vegetation reconstruction transects presented in Figures 6.3a-d. The aerial photograph is courtesy of Geoff Nichols.

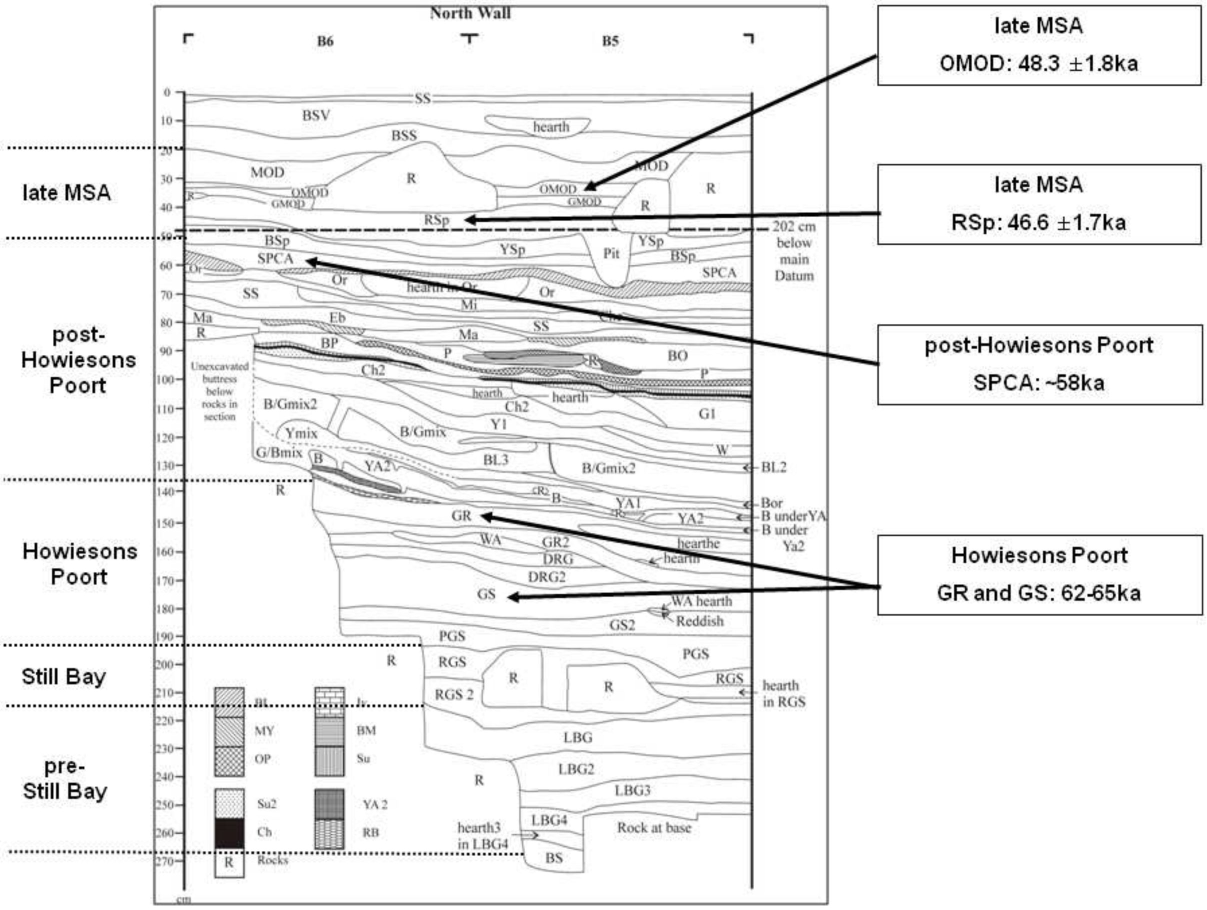

Figure 6.2. Stratigraphy of the trial trench in the northern grid from Sibudu Cave. The layers and available ages (Jacobs *et al.*, 2008a, b) from where charcoal samples for this study were collected are indicated.

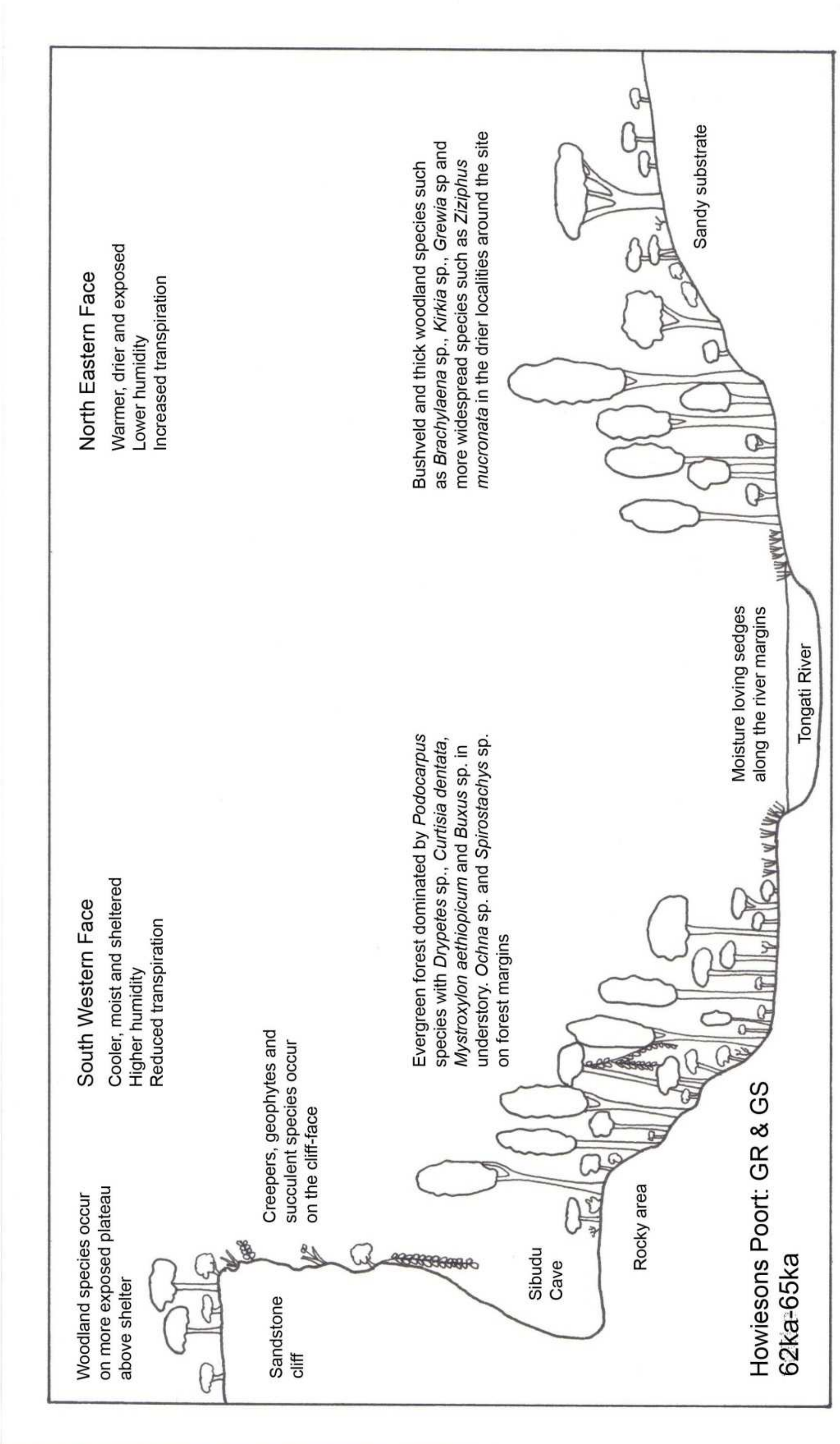

Figure 6.3a. Schematic reconstruction of Howiesons Poort period vegetation communities around Sibudu Cave based on botanical evidence (Allott, 2006; Renaut and Bamford, 2006; Sievers, 2006; Wadley, 2004).

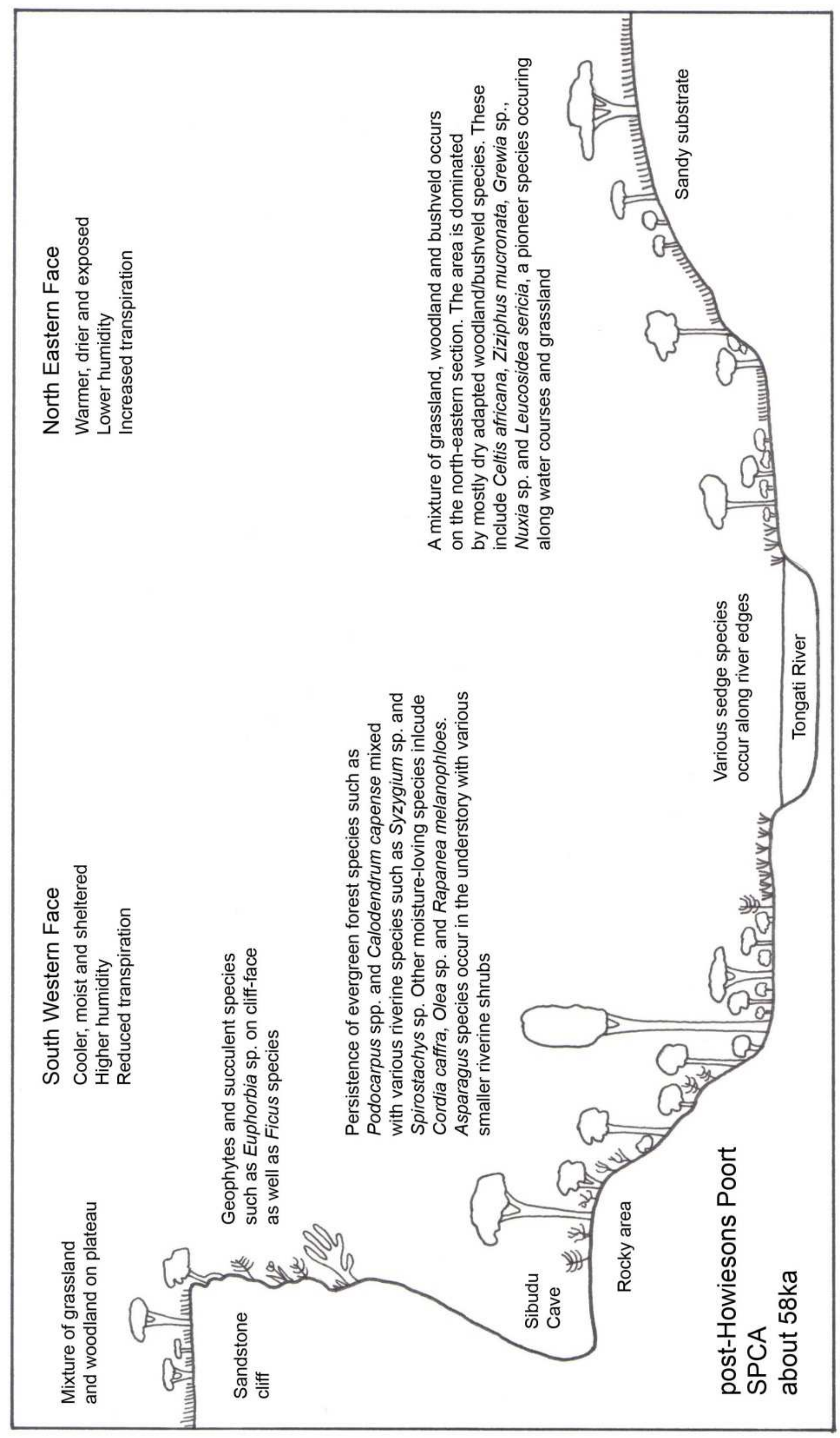

Figure 6.3b. Schematic reconstruction of post-Howiesons Poort vegetation communities around Sibudu Cave based on botanical evidence (Allott, 2006; Renaut and Bamford, 2006; Sievers, 2006; Wadley, 2004).

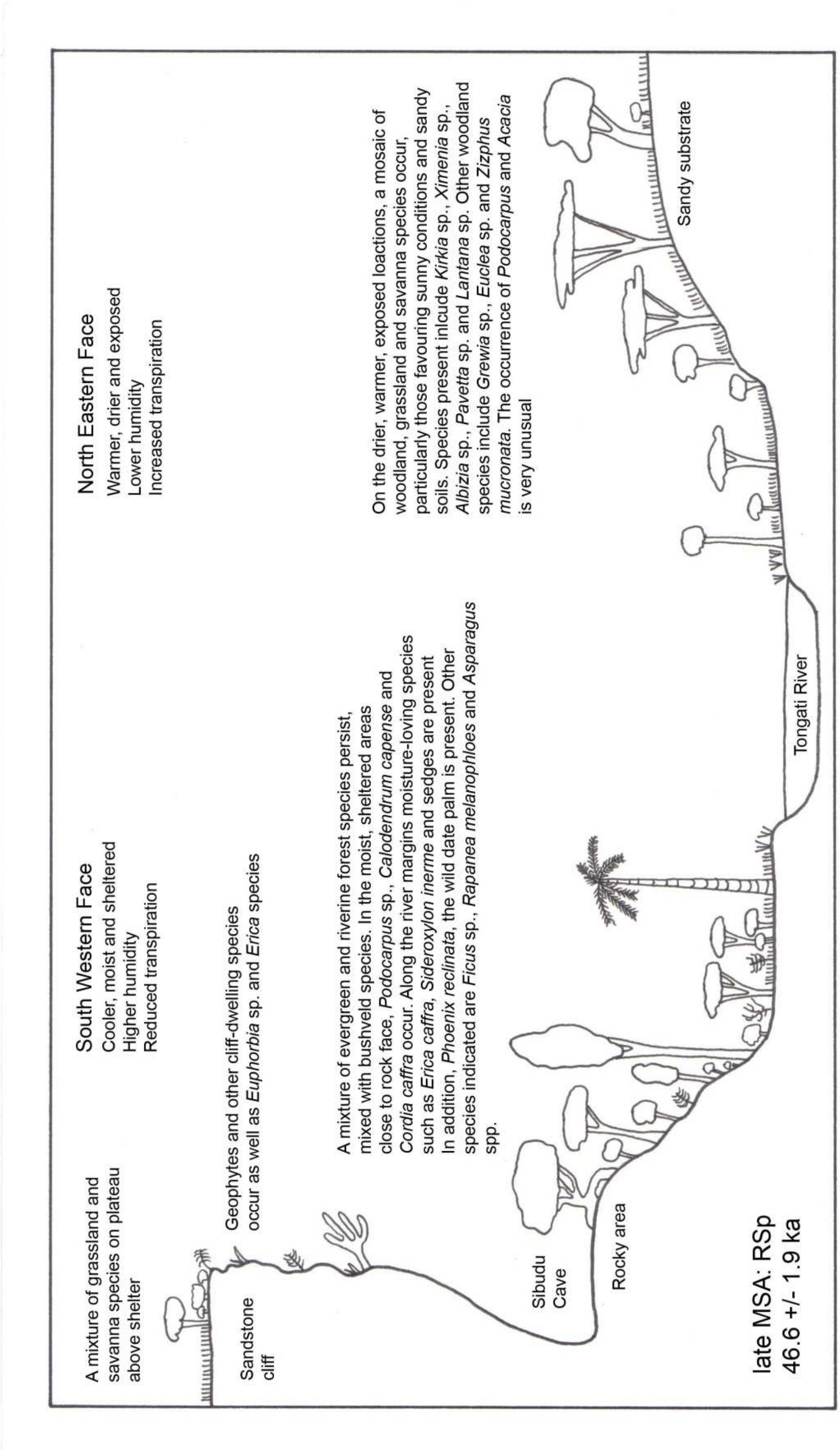

Figure 6.3c. Schematic reconstruction of late MSA vegetation communities around Sibudu Cave based on botanical evidence (Allott, 2006; Renaut and Bamford, 2006; Sievers, 2006; Wadley, 2004) from layer RSp.

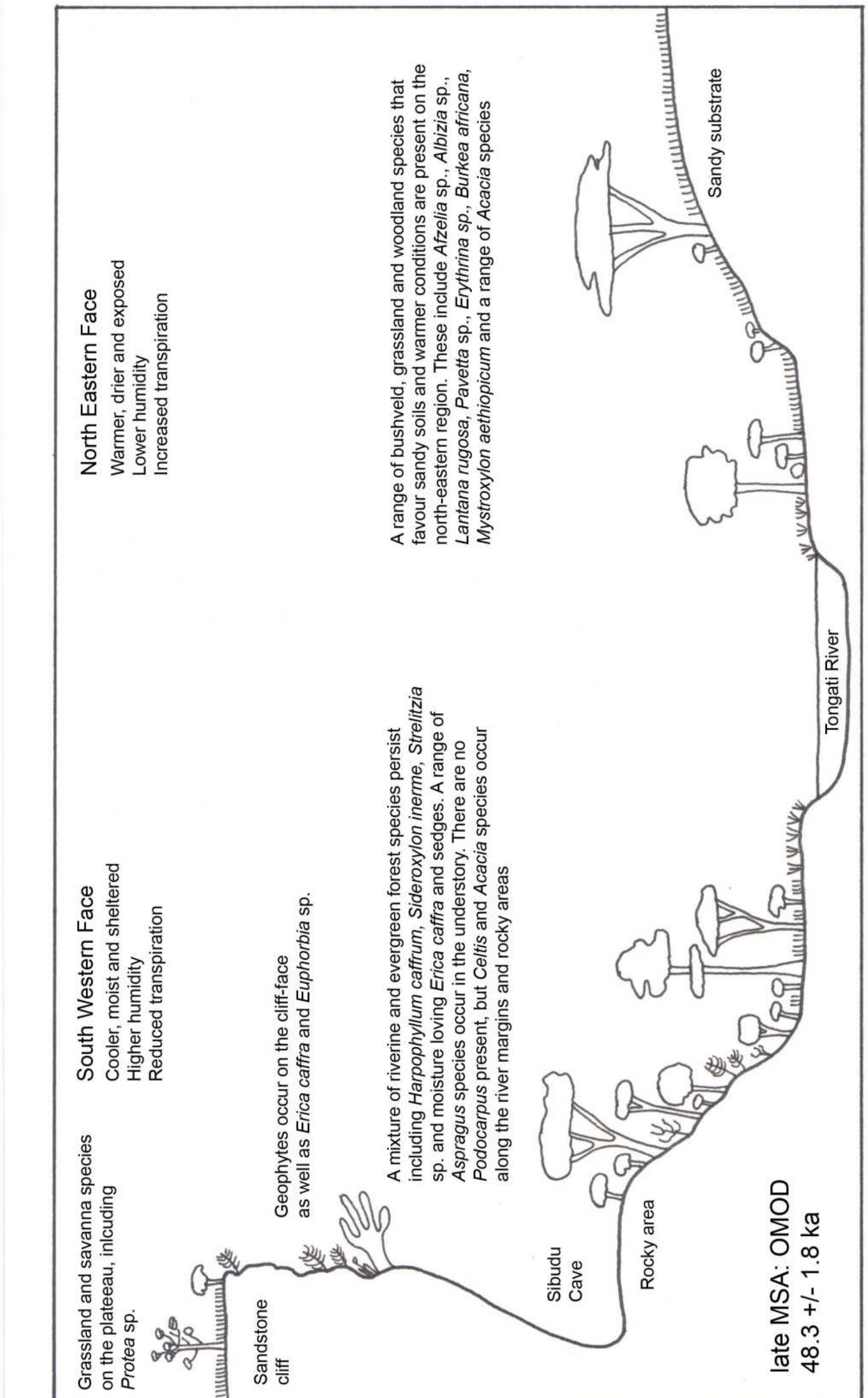

Figure 6.3d. Schematic reconstruction of late MSA vegetation communities around Sibudu Cave based on botanical evidence (Allott, 2006; Renaut and Bamford, 2006; Sievers, 2006; Wadley, 2004) from layer OMOD.

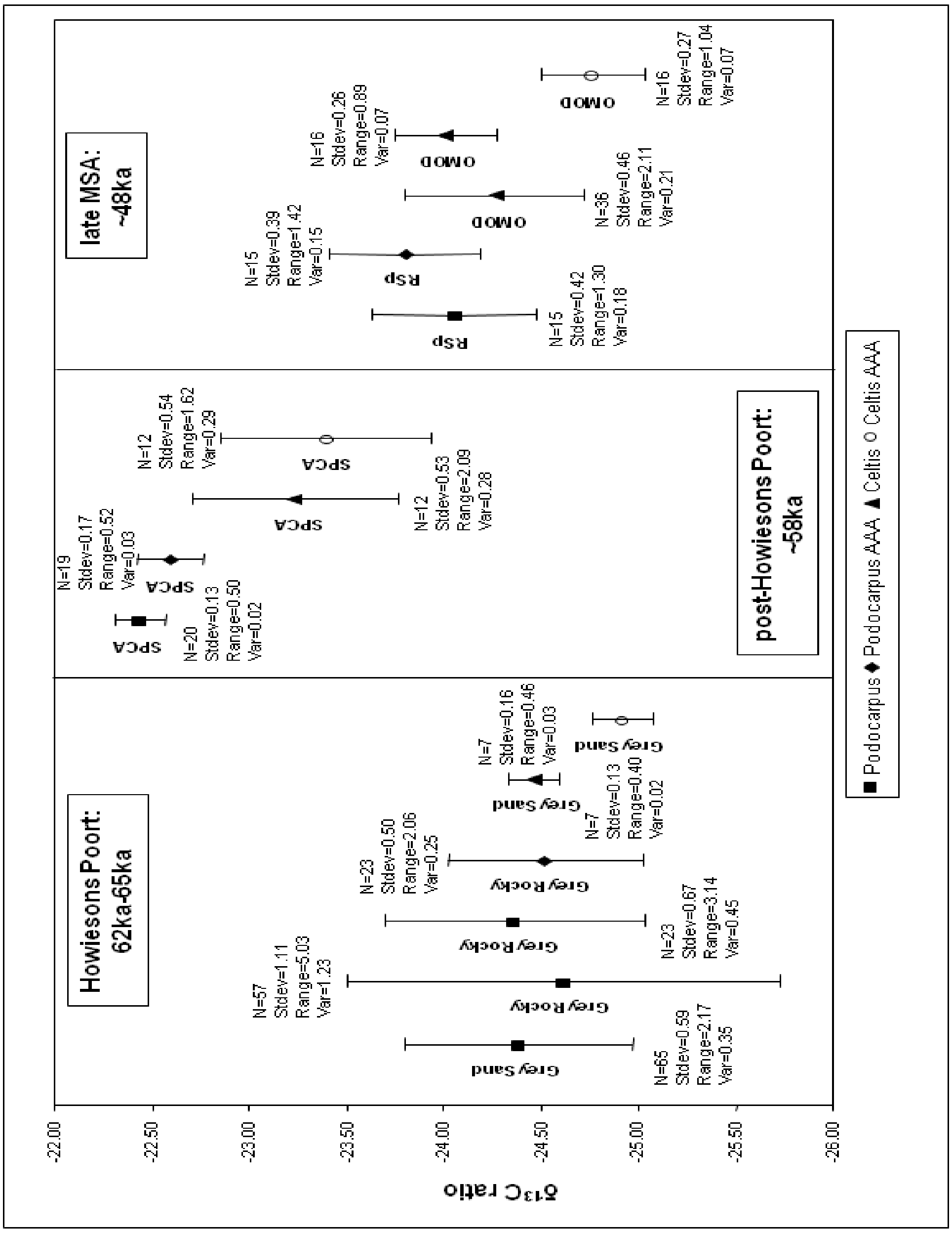

Figure 6.4. Mean carbon isotope values for *Podocarpus* and *Celtis* archaeological charcoal showing changes in carbon isotope values over time (adapted from Hall *et al.*, 2008). Error bars represent the standard deviation for each sample set. The number of samples, standard deviations, ranges and sample variances for each sample set is provided. The sample size from each sample set is large enough to allow meaningful inferences regarding the climatic conditions during each archaeological period.

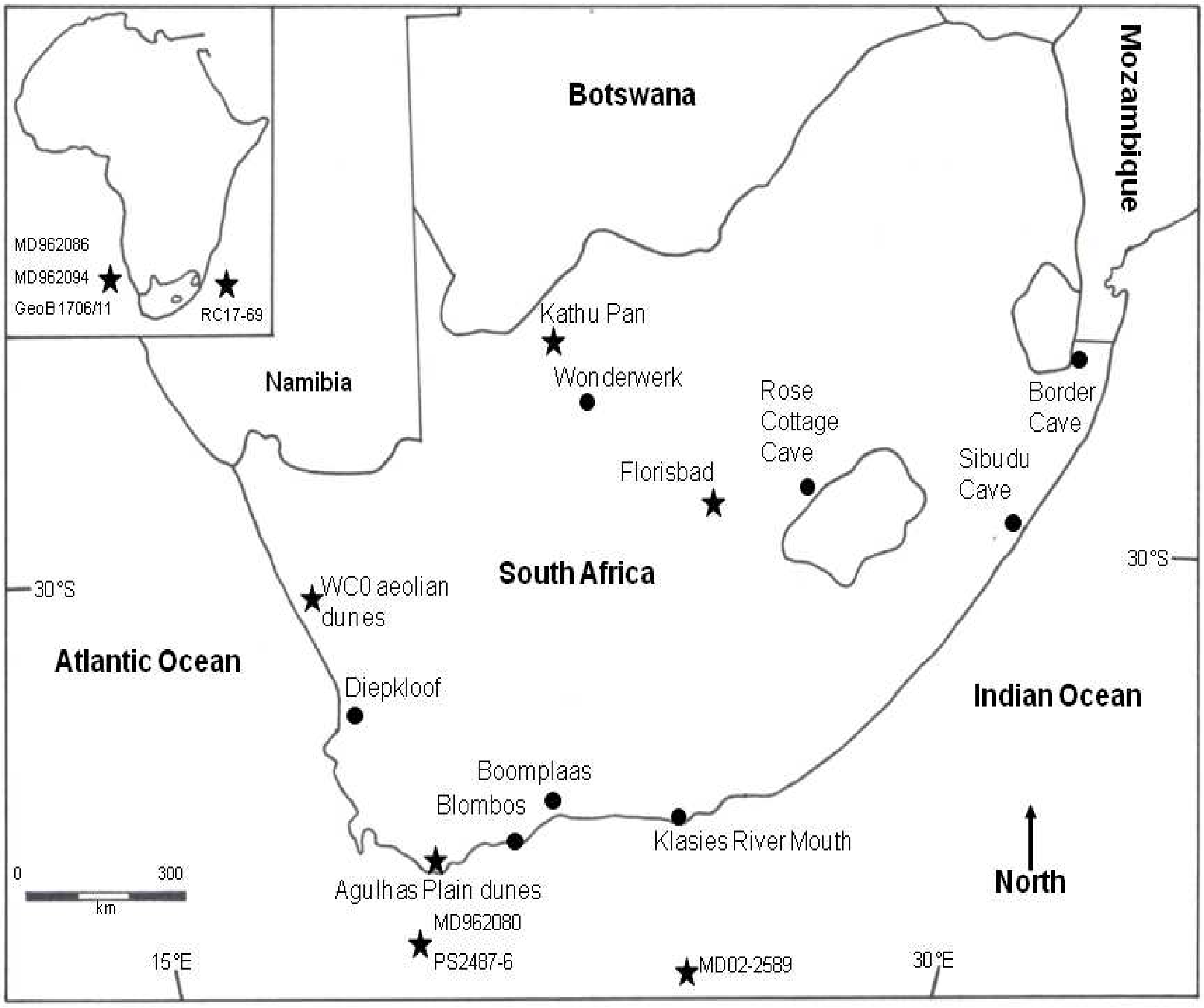

Figure 7.1. Map of southern Africa showing the locations of Middle Stone Age archaeological sites (black circles), deep sea cores and aeolian sediments (black stars) mentioned in the text.

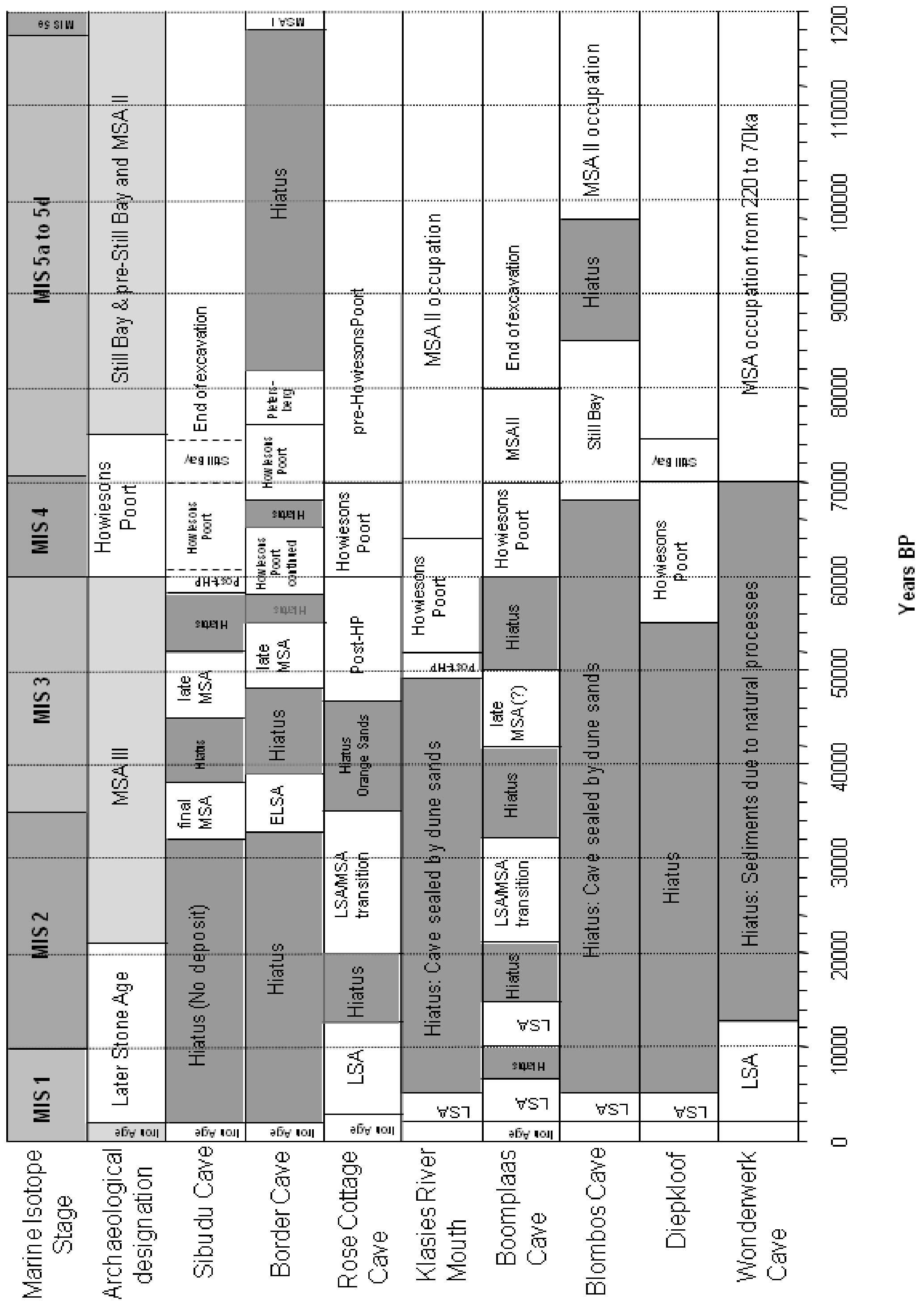

Figure 7.2. Summary graph of Marine Isotope Stages 1 to 5, archaeological designations and occupation/hiatus periods for Sibudu Cave and other Middle Stone Age sites from South Africa during the last 120ka.

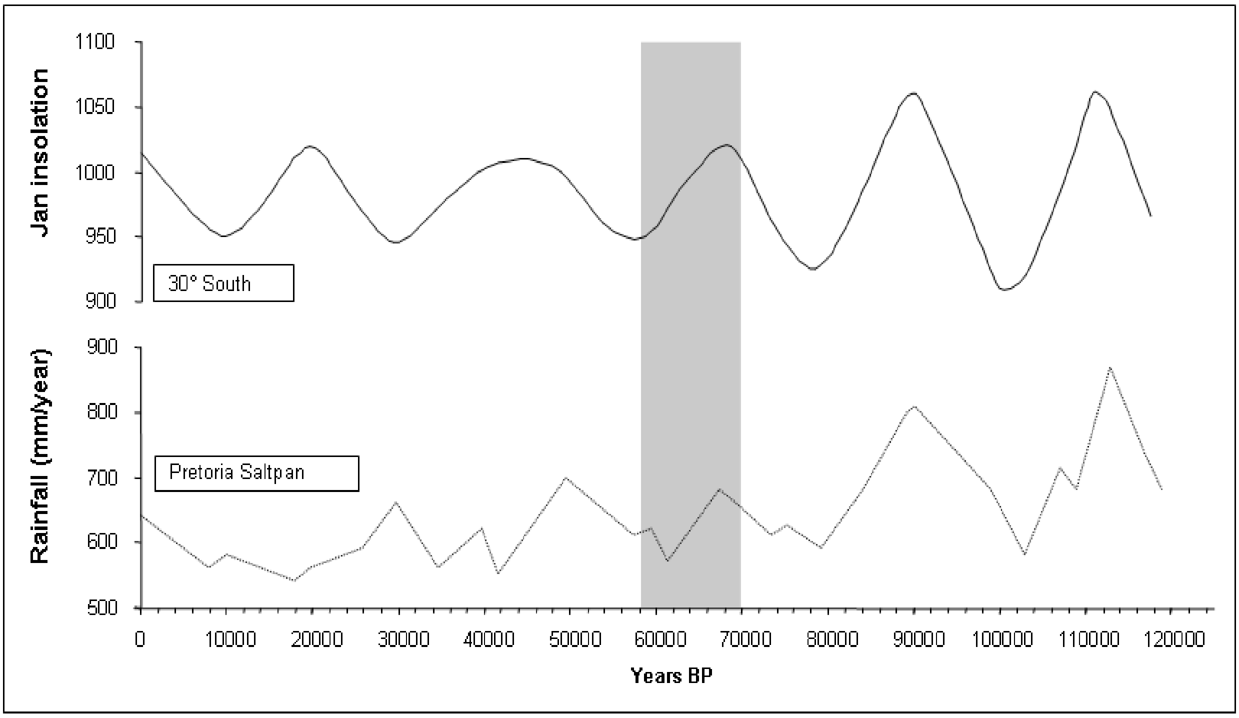

Figure 7.3. Southern African January insolation, 30° south (Partridge *et al*., 1997) and Pretoria Saltpan (Tswaing Crater) tuned rainfall (mm/year) time series (Partridge *et al*., 1997). The shaded area indicates the period of interest for this study.

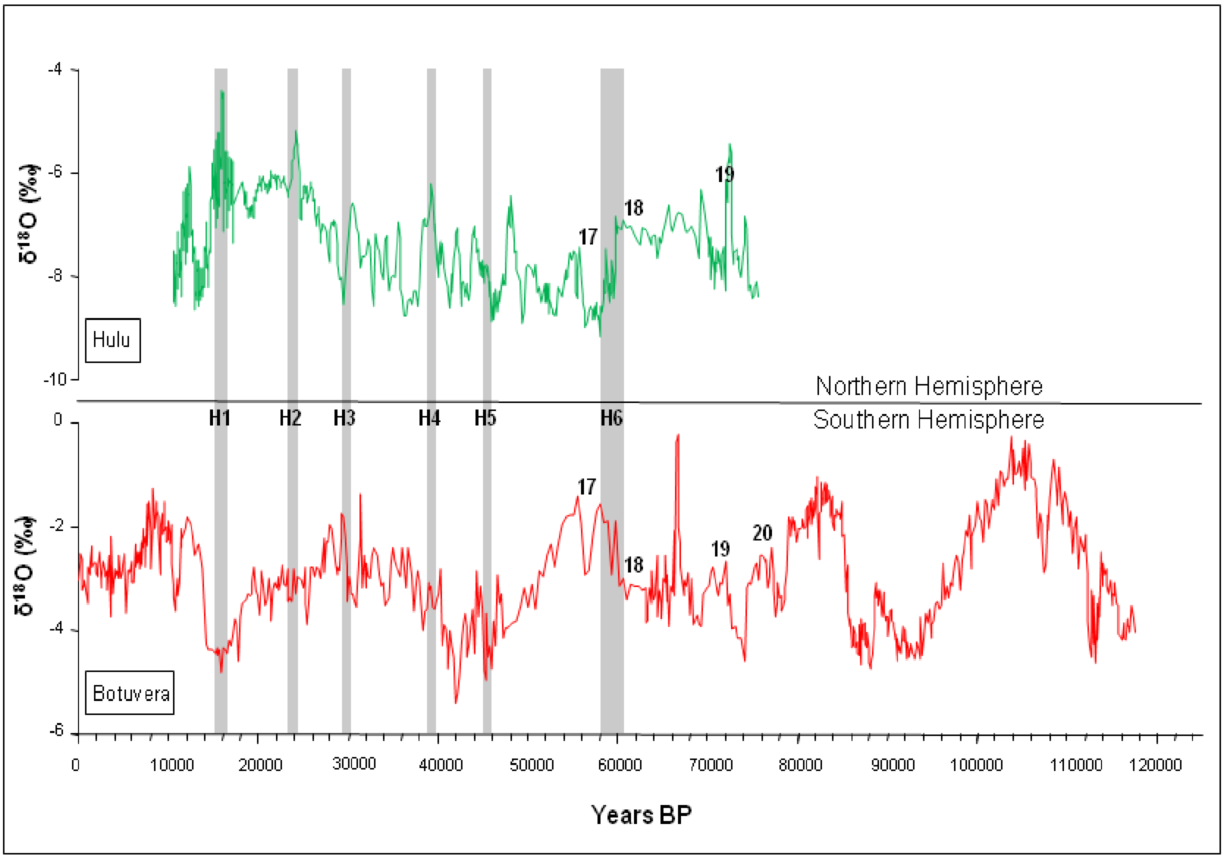

Figure 7.4. High-resolution $\delta^{18}O$ time series from northern and southern hemisphere speleothems for the last 120ka. Dansgaard/Oeschger events 20-17 (numbered) and Heinrich events 1-6 (shaded areas) are presented. Top: Combined oxygen isotope ratios from five speleothems from Hulu Cave, China (Wang *et al.*, 2004). Bottom: Oxygen isotope ratios from speleothems from Botuvera Cave, south-eastern Brazil (Cruz *et al*., 2005).

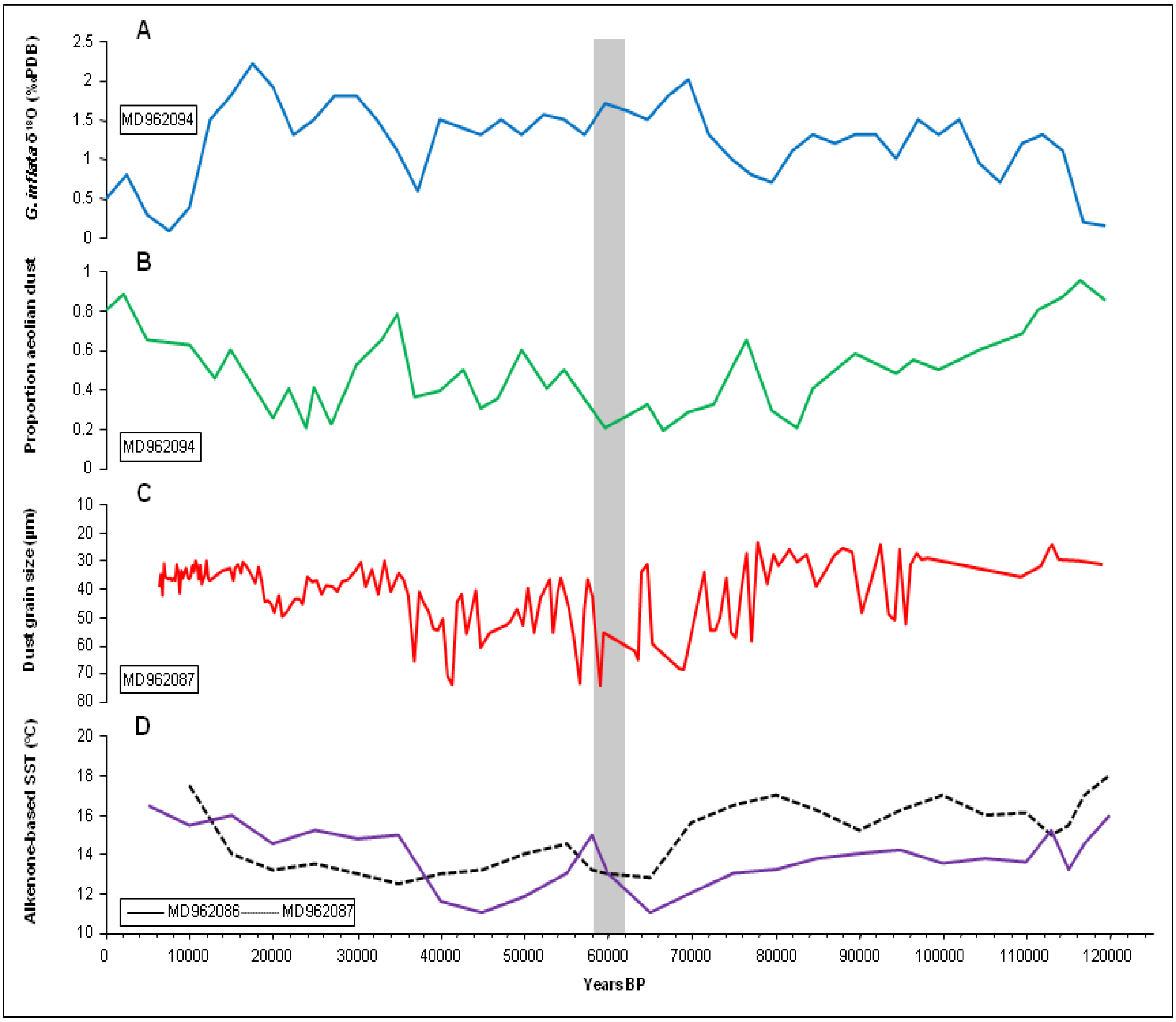

Figure 7.5. Palaeoenvironmental proxy data sets from deep sea cores of the western coast of southern Africa for the last 120ka. Age models and stratigraphy of the cores are mostly created by correlating $\delta^{18}O$ records of selected planktonic and/or benthic foraminifera with the SPECMAP record developed by Imbrie *et al*. in 1984. The shaded area indicates the period of interest for this study. A: $\delta^{18}O$ record for *Globorotalia inflata* from deep sea core MD962094 (Stuut *et al*., 2002). B: The proportion of aeolian dust from deep sea core MD962094 (Stuut *et al*., 2002). C: Time series of dust grain size (µm) from deep sea core MD962087 (Pichevin *et al*., 2005). D: Alkenone-based sea surface temperatures (SST) for deep sea cores MD962086 and 87 (Pichevin *et al*., 2005).

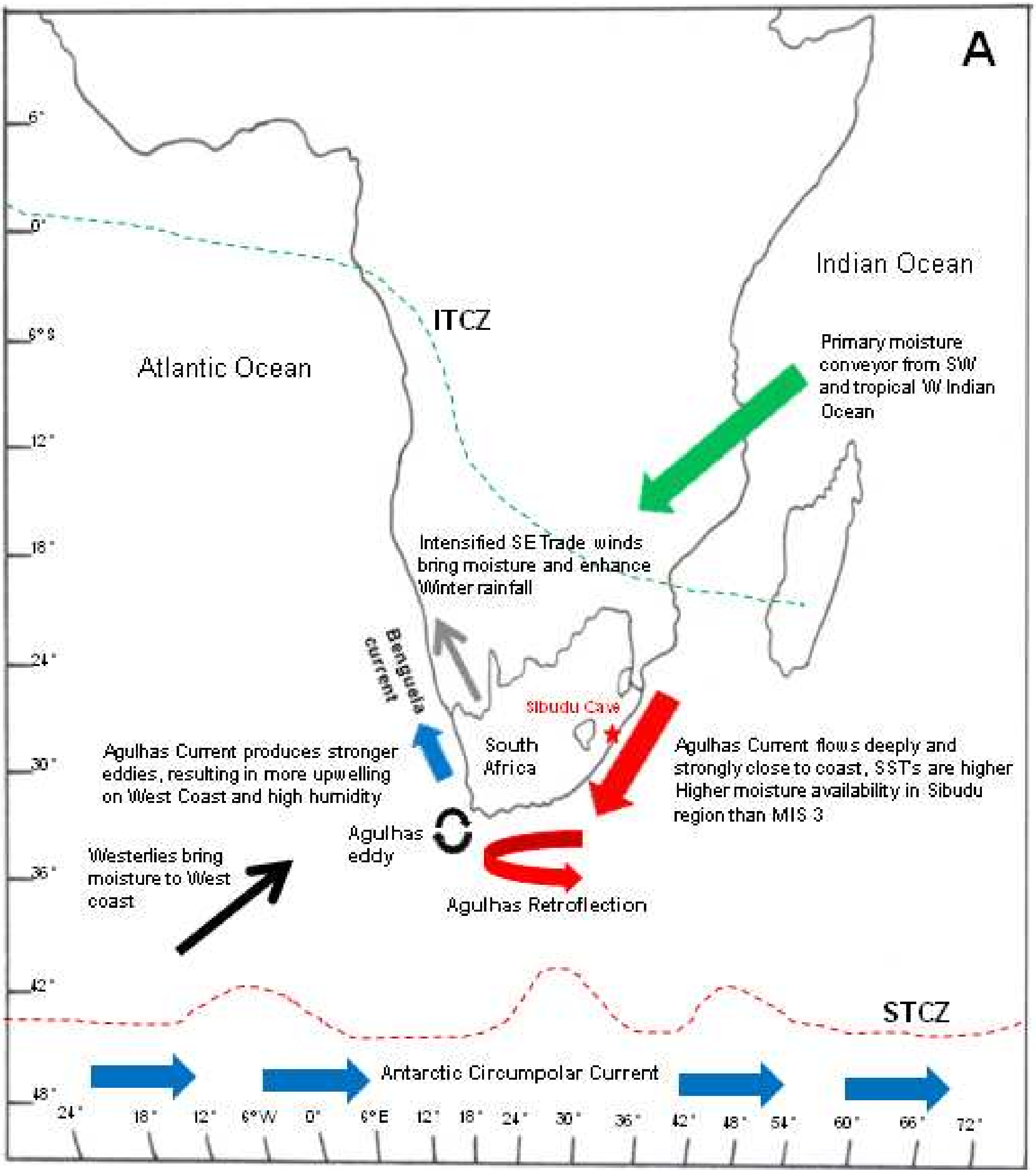

Figure 7.6a. Schematic diagram showing the relative positions and strength of the Agulhas, Benguela and Antarctic Circumpolar currents, the Agulhas Retroflection, Westerlies, South East trade winds, Intertropical Convergence Zone (ITCZ) and the Subtropical Convergence Zone (STCZ) during MIS 4. The location of the MSA site of Sibudu Cave is represented by a red star.

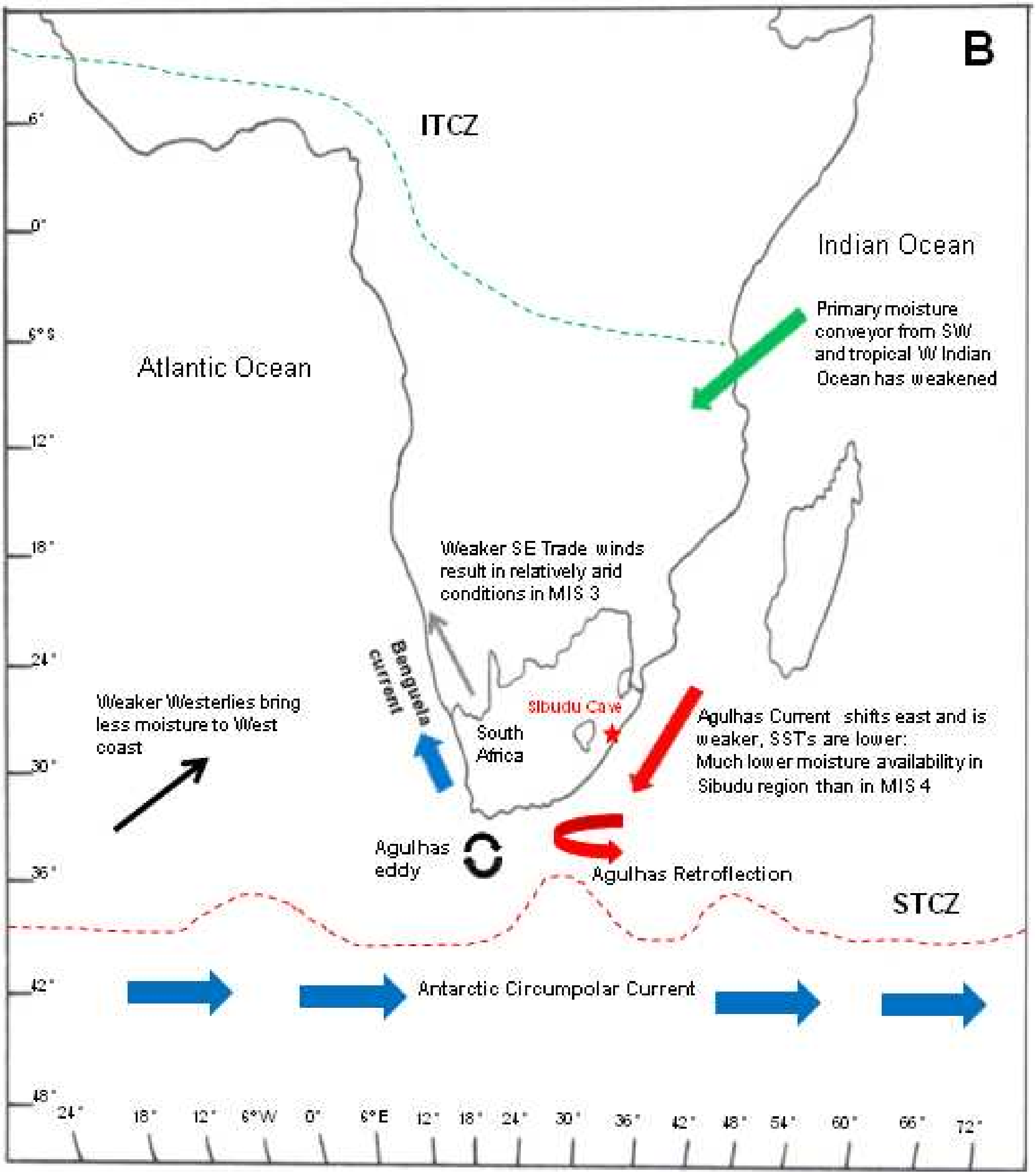

Figure 7.6b. Schematic diagram showing the relative positions and strength of the Agulhas, Benguela and Antarctic Circumpolar currents, the Agulhas Retroflection, Westerlies, South East trade winds, Intertropical Convergence Zone (ITCZ) and the Subtropical Convergence Zone (STCZ) during early MIS 3. The location of the MSA site of Sibudu Cave is represented by a red star.

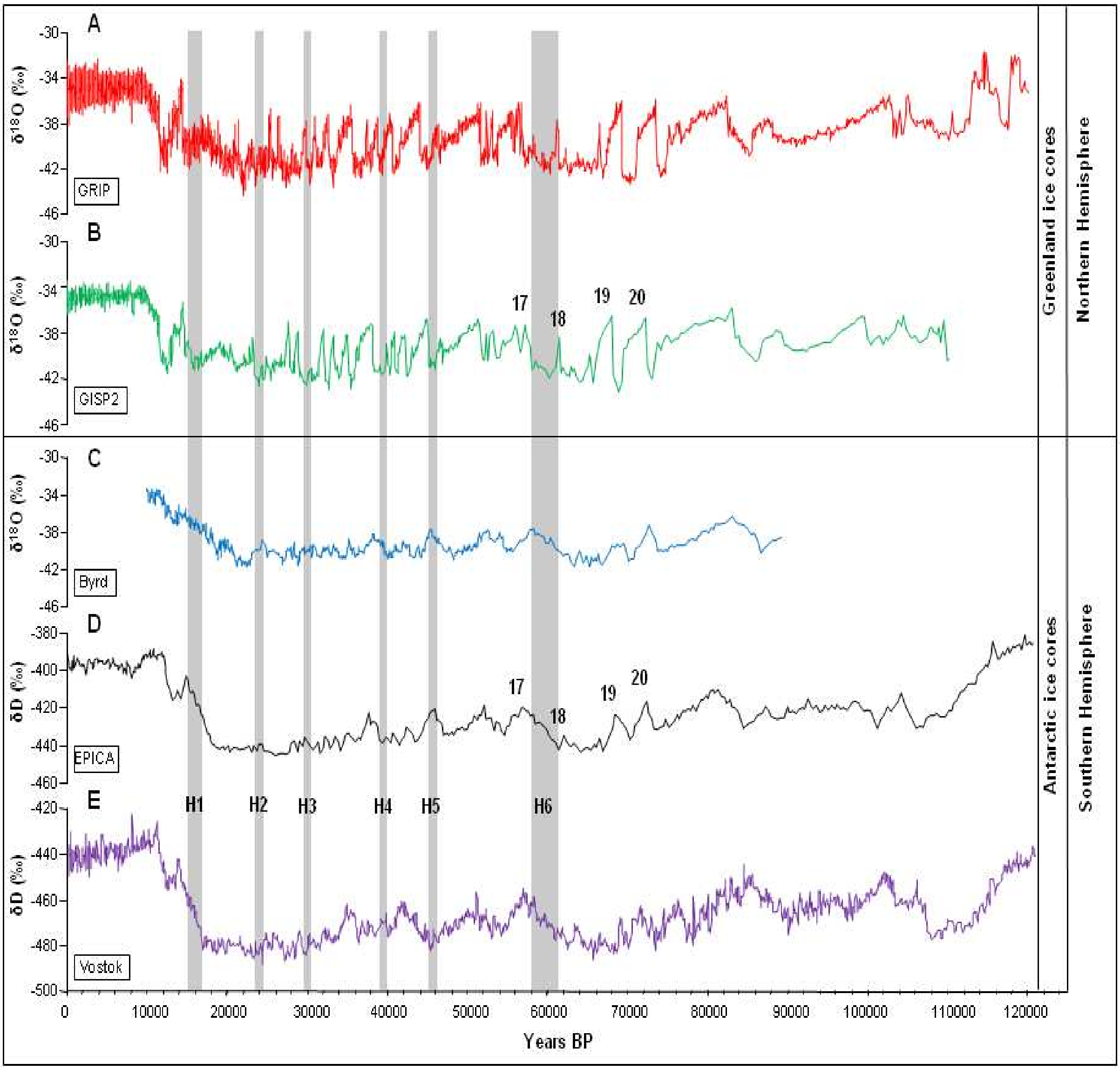

Figure 7.7. High-resolution $\delta^{18}O$ and δD time series from northern and southern hemisphere ice cores for the last 120ka. Dansgaard/Oeschger events 20-17 (numbered) and Heinrich events 1-6 (shaded areas) are presented. A: Oxygen isotope ratios from GRIP, Greenland (Blunier and Brook, 2001). B: Oxygen isotope ratios from GISP2, Greenland (Blunier and Brook, 2001). C: Oxygen isotope ratios from the Byrd ice core, Antarctica (Blunier and Brook, 2001). D: Deuterium isotope ratios from the EPICA ice core, Antarctica (Jouzel *et al*., 2004). E: Deuterium isotope ratios from the Vostok ice core, Antarctica (Petit *et al*., 2001).

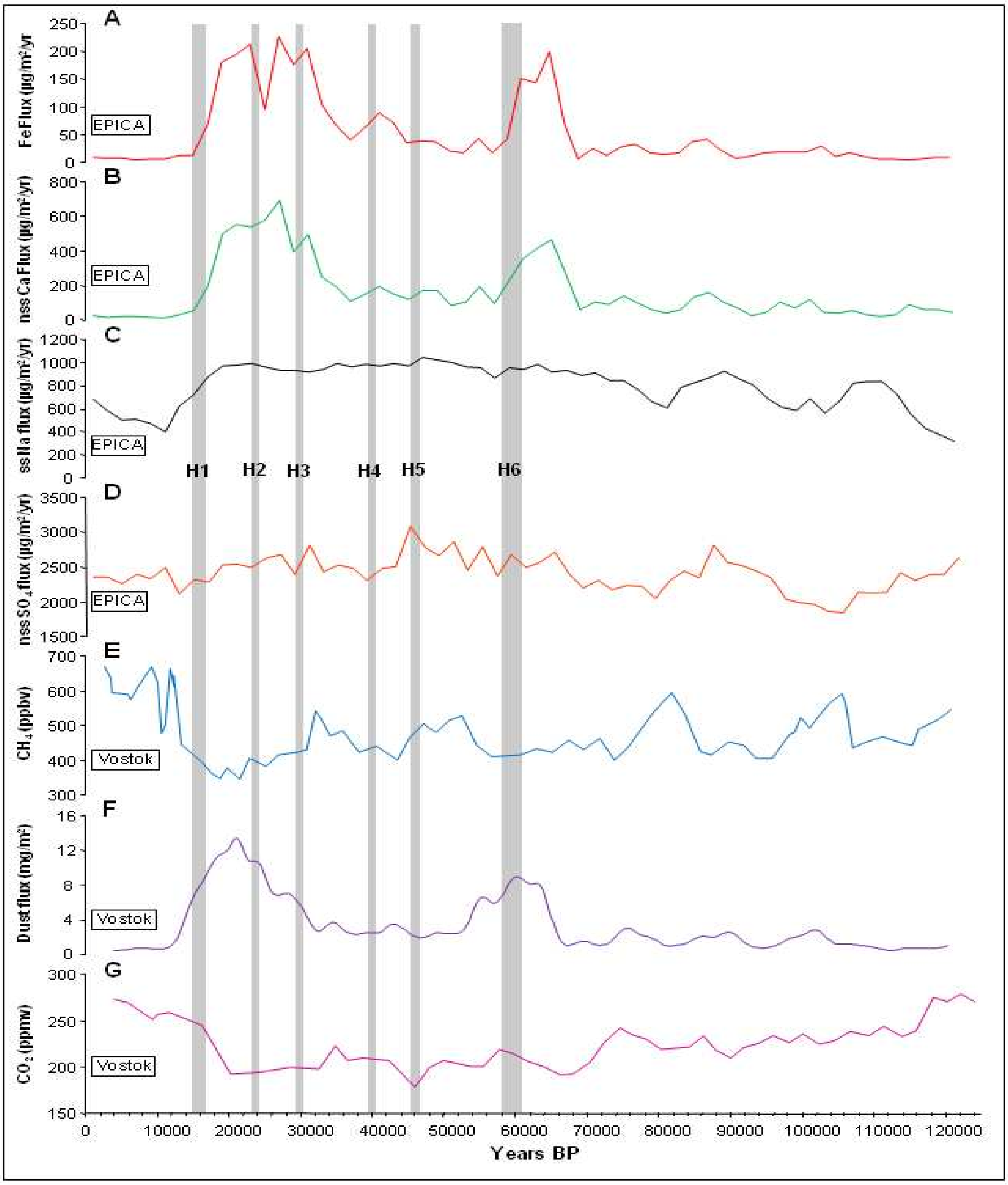

Figure 7.8. Chemistry data time series from the EPICA and Vostok ice cores, Antarctica for the last 120ka. The shaded areas indicate Heinrich events 1-6. A: Iron (Fe) flux from EPICA (Wolff *et al*., 2006). B: Non sea salt calcium (nssCa) flux from EPICA (Wolff *et al*., 2006). C: Sea salt sodium (ssNa) flux from EPICA (Wolff et al., 2006). D: Non sea salt sulphate ($nssSO_4$) flux from EPICA (Wolff *et al*., 2006). E: Methane (CH_4) variability from the Vostok ice core (Chappellaz *et al*., 1990). F: Dust flux record from the Vostok ice core (Petit *et al*., 1990). G: Carbon dioxide (CO_2) concentrations from the Vostok ice core (Barnola *et al*., 1987).

TABLES

Table 2.1. A summary of papers that have utilised stable isotope data from tree rings, fossils and other plant material for palaeoenvironmental research.

Reference	Species/ material	Location	Sampling methods	Wood component	Method	Data analysis	Results
Anderson *et al*., 2005	*Taxadium ascendens* (Pond Cypress) *T. distichum* (Bald Cypress)	South Florida, USA	Core samples from 2 wetland sites Rings identified, dated using standard dendrochronological methods Samples from individual rings and 10 ring pooled samples	α-cellulose extracted from homogenised wholewood	On-line, con-flo system	Data corrected for changing atmospheric CO_2, compared differences between locations and local climatic data	Time series for *T. ascendens* positive correlation with annual rainfall. Time series for *T. distichum* affected by saltwater stress
Ando *et al*., 2003	Detrital woody material, Aptian Stage	Hokkaido, Japan	Soil organic matter extracted from mudstone samples from 4 sample sites	Pre-treated bulk soil organic matter	On-line combustion	Creation of time series of carbon isotope variation and comparison with other proxy environmental records	Creation of a temporal record of changes in $\delta^{13}C$ of the ocean-atmosphere-biosphere system
Bechtel *et al*., 2002	Fossil gymnosperms from Early Miocene	Styrian Basin, Austria	Collected gelified and ungelified wood samples from borehole cores	Homogenised wholewood, cellulose and coal	On-line combustion	Compared mean isotope values of sample types and geochemical data	Isotope data showed shifts in vegetation due to climatic change and the effects of decay on various tissue types
Bechtel *et al*., 2003	Pliocene gymnosperm fossils	Slovenia	31 samples of fossil wood and charcoal extracted from borehole cores in lignite seam	Cellulose extracted from pre-treated samples	On-line combustion	Isotope values compared with petrographic and geochemical parameters	The $\delta^{13}C$ data shows that there is differential decomposition between wood and charcoal and the time series show shifts in vegetation communities
Benner *et al*., 1987	Variety of C_4 grasses and C_3 trees	USA	Collected samples of various plant parts	Whole tissue, hemicellulose, cellulose and lignin from pooled samples	No data	Statistical comparisons of various tissue types	Lignin values are highly depleted in ^{13}C with respect to whole tissue and cellulose and this effects isotope values of decayed wood
Biedenbender et al., 2004	Soil organic matter	SE Arizona, USA	Soil samples from 5 profiles across a watershed Relative age of soil organic matter derived from ^{14}C dating	Soil organic matter	Off-line combustion	Statistical analyses of isotope data and models of C_3/C_4 mixing to determine changes in vegetation and landscape	Data showed climate induced shifts in proportions of C_3/C_4 plants during Holocene, effect of aridity

Reference	Species/ material	Location	Sampling methods	Wood component	Method	Data analysis	Results
Brendel *et al*., 2002	*Pinus sylvestris* (Scots Pine)	N & central Scotland	Core samples from 150 trees from 5 natural populations 3 cores per tree, annual rings pooled and samples from clone bank	Cellulose from pooled annual ring samples	On-line, con-flo system	Statistical analysis of $\delta^{13}C$ data from natural and cloned populations with climatic data for the region	Isotopic values varied significantly in natural populations and correlated with climatic conditions, not the case with cloned population
Buhay *et al*., 2008	*Picea glauca* (White Spruce)	NW Territories, Canada	2 cores/tree, 6 trees from 3 sites Ring width chronologies created for all specimens (1689-2003)	α-cellulose extracted from combined early and late wood from each ring	On-line, con-flo system	$\delta^{13}C$ time series detrended to remove atmospheric and juvenile effects and statistically correlated with historic climate data from region	Time series showed best correlation with precipitation, rather than temperature At decreased temporal resolution $\delta^{13}C$ values capture generalised climatic trends
Comstock and Ehleringer, 1992	*Hymenoclea salsola*	W USA	Seed samples from 8 natural populations representing a range of environments. Seeds cultivated on common plot for 2 years and then analysed	Whole tissue from twigs and leaves	No data	Compared isotope data and proportions of leaf/twig photosynthetic tissue with climate data from each site of origin	Variation due to genetic differences Plants had substantial control of water use efficiency over large environmental gradients of temperature and water availability
Cullen and Grierson, 2006	*Callitris glaucophylla (Conifer)*	NW Australia	9-11 cores from 7-8 trees All cores cross-dated to assign assign calendar date Annual ring samples pooled	Wholewood and α-cellulose from annual rings	On-line, con-flo system	Statistical analysis of $\delta^{13}C$ and $\delta^{18}O$ data from tissue types and comparison with local climatic data	Isotopic time series of both tissue types have similar annual variation and can provide proxies for climate. $\delta^{13}C$ of cellulose more sensitive to high frequency variation, wholewood for long-term trends
Czimczik *et al*., 2002	*Pinus sylvestris* (Scots Pine) *Betula pendula* (Birch) Samples of rotted wood	NW Germany & Canada	Bulk samples of each wood type Air dried and milled Subject to controlled combustion times and temperatures in laboratory	Wholewood, holocellulose, lignin and pyrolysis products	On-line, con-flo system	Compared isotopic data from various tissue types and pyrolysis products	Soft wood species have more depleted isotope values than hard wood due to difference in cellulose: lignin ratio Temperature and length of burn affects the $\delta^{13}C$ values of product released
Danis *et al*., 2006	*Quercus robur* (Common Oak)	SE France	Collected core samples (3/tree) from 2 natural populations Looked at the latewood from rings 1971-2001, samples pooled	α-cellulose extracted from pooled latewood	On-line, con-flo system	Statistical analysis of $\delta^{13}C$ and $\delta^{18}O$ time series with local monthly temperature and relative humidity and oxygen isotope record of precipitation	$\delta^{18}O$ inter-annual variability mainly due to changes in isotopic composition of precipitation and relative humidity Combined carbon and oxygen time time series can allow reconstruction of past summer precipitation isotope record
Dodd *et al*., 2008	*Picea glauca* (White Spruce) *Larix laricina* (Tamarack)	Canada & USA	Core and disc samples from specimens from natural forest ecosystems	α-cellulose extracted from milled wood tissue	On-line, con-flo system	$\delta^{13}C$ time series detrended to better illustrate relationship between	Time series showed sub-seasonal variation seen in precipitation

Reference	Species/ material	Location	Sampling methods	Wood component	Method	Data analysis	Results
	Populus grandidentata (Popular)		Used a computer controlled micromill to obtain multiple samples (2-12, mean=4) per growth ring			isotope values and precipitation	
Dongarra and Varrica, 2002	*Plantanus hybrida* sp.	Palermo, Italy	Annual growth rings sampled in 5-year blocks from 3 trees for period 1880-1998 Dated using chronological ring counts	Wholewood samples	On-line combustion	Statistical comparison of isotope data with modern atmospheric CO_2 data to reconstruct past atmospheric CO_2	$\delta^{13}C$ time series of trees showed more negative values over time in response to changing atmospheric CO_2 concentration due to burning of fossil fuels
Hunter *et al.*, 2006	Various conifer species from Holocene	Lake Huron, USA	20 cross-sections from submerged roots, stumps and logs All ^{14}C dated to about 7350 BP	Holocellulose from selected ring intervals	On-lime combustion	Statistical analysis of $\delta^{13}C$ and $\delta^{18}O$ data from Holocene trees with modern data from Holocene trees with modern data and development of proxy data for past climates	Isotopic data indicates environment with high inter-annual climate variability Also suggests local environment was warmer than present
Dupouey *et al.*, 1993	*Fagus sylvatica* (Beech)	Nancy, France	4 cores/tree from 4 trees Individual rings from cores combined to have pooled sample of 16 rings/year	Holocellulose extracted from whole ring early and latewood combined	Off-line combustion	Statistical analysis of data and modelling of $\delta^{13}C$	$\delta^{13}C$ time series provided a proxy for past water availability and showed decreasing trend over time due to changes in atmospheric CO_2
Edwards *et al.*, 2000	*Vicia faba (Bean), Abies alba* (Black Forest Fir)	Germany	80 bean plants grown under 4 treatments 5 trees from Black Forest	Bean stem and leaf cellulose Annual ring latewood cellulose	No data	Statistical comparison of $\delta^{13}C$ data with relative humidity and temperature for the 4 treatments and local rainfall, temperature and relative humidity from Black Forest	Multivariate analysis of data is needed to show effect of moisture and temperature on carbon isotope values
Feng and Epstein, 1995	*Pinus coulteri, P. langaza* *Juniperus phoenica* *Quercus lobata*	California, USA Sinai Peninsula, Egypt	1 radial segment per tree, samples taken from annual rings annual rings and 5-year intervals ^{14}C dating and annual ring counts	Cellulose converted into cellulose nitrate	Off-line combustion	Modelling using low frequency signal (trend) and high frequency signal reflecting response to rainfall	$\delta^{13}C$ time series show declining trend due to changing atmospheric CO_2 High frequency effect directly related to amount of precipitation, water use efficiency
Gagen *et al.*, 2008	*Pinus sylvestris* (Scots Pine)	Lapland, N Finland	32 trees cored to produce 6 chronologies 3 sites in open semi-natural forest Each chronology composed of 5 trees Dated using standard ring width methods	Pooled α-cellulose extracted from latewood of annual rings	On and off-line combustion	$\delta^{13}C$ time series detrended to remove atmospheric and juvenile effects These are non climatic trends	The atmospheric trend is removed mathematically. Use of Regional Curve Standardisation removes the juvenile effect
Garciá-G *et al.*, 2004	*Pinus greggii*	Central Mexico	Sampled 3 populations from 2 plantations	α-cellulose from growth rings	On-line, con-flo	ANOVA analysis of isotope data,	Differences in $\delta^{13}C$ values between

Reference	Species/ material	Location	Sampling methods	Wood component	Method	Data analysis	Results
			12mm cores taken from 5 trees at each site Examined the most recent 5 annual rings			basal area increments and local meteorological variables and comparison of the 2 populations	sites due to precipitation and altitude High, dry site less negative than low, wetter site. Good correlations with climate variables at wetter site, not at dry site
Gouveia *et al*., 2002	Soil organic matter and charcoal	SE & CW Brazil	Soil organic matter and charcoal removed at 10cm intervals from 5 soil profiles	Bulk samples of fine sieved organic matter	No data	Created carbon isotope time series for the soil profiles, ^{14}C dating of humin and charcoal	Time series showed shifts in proportion of C_3 and C_4 plants due to shifts in level of aridity through Holocene
Guo and Xie, 2006	4 C_3 species	Tibetan Plateau, China	Leaf samples collected from a N-S transect across climate zones Samples washed and dried	Whole leaf tissue	On-line, con-flo system	Isotopic data statistically correlated with altitude and climatic data Also correlated isotope values with satellite data on normalised difference vegetation index (NDVI)	Northern $\delta^{13}C$ values correlated positively with altitude and precipitation Southern $\delta^{13}C$ values correlated negatively NDVI data can approximate $\delta^{13}C$
Kirdyanov *et al*., 2008	*Larix cajanderi* (Cajander Larch)	E Siberia, Russia	Core and discs from 10 dominant trees Obtained latewood density and ring width data using computer program Latewood manually removed from each ring	Cellulose from homogenised wood samples	On-line combustion	$\delta^{13}C$ time series detrended to remove atmospheric effects, anthropological and physiological. Then statistically correlated with latewood density, ring widths and local climatic variables	Time series showed significant correlations with precipitation and temperature, combined with other data allows creation of long-term palaeoclimate records
Krull *et al*., 2003	Variety of woody species and C_3/C_4 grasses	Australia	Grass, leaves, wood and char samples from natural burns and material from laboratory combustion experiments	Whole bulk samples and char from various burning regimes	On-line combustion	Comparison of isotope results from a variety of burning regimes	Cannot use laboratory chars to infer changes seen in natural burns C_4 chars show significant ^{13}C depletion C_3 chars do not
Leavitt, 2002	11 tree species	Great Lakes, USA	Punch core samples taken from trees from 3 sites during 1990 growing season, 2 core/tree	Composite holocellulose sample	Off-line combustion	Comparison of seasonal $\delta^{13}C$ values with climatic data	Shows trees produced a representative isotopic pattern that shows the ecophysiological response to seasonal climate change
Leavitt and Long, 1982	3 species of *Juniperus*	Arizona, USA	Leaf samples from 4 cardinal points, rings representing 10 growing seasons from 10 trees growing at various altitudes	Wholewood from rings and cellulose from pooled leaf samples and wood	Off-line combustion	Comparison of $\delta^{13}C$ values of tissue types to determine magnitude of fractionation between leaves and wood	Leaves on average 2‰ isotopically lighter than wood tissue. Also a seasonal response to temperature, $\delta^{13}C$ values become more negative and then more positive through season
Li *et al*., 2004, 2005	*Pinus tabulaeformis* (Chinese Pine)	N China	Discs from 3 trees taken, dated using standard dendrochronological	α-cellulose from growth rings	Off-line combustion	Statistical analysis of long-term inter-annual $\delta^{13}C$ variability and	Isotope time series show inter-annual and seasonal variability in response to

Reference	Species/ material	Location	Sampling methods	Wood component	Method	Data analysis	Results
			techniques			seasonal variability	changes in soil moisture, precipitation and relative humidity. Differences between early and latewood and declining trend due to changes in atmospheric CO_2
Lipp *et al*., 1996	*Tamarix jordanis*	Jordan Rift Valley, Israel	Branch samples taken from 9 trees from 4 ecoclimatic regions	α-cellulose from growth rings from 1991-1992	No data	Compared $\delta^{13}C$ and $\delta^{18}O$ data from rings with stem/leaf water values and relative humidity, temperature and precipitation data from each site	$\delta^{13}C$ values less negative at lower relative humidity, also affected by higher water availability, no clear link between temperature and precipitation
Liu *et al*., 2004	*Pinus tabulaeformis* (Chinese Pine)	NW China	2 cores/ tree for cross-dating, third for carbon isotope analysis, 6 trees/site	Composite samples of annual rings reduced to cellulose	Off-line combustion	Statistical analyses of isotope time series with temperature and precipitation. Isotope data detrended for atmospheric and juvenile effects	Time series have a negative correlation with precipitation and provide proxy record of historical wet. dry fluctuations
Loader *et al*., 2003	*Quercus robur* (Oak)	East Anglia, UK	12mm cores taken from 2 trees Absolutely dated against local and regional dendrochronologies 55 year sequence (1946-2000) of annual rings	Wholewood, lignin and cellulose from latewood of each ring	On-line, con-flo	Correlation of isotope values for each tissue type and their associations with climate	Cellulose values are enriched with respect to lignin. Wholewood $\delta^{13}C$ retains the strongest climate signal
Loader *et al*., 2008	*Quercus robur* (Common Oak)	SW Scotland	12mm cores taken from 4 mature trees Dated using cross-dating chronology previously developed Latewood removed from each annual ring All 4 samples pooled	Homogenised α-cellulose	On-line combustion	$\delta^{13}C$ time series detrended to remove atmospheric effects, anthropological and physiological. Then statistically correlated with local climatic data	Time series reflected influence of higher temperatures, increased insolation, low humidity and reduced precipitation. Possible to extract strong, coherent summer climate signal
Lockheart *et al*., 1998	*Fagus sylvatica* (Beech)	Gloustershire, UK	Leaves collected from 4 cardinal points from direct sun and shaded areas	*n*-C_{27} hydrocarbon extract and bulk leaf tissue	On-line combustion	Compared isotope values with stomatal density	Lipid $\delta^{13}C$ more negative than bulk leaf values. Sun leaves less negative than shade due to reduced fractionation Has implication for obtaining proxy data from fossil leaves
Lücke *et al*., 1999	Fossil wood from 7 taxa of angiosperms and gymnosperms	Garzwieler Seam, Germany	Fossil wood and brown coal samples taken from 20cm sections through coal seam profile	Fossil wholewood, cellulose and brown coal	On-line combustion	Compared mean isotope values of sample types through time Middle Miocene	Isotope data provide proxy record showing shifts in vegetation due to changing environment, cooling trend
Mazany *et al*., 1980	Archaeological samples of *Pinus*	Chaco Canyon	Tree ring sections from two	Cellulose and lignin from pooled	Off-line combustion	Statistical comparison of isotope values	Cellulose most sensitive to climatic

Reference	Species/ material	Location	Sampling methods	Wood component	Method	Data analysis	Results
	ponderosa and *Abies concolour*	New Mexico, USA	dendrochronologically dated specimens	ring samples representing 10-year periods		of tissue types and creation of a time series to determine variation in $\delta^{13}C$ values	changes and time series has potential to provide a record of past climates
Nguyen Tu *et al*., 2002	Fossil plants from Cenomanian	Bohemia	Fossil leaf samples from deposits Pre-treated to remove contaminants	Leaf cuticle and petiole tissue and extracted leaf lipids	On-line combustion	Looked at preservation of isotopic signal in fossils, range of variation in fossils and modern plants and changes in palaeoenvironment	There were significant differences in isotope values of leaf components Overall $\delta^{13}C$ values not significantly altered diagenetically, allowing reconstruction of palaeoenvironment
Pearman *et al*., 1976	*Arthrotaxis selaginoides* (King Billy pine)	Tasmania	Removed 5-yr blocks of rings from two trees	Pooled samples of wholewood	Off-line combustion	Statistical comparison of isotope data with local temperature records	Showed a significant correlation with temperature, but not the sole influence on the isotopic composition
Pennington *et al*. 1999	*Prosopis glandulosa* (Honey Mesquite)	SW USA	Seeds from 15 maternal families growing along a precipitation gradient Grown under controlled conditions	Pooled whole leaf tissue 20 seedlings/family	No data	Looked at variation in $\delta^{13}C$ amongst families to show genetic effects and compared data with climatic records	The isotopic data indicates there is genetic variability across the families adaptation for local environmental conditions
Poole *et al*., 2002	*Pisum sativum* (Peas)	Netherlands	Sets of 10 peas (seed coat removed) subject to series of controlled combustion conditions in laboratory	Whole tissue	On-line combustion	Examined changes in isotope values due to combustion under range of temperatures and the implications for palaeoclimate reconstructions	The plant part examined is important Combustion temperature is main influence of isotope value, but can be corrected for.
Poussart and Schrag, 2005	6 tropical tree species	N Thailand	Cross-sections collected from felled trees from 4 locations Age models from 14C dating	α-cellulose from visible rings or microtome slivers at constant intervals across section	On-line combustion	Compared $\delta^{13}C$ and $\delta^{18}O$ data from time series with rainfall variability and create isotopic age models for trees with no visible ring structure	$\delta^{13}C$ time series showed correlations with regional rainfall variability Isotopic age models used to reconstruct growth rates, significant correlation
Poussart *et al*., 2004	*Tectona grandis* (Teak) *Samanea saman* (Saur) *Podocarpus neriifolius* (Yellowwood)	Indonesia Thailand	Core or wedge samples from 2 trees per species	α-cellulose from growth rings or specific intervals across core when rings not clear	On-line, con-flo	Compared $\delta^{13}C$ and $\delta^{18}O$ data from tropical species with visible rings partial rings and no ring structure and local climate data	Possible to obtain sub-annual isotope time series from tropical species reflecting local climatic conditions
Rakowski *et al*., 2008	*Pinus sylvestris* *Pinus densiflora* *Pinus radiata*	Poland, Japan & Peru	3 core samples/tree Samples from annual rings removed using hollow drill, Samples pre-treated for AMS dating using acid-alkaline-acid treatment	Wholewood	On-line	Examining the Suess effect-lower radiocarbon concentrations due to anthropogenic activities	Can use carbon isotope values from tree rings to obtain secular variations of ^{14}C concentrations of atmospheric CO_2 and reconstruction of past radiocarbon concentrations

Reference	Species/ material	Location	Sampling methods	Wood component	Method	Data analysis	Results
Rinne *et al*., 2005	*Pinus sylvestris* (Scots Pine) modern and sub-fossil	N Finland, UK & Russia	Bulk heartwood and sapwood samples Sub-fossils grouped sample of 5 trees ^{14}C dated	Resin extracted α-cellulose α-cellulose without resin extracted	On-line combustion	Compared two pre-treatments isotope values and also did Fourier transform infrared spectroscopy	Found no difference between the isotopic values of the two methods
Robertson *et al*., 2004	*Shorea superba* (Selangan batu)	Sabah, Malaysia	Radial segment from fallen specimen Age model from 5 high-resolution ^{14}C dates, ring counts and computerised calibration program	Resin extracted wholewood from 173 rings	On-line combustion	Compared the carbon isotope time series with local climatic data	δ^{13}C time series showed the "juvenile" and anthropogenic effects No evidence of a seasonal response to climate
Roden, 2008	*Pinus ponderosa* (Ponderosa Pine) *Sequoia sempervirens* (Redwood)	California, USA	4 12mm cores/tree from 5 sites Ring width measured using computerised system	Pooled α-cellulose extracted from latewood samples and sub-annual levels	On-line combustion	Ring width, δ^{13}C and δ^{18}O data statistically analysed using computer program (COFECHA)	Demonstrated the possibility to use isotopic time series to cross-date tree ring sequences
Schleser *et al*., 1999	*Quercus robur, Fagus sylvatica* *Pinus sylvestris* *Sequoiadendron giganteum* and fossil tree trunks	Germany	Homogenised wood from whole cross section 10 samples per species, subjected to artificial aging using water and heat treatments	Cellulose extracted from range of aged samples & fossils	On-line combustion	Examined changes in carbon isotope values during aging and compared with fossil material	There is a 2-stage degradation of isotope values, depletion (more negative) followed by enrichment (more positive)
Stuiver and Braziunas, 1987	6 species of conifer	USA	Pooled samples of tree rings from trunk sections of 19 deciduous and evergreen conifers	Cellulose extracted	No data	Statistical analysis of pre-1850 isotope data with latitude and climatic data and Greenland ice cores (temperature)	Found a strong dependency on latitude. Strong negative correlation with temp Strong positive one with relative humidity Also correlations with ice core record
Tardif *et al*., 2008	*Picea glauca (White Spruce)*	Subarctic Manitoba, Canada	Cross-sections from 8 trees Ring width chronologies created (1756-2000) using computer program Analysed 5-year blocks of pooled samples and individual rings	α-cellulose extracted from entire ring	On-line, con-flo system	Statistical and mathematical detrending of δ^{13}C time series to remove the anthropogenic effect, correlated data with ring widths and climatic data	Time series had no correlation with ring width, positive correlation with summer temperatures and length of growing season. Can provide long-term climate proxy records
Tarhule and Leavitt, 2004	*Isoberlina daka* *Daniella oliverim* *Tamarindus indica*	West Africa	Core. disc samples from 9 trees from 4 locations Cross-dated using ring sequences	Holocellulose from growth rings	On-line, con-flo system	Comparison of carbon isotope time series of the 3 species	All time series showed inter-annual and season response to climate and can provide proxy for seasonal rainfall
Turekian ***et al*.**, 1998 Ballentine *et al*., 1998	2 C_3 tree spp. and 3 C_4 grass spp.	Namibia South Africa	Collected ash & aerosol samples from natural burns	Whole leaf bulk samples, ashed material, aerosol	Off-line combustion	Compared mean isotope values of sample types.	C_3 values showed no difference in δ^{13}C values between sample types

Reference	Species/ material	Location	Sampling methods	Wood component	Method	Data analysis	Results
		California, USA	Controlled burns in laboratory	components and lipids			C_4 samples show fractionation effect between bulk and combusted material
Turney *et al*., 2006	*Eucalyptus* spp. *Quercus robur* *Pinus radiata*	Australia	Wood samples from 6 years of growth rings collected from each species, chipped, homogenised and combusted at range of temperatures and times under reducing and oxidising conditions	Wholewood and charcoal	On-line, con-flo system	Compared isotopic values to determine the effects of combustion temperature and length on carbon isotope fractionation	The time length of combustion has no effect on the final $\delta^{13}C$ result, but values become progressively depleted in ^{13}C as temperature increases
van Bergen and Poole, 2002	Archaeological and fossil wood	Antarctica Germany	Samples of fossil wood and sub samples from archaeological wood from exterior to interior	Pre-treated insoluble wood organic matter and products of pyrolysis	On-line combustion	Examined variation in isotope values from range of fossils and archaeological wood to determine possible source for this variation	Differences in $\delta^{13}C$ values due to changes in chemical composition of wood over time
Van de Water, 2002	Various C_3, C_4 and CAM species	Utah, New Mexico, USA	5 random plants from transects representing range of environmental conditions Twigs, leaves, spines from cardinal points of each plant, pooled for analysis	Whole tissue. hemicellulose, α-cellulose and nitro-cellulose	Off-line combustion	Statistical comparison of the $\delta^{13}C$ values for the various tissues	Carbon isotopes show significant differences between C_3, C_4 and CAM Also differences due to pre-treatment and tissue type used
Van de Water *et al*., 1994	*Pinus flexilis*	Idaho, Utah, Arizona Nevada, USA	41 collections of pine needles from pack rat middens from last 40ka, AMS dating of needles	Leaf cellulose extracted from needles	No data	Statistical analysis of isotopic data, stomatal densities from last glacial-interglacial cycle	$\delta^{13}C$ time series provided a proxy record of climate change for the last 30ka and showed changes in water use efficiency over time
Verheyden *et al*., 2004, 2005	*Rhizophora mucronata* (Mangrove)	Gazi Bay, Kenya	Stem discs from 2 trees Growth rings identified and counted and age models developed	Wholewood, α-cellulose from early and latewood	On-line, con-flo system	Statistical comparison between the isotopic values of the tissue types	Isotope values of wholewood and cellulose high correlated, can use wholewood for creation of proxy records
Weigl *et al.*, 2008	*Quercus patraea* (Sessile Oak)	Vienna, Austria	Single trunk disc, annual rings divided into 4 components Early and latewood, complete ring and transfer ring (subsequent early and current latewood used)	Wholewood from 50 year sequence (1936- 1985)	On-line combustion	$\delta^{13}C$ time series corrected for changes in atmospheric $\delta^{13}C$ Data correlated with ring component width	Latewood values showed best sensitivity to climatic variables. No significant correlation to width
Wilson and Grinsted, 1977	*Pinus radiata*	New Zealand	Trunk section of single specimen, samples taken from three annual rings	Cellulose and lignin	Off-line combustion	Compared time series of the two tissue types to show inter-annual variability	Both time series similar amplitude, varied with temperature and showed seasonal variation

Reference	Species/ material	Location	Sampling methods	Wood component	Method	Data analysis	Results
							Lignin values more negative than cellulose Need to compensate for juvenile effect
Wooler *et al*., 2004	*Rhizophora mangle* (Red Mangrove)	Twin Cays, Belize	Leaf samples collected from a mangrove peat core, 5cm intervals 5 AMS dates for core (850-7840 BP)	Whole leaf tissue	On-line, con-flo system	Comparison of carbon isotope data with pollen analysis to create time series	$\delta^{13}C$ data indicated significant changes in environment through Holocene, allowing reconstruction of mangrove ecosystem shifts
Zhao et al., 2006	*Cryptomeria fortunei* (Cryptomeria)	Zheijiang Province China	Trunk discs collected from 3 trees in sub-tropical monsoon zone All ring sequences cross-dated using International Tree Ring Data Bank	α-cellulose extracted from entire ring	Off-line combustion	Used $\delta^{13}C$ time series to model past atmospheric CO_2 concentrations, statistically removed high-frequency climate driven signal	All 3 time series showed a declining trend (more negative) in response to changes in atmospheric CO_2 concentration Can provide a proxy for past atmospheric CO_2 variability

Table 2.2. A summary of papers that have utilised stable isotope data from tree rings for palaeoenvironmental research in southern Africa.

Reference	Species	Location	Sampling methods	Wood component	Method	Data manipulation	Results
February, 1992	*Widdringtonia cedarbergensis* Clanwilliam Cedar	SW Cape Province	Selected rings from cores, 2 cores per tree from 6 trees	Holocellulose from pooled corresponding rings	Off-line combustion	Tested relationship between isotopes and rainfall	Shows declining atmospheric CO_2 $\delta^{13}C$ trend No correlation to rainfall
	Eucalyptus grandis Eucalyptus	Mpumulanga	Cuttings from trees grown under 2 water treatments	Whole leaf tissue, leaf cellulose and trunk cellulose	Off-line combustion	Tested relationship between isotopes and water availability	No significant correlations
	Combretum apiculatum, Protea roupelliae	Mpumulanga & KwaZulu-Natal	Modern charred specimens along a rainfall gradient	Wholewood, cellulose and charcoal	Off-line combustion	Tested relationship between species, tissue type and rainfall variation	$\delta^{13}C$ differs between 2 species No correlation for $\delta^{13}C$ charcoal with rainfall, suggests not possible to use charcoal for climate reconstruction
February and van der Merwe 1992	*Rhus* sp, *Diospyros glabrata* Ebenaceae archaeological charcoal	SW Cape Province	Wood samples from 4 locations and 3 archaeological sites. Modern wood samples combusted in muffle furnace	Pre-treated bulk charcoal	Off-line combustion	Tested relationship between species, tissue type and rainfall variation	Archaeological $\delta^{13}C$ values vary through time Thought to be due to climatic changes, particularly precipitation
February and Stock, 1999	*Widdringtonia cedarbergensis* Clanwilliam Cedar	SW Cape Province	Selected rings from cores, 2 cores per tree from 6 trees	Holocellulose from pooled corresponding rings	Off-line combustion	Tested relationship between isotopes and rainfall	Time series shows shows declining atmospheric CO_2 $\delta^{13}C$ trend No correlation to rainfall variability
Le Roux *et al.*, 1996	*Eucalyptus grandis* & two hybrids Eucalyptus	Sabie, Mpumulanga	Sampled 3 trees clone type, 6 types grown under controlled water treatments	Combined crude leaf fibre extracts	On-line combustion	Statistical testing against water use efficiency and ci/ca data	Examined relationship between $\delta^{13}C$ and water use efficiency, significant + correlation under high soil water conditions
Norström *et al.*, 2005	*Breonadia salicina* Matumi	Limpopo Province	Discs from 2 trees Age models from AMS dating and "wiggle matching"	Cellulose from visible rings and 5mm intervals across disc to centre	On-line combustion in con-flo system	Detrended to remove non-climatic trends Changing atmospheric ^{13}C composition	Compared $\delta^{13}C$ time series with wood anatomy and local rainfall record Shows response to water stress and provides proxy for past rainfall

Reference	Species	Location	Sampling methods	Wood component	Method	Data manipulation	Results
Robertson *et al.*, 2006	*Adansonia digitata* Baobab	Kruger National Park, Mpumulanga	Disc and core samples from 2 trees ^{14}C dated, rings are annual	Wholewood from 22 rings	On-line combustion in con-flo system	Detrended to remove non-climatic trends Changing atmospheric ^{13}C composition	Time series correlates positively with rainfall Has potential for producing long-term proxy record of palaeoclimates with high temporal resolution
West *et al.*, 2001	6 forest species including *Podocarpus, Olea & Celtis*	W Cape Province & KwaZulu-Natal	Cores and leaf samples from trees growing in shaded and open areas	Whole tissue and Holocellulose from leaves and cores	On-line combustion	ANOVA testing of categories of tissue type and location (open vs. closed)	$\delta^{13}C$ values of both tissue types showed similar variability, can determine recruitment environment based on differences in inner and outer ring isotope values
Woodborne and Robertson, 2000, 2001	*Acacia erioloba*, *Prosopis spp.*	Namibia	Trunk discs from felled trees, dated using high-resolution ^{14}C dating	Wholewood from annual rings	On-line combustion	Statistical comparison between the isotope values of both species and local rainfall	$\delta^{13}C$ values of the 2 species show different adaptations to variations in local water availability and precipitation
Woodborne *et al.*, 2003	*Pinus elliottii*, *P.patula*	Swaziland & Eastern Cape Province	3 transects along riparian zones, discs from 10 trees/transect	Wholewood taken from latewood of each growth ring	On-line combustion		$\delta^{13}C$ values reflected degree of water stress and response to variations in annual rainfall for individuals grouped samples along transect

Table 3.1. Full listing of all excavated layers and their associated letter codes from the trial trench.

Layer name	Abbreviation	Grid position
Coffee	Co	
Buff	Bu	
Light Brown Mottled Deposit	LBMOD	
Milk Chocolate	MC	EAST-ONLY
Espresso	Es	squares C2, D2
Mousse, Dark Mousse	Mou, D Mou	D3, E2, E3
Polar Bear	PB	
Oreo, Oreo 2	Ore, Ore2	
Red Decomposed	RD	
Cadbury, Pumpkin	Cad, Pu	
Mottled Deposit	MOD	
Orange Mottled Deposit	OMOD	
Black Lens in Orange Mottled Deposit	OMODBL	
Orange Mottled Deposit 2	OMOD2	
Black Lens in Orange Mottled Deposit 2	OMOD2BL	NORTH
Grey Mottled Deposit	GMOD	
Brown Mottled Deposit	BMOD	squares A4, A5
Red Speckled	RSp	A6, B4, B5, B6,
Yellow Speckled	YSp	C3, C4, C5, C6
Brown Speckled	BSp	D4, D5, D6
Brown Speckled 2	BSp2	E4, E5, E6
Spotty Camel	SPCA	
Black Lens, Orange	BL, Or	
Midnight	Mi	
Speckled Sunrise	SS	
Chestnut, Ebony	Che, Eb	
Mahogany, Mexican Yellow	Ma, MY	
Burnt Ochre	BO	
Pox	P	
Orange Pox	OP	
Brown Pox	BP	
Ivory	Iv	
Black Magic	BMOD	
Chocolate	Ch	
Sulphur, Sulphur 2	Su, Su2	
Pink 1	P1	NORTH
Grey 1	G1	
Chocolate 2	Ch2	TRIAL TRENCH
Yellow 1	Y1	ONLY
Brown/Grey Mix	B/Gmix	squares B5, B6
Black Lens 2, Black Lens 3	BL2, BL3	
Brown Organic, Yellow Mix	BOr , Ymix	These layers
Yellow Ash 1	YA1	are still to be
Yellow Ash 2	YA2	excavated in
Brown under Yellow Ash 2	Br under YA2	the other
Dark Reddish-grey	DRG	squares
Grey Rocky	GR	
Grey Rocky 2	GR2	
Grey Sand	GS	
Grey Sand 2	GS2	
Pinkish-grey Sand	PGS	
Reddish-grey Sand	RGS	
Reddish-grey Sand 2	RGS2	
Light Brownish-grey	LBG	
Light Brownish-grey 2	LBG2	
Light Brownish-grey 3	LBG3	
Light Brownish-grey 4	LBG4	

Layer name	Abbreviation	Grid position
Brown Sand	BS	
BEDROCK?		

Table 3.2. Radiocarbon (^{14}C) dates (Wadley and Jacobs, 2004, 2006) and OSL dates (Jacobs *et al*., 2008a, b, Jacobs and Roberts, 2008) from selected layers from Sibudu Cave.

Radiocarbon dates				
Lab no.	**Location**	**Level**	**Sample**	**Age (BP)**
Pta-8142	North	OMOD2	Charcoal	34 300 ± 2000
Pta-8136	North	OMOD2-BL	Charcoal	> 45 000
Pta-7775	North	RSp	Charcoal	> 41 400
Pta-8017	East	Bu	Charcoal	42 300 ± 1300
Pta-8137	East	RSp	Charcoal	> 45 200
GrA19670	East	BSp2	Bone	28 880 ± 170
OSL dates				
final MSA	**Location**	**Level**	**Sample**	**Age (ka)**
SIB11	East	Co	Sediment	34.7 ± 1.7
SIB10	East	Bu	Sediment	35.6 ± 2.0
SIB22	East	LBMOD	Sediment	48.9 ± 2.8
late MSA				
SIB14	North	MOD	Sediment	48.3 ± 2.0
SIB8	North	OMOD	Sediment	48.3 ± 1.8
SIB13	North	OMOD-BL	Sediment	47.0 ± 1.8
SIB7	North	RSp	Sediment	46.6 ± 1.9
SIB12	East	RD	Sediment	49.0 ± 2.0
post-HP				
SIB6	North	BSp	Sediment	58.0 ± 2.1
SIB4	North	SS	Sediment	53.6 ± 2.0
SIB9	North	P	Sediment	59.1 ± 2.2
SIB3	North	Ch2	Sediment	58.6 ± 1.9
SIB2	North	Y1	Sediment	58.2 ± 2.5
SIB1	North	B/Gmix	Sediment	57.8 ± 2.3
Howiesons Poort				
SIB15		GR2	Sediment	61.6 ± 1.5
SIB17		GS2	Sediment	63.8 ± 2.5
SIB19		PGS	Sediment	64.7 ± 1.9
Still Bay				
SIB20		RGS	Sediment	70.5 ± 2.0
Pre-Still Bay				

SIB21		LBG	Sediment	72.5 ± 2.0
SIB24		LBG2	Sediment	73.2 ± 2.3
SIB23		BS	Sediment	77.3 ± 2.2

Table 4.1. Radiocarbon analyses of selected *Mimusops caffra* rings from Umhlanga 1. The range for the possible calibrated dates for Pta-9518 is 1σ.

Anal. No.	Sample designation	$\delta^{13}C$ (‰)$_{PDB}$	Percent Modern Carbon	Calibrated date
Pta-9503	Umhlanga 1 ring 17	-25.5	118.6 ± 0.2	AD 1961 or 1987
Pta-9515	Umhlanga 1 ring 25	-25.3	131.6 ± 0.2	AD 1963 or 1979
Pta-9518	Umhlanga 1 centre rings	-26.2	98.8 ± 0.95	AD 1688-1732 or AD 1811-1938

Table 5.1. Statistical relationships and correlations between modern core and branch $\delta^{13}C$ values and annualised local rainfall, temperature and humidity data.

Sample	n	r^2	P-value	Correlation
Core 2				
Rainfall	47	0.003	0.295	-0.16
Temperature	**47**	**0.285**	**<0.000001**	**-0.55**
Humidity	21	0.246	0.013	-0.53
Core 3				
Rainfall	43	0.066	0.053	-0.30
Temperature	43	-0.0006	0.329	0.15
Humidity	**20**	**0.41**	**0.001**	**-0.66**
Branch B				
Rainfall	11	0.292	0.049	-0.60
Temperature	11	-0.09	0.765	-0.10
Humidity	**11**	**0.81**	**<0.000001**	**-0.91**
Core 4				
Rainfall	41	0.014	0.216	-0.20
Temperature	**41**	**0.268**	**0.0003**	**-0.54**
Humidity	19	-0.01	0.403	0.20
Branch C				
Rainfall	13	0.28	0.036	-0.58
Temperature	13	-0.03	0.444	0.23
Humidity	13	0.218	0.061	-0.53

Table 5.2. Summary statistics for the mean modern (Seaton Park and Baviaans Kloof) *Podocarpus* carbon isotope data and mean archaeological *Podocarpus* and *Celtis* charcoal carbon isotope data from Sibudu Cave.

Modern	**Seaton Park Branches**			**Baviaans**
	Wholewood	**Reduced**	**Oxidised**	**Wholewood**
Period	Modern	Modern	Modern	Modern
Age	2005	2005	2005	~1994
Mean	-24	-25.23	-24.86	-21.70
Median	-23.92	-25.04	-24.68	-21.66
Std dev.	0.95	0.97	1.01	0.69
Variance	0.9	0.95	1.03	0.47
Range	4.55	4.65	4.92	5.25
Minimum	-26.44	-28.07	-27.92	-25.32
Maximum	-21.89	-23.42	22.8	-20.07
N	97	75	71	303
Archaeological	***Podocarpus***			
	RSp	**SPCA**	**G Rocky**	**G Sand**
Lithic designation	late MSA	post-HP	HP	HP
Age	46.6±1.9ka	~58ka	>60ka	>60ka
Mean	-24.06	-22.44	-24.62	-24.39
Std dev.	0.42	0.13	1.11	0.59
Variance	0.18	0.02	1.23	0.35
Range	1.30	0.50	5.03	2.17
Minimum	-24.72	-22.68	-27.08	-25.07
Maximum	-23.42	-22.17	-22.06	-22.90
n	15	20	57	65
	Celtis			
	OMOD	**SPCA**		**G Sand**
Lithic designation	late MSA	post-HP		HP
Age	48.3 ± 2.0ka	~58ka		>60ka
Mean	-24.27	-23.24		-24.47
Std dev.	0.46	0.53		0.13
Variance	0.21	0.28		0.02
Range	2.11	2.09		0.40
Minimum	-25.67	-24.86		-24.72
Maximum	-23.56	-22.77		-24.32
n	36	12		7

Table 6.1. Sibudu Cave: summary of proxy environmental evidence. Stratigraphy (Wadley and Jacobs, 2006), ages (Jacobs *et al*., 2008a, b), formal and informal lithic designation (Wadley and Jacobs, 2006), isotopic data (Hall *et al*., 2008), botanical (Allott, 2006; Renaut and Bamford, 2006; Sievers, 2006; Wadley, 2004) and faunal data (Cain, 2006; Clark and Plug, 2008; Glenny, 2006; Plug, 2004, 2006; Wells, 2006), geology and mineralogy (Pickering, 2006, Schiegl *et al*., 2004; Schiegl and Conard, 2006) and magnetic susceptibility (Herries, 2006).

Layer	**Age (ka)**	**Lithic Designation**	**General environmental trends**	**Carbon Isotopes**	**Seeds**	**Charcoal**	**Phytoliths & Pollen**	**Macrofauna**	**Microfauna**	**Mineralogy**	**Mag Sus.**
					Occupational hiatus						
					~48ka occupation						
PB		**late MSA**			Also overall increase					High calcite, high gypsum	
Ore, Ore2					in deciduous species					High calcite, high gypsum	
RD, RSp	49.0 ± 2.0									Calcite, high gypsum	
Cad, Pu										Gypsum	
MOD	48.3 ± 2.0				*Pavetta* sp., Sedges	*Acacia, Erica*		Large and med.		High calcite, high gypsum	Warmer
OMOD	48.3 ± 1.8		Cooler with more	*Celtis*	*Pavetta* sp., Sedges	*Acacia, Erica*		bovids		High calcite, high gypsum	Warmer
OMODBL	47.0 ± 1.8		deciduous taxa	more negative	*Pavetta* sp.			Large and med.			
OMOD2					*Pavetta* sp.			bovids			
OMODBL					*Pavetta* sp.			Large and med.			
GMOD, BMOD					*Pavetta* sp.			bovids			
RSp	46.6 ± 1.9		Warming period with	*Podocarpus*	*Phoenix reclinata*	*Acacia, Erica, Podocarp*		Large and med.	*Mastomys natalensis*	Calcite, high gypsum	Warmer
Ysp			highly mosaic environment	more negative	*Pavetta* sp., Sedges		Grass	bovids	indicates succession	Gypsum	
					Occupational hiatus						
					~58ka occupation						
BSp	58.0 ± 2.1	**Post-Howiesons**	Cooler and drier phase with		*Asparagus* sp.	*Erica, Acacia, Ficus*		Large and med.		High calcite, gypsum	
BSp2		**Poort**	increased grasslands		*Asparagus* sp., Sedges			bovids		Calcite, gypsum	
SPCA			Warmer conditions with	*Celtis* & *Podocarpus*	*Asparagus* sp., Sedges	*Erica, Podocarp, Leuco*		Very large bovids		High calcite, high gypsum	
BL, Or			increased woodlands	less negative			Sedge, *Acacia*,	Large bovids			
Mi			Cooler phase, more grassland		Overall seed assemblage		Grass	Large bovids		High gypsum	
SS	53.6 ± 2.0				dominated by evergreen			Large bovids		High gypsum	

Layer	Age (ka)	Lithic Designation	General environmental trends	Carbon Isotopes	Seeds	Charcoal	Phytoliths & Pollen	Macrofauna	Microfauna	Mineralogy	Mag Sus.
Che, Eb			Warm, dry period		species	Dry-adapted species		Large bovids	*Mastomys natalensis*	Gypsum	Cool
Ma, MY						present in assemblage		Large bovids	indicates succession	Gypsum	
BO			Cold phase and very dry with		*Asparagus* sp.	*Acacia, Erica, Ziziphus*		Large bovids		Gypsum	
P	59.1 ± 2.2		very reduced forested areas		*Asparagus* sp.			Large bovids		Gypsum	Warm
OP					*Asparagus* sp.			Large bovids		High gypsum	Warm
BP			Warming period, cooler and		*Asparagus* sp., *Podocarps*		*Acacia*, Grass,	Large bovids		Gypsum	
Iv			drier than present		*Asparagus* sp., *Podocarps*		Fern, Sedge	Large bovids		Gypsum	
BM					*Asparagus* sp., *Podocarps*			Large bovids		Gypsum	
Ch					*Asparagus* sp., *Podocarps*			Large bovids		High gypsum	
Su, Su2					*Asparagus* sp., *Podocarps*			including species		High gypsum	Warming
G1					Sedges			such as buffalo and		High gypsum	Cold
Ch2	58.6 ± 1.9		Coldest period in the MSA with		Sedges		Grass, Sedge	equids present		High gypsum	Cold
Y1	58.2 ± 2.5		more open savanna and		Sedges			Large bovids		High gypsum	Cold
B/Mix	57.8 ± 2.3		grassland environments		Sedges		*Acacia*, Grass	Large bovids		High gypsum	Cold
BL2, BL3					Sedges			Large bovids		High gypsum	Cold
Bor, Ymix					Sedges			Large bovids		Gypsum	Cold
YA1					Sedges			Large bovids		Calcite, gypsum	Cold
YA2					Sedges			Large bovids		Calcite, gypsum	Cold
Br under YA2											
Potential hiatus											
62ka to 65ka occupation											
GR		**Howiesons Poort**	Cold, humid and moist	*Celtis* & *Podocarpus*	Sedges	*Podocarpus* dominates		Small forest species	Gambian Giant Rat &	Calcite, gypsum	
GR2			conditions with predominance	more negative	Sedges	the assemblage and		and lots of aquatic	Geoffroy's Horseshoe	Calcite, gypsum	
GS			of evergreen forests dominated	Podocarpus values	Sedges	other forest species		species	Bat indicate forests &	Calcite	
GS2			by *Podocarpus*	have high variability	Sedges	present		Blue duiker dominant	humid conditions	Calcite	
PGS					Sedges					High calcite	

Table 6.2. Summary statistics for the mean modern (Seaton Park and Baviaans Kloof) *Podocarpus* $\delta^{13}C$ data and mean archaeological *Podocarpus* and *Celtis* charcoal carbon isotope data from Sibudu Cave. This table incorporates isotope data from Hall *et al* (2008) and new values obtained from subsets of charcoal samples that were further treated using the acid-alkali-acid (AAA) method.

Modern	***Podocarpus***									
	Seaton Park Branches, KwaZulu-Natal			**Baviaans Kloof, Eastern Cape**						
Period		Modern		Modern						
Date		2005		~1994						
	Wholewood	**Reduced**	**Oxidised**	**Wholewood**						
Mean	-24	-25.23	-24.86	-21.70						
Std dev.	0.95	0.97	1.01	0.69						
Variance	0.9	0.95	1.03	0.47						
Range	4.55	4.65	4.92	5.25						
Minimum	-26.44	-28.07	-27.92	-25.32						
Maximum	-21.89	-23.42	22.8	-20.07						
n	97	75	71	303						
Archaeological	***Podocarpus***									
		RSp		**SPCA**			**G Rocky**		**G Sand**	
Period		Late MSA		Post-Howiesons Poort			Howiesons Poort		Howiesons Poort	
Date		48.4 ±1.7ka		~58ka			62ka-65ka		62ka-65ka	
	Original	**AAA subset**		**Original**	**AAA subset**	**Original**	**Original subset**	**AAA subset**	**Original**	
Mean	-24.06	-23.80		-22.44	-22.60	-24.62	-24.37	-24.52	-24.39	
Std dev.	0.42	0.39		0.13	0.17	1.11	0.67	0.50	0.59	
Variance	0.18	0.15		0.02	0.03	1.23	0.45	0.25	0.35	
Range	1.30	1.42		0.50	0.57	5.03	3.14	2.06	2.17	
Minimum	-24.72	-24.62		-22.68	-22.98	-27.08	-25.48	-25.04	-25.07	
Maximum	-23.42	-23.20		-22.17	-22.41	-22.06	-22.34	-22.98	-22.90	
n	15	15		20	19	57	23	23	65	
Correl		0.68			0.38			0.61		
Covar		0.10			0.01			0.20		
	Celtis									
		OMOD		**SPCA**					**G Sand**	
Period		Late MSA		Post-Howiesons Poort					Howiesons Poort	
Date		50.3 ± 2.1ka		~58ka					62ka-65ka	
	Original	**Original subset**	**AAA subset**	**Original**	**AAA subset**				**Original**	**AAA subset**
Mean	-24.27	-24.01	-24.77	-23.24	-23.40				-24.47	-24.92
Std dev.	0.46	0.26	0.27	0.53	0.54				0.13	0.16
Variance	0.21	0.07	0.07	0.28	0.29				0.02	0.03
Range	2.11	0.89	1.04	2.09	1.62				0.40	0.46
Minimum	-25.67	-24.45	-25.39	-24.86	-24.39				-24.72	-25.20
Maximum	-23.56	-23.56	-24.35	-22.77	-22.78				-24.32	-24.74
n	36	16	16	12	12				7	7
Correl			0.68		0.75					-0.13
Covar			0.18		0.01					-0.01

Table 7.1. Optically Stimulated Luminescence (OSL) dates for the pre-Still Bay, Still Bay, Howiesons Poort, post-Howiesons Poort, late and final Middle Stone Age levels from Sibudu Cave (Jacobs and Roberts, 2008; Jacobs *et al.*, 2008a, b).

Sibudu OSL dates				
final MSA	**Location**	**Level**	**Sample**	**Age (ka)**
SIB11	East	Co	Sediment	34.7 ± 1.7
SIB10	East	Bu	Sediment	35.6 ± 2.0
SIB22	East	LBMOD	Sediment	48.9 ± 2.8
late MSA				
SIB14	North	MOD	Sediment	48.3 ± 2.0
SIB8	North	OMOD	Sediment	48.3 ± 1.8
SIB13	North	OMOD-BL	Sediment	47.0 ± 1.8
SIB7	North	RSp	Sediment	46.6 ± 1.9
SIB12	East	RD	Sediment	49.0 ± 2.0
post-HP				
SIB6	North	BSp	Sediment	58.0 ± 2.1
SIB4	North	SS	Sediment	53.6 ± 2.0
SIB9	North	P	Sediment	59.1 ± 2.2
SIB3	North	Ch2	Sediment	58.6 ± 1.9
SIB2	North	Y1	Sediment	58.2 ± 2.5
SIB1	North	B/Gmix	Sediment	57.8 ± 2.3
Howiesons Poort				
SIB15		GR2	Sediment	61.6 ± 1.5
SIB17		GS2	Sediment	63.8 ± 2.5
SIB19		PGS	Sediment	64.7 ± 1.9
Still Bay				
SIB20		RGS	Sediment	70.5 ± 2.0
Pre-Still Bay				
SIB21		LBG	Sediment	72.5 ± 2.0
SIB24		LBG2	Sediment	73.2 ± 2.3
SIB23		BS	Sediment	77.3 ± 2.2

Table 7.2. Summary table for Sibudu Cave and other Middle Stone Age sites cited. The general location, age range, dating techniques, dating references, available range of environmental proxies and hiatus type is provided for each site. Highlighted OSL ages correspond to highlighted references and are considered to be the most applicable.

Site	Location	Age range	Dating techniques	Dating references	Environmental proxies	Hiatus type
Sibudu Cave	40km north of Durban	Iron Age: ~1000 BP	Radiocarbon (^{14}C)	Wadley and Jacobs, 2004	Botanical: seeds, charcoal,	
	15km form coastline	final MSA: ~35ka	OSL	**Jacobs, 2004**	pollen, phytoliths	3 hiatuses with no deposit
	KwaZulu-Natal	**late MSA: ~48ka**	OSL	**Jacobs and Wadley, 2006**	Faunal: Macro & microfauna,	present, may have been
		post-HP: ~58ka	OSL	**Jacobs et al., 2008a, b**	molluscs	removed by wind action
		HP: 65ka-62ka	OSL	**Jacobs and Roberts, 2008**	Sedimentology & geology	
		Still Bay: 70.5ka	OSL		Magnetic Susceptibility	
		Pre-Still Bay: 77ka-72ka	OSL		Isotopic analysis of charcoal	
Border Cave	Southern Lebombo Mountains	Iron Age	Radiocarbon (^{14}C)	Butzer *et al*., 1978; Beaumont *et al.,* 1978	Faunal: Macro & microfauna	
	Close to Swaziland border	ELSA: ~38ka	AAR	Miller *et al*., 1993	Sedimentology & geology	Numerous, culturally sterile
	Northern KwaZulu-Natal	**Howiesons Poort: ~55-75ka**	ESR	**Grün *et al*., 1990a**	Lithostratigraphy	deposits formed by natural
		MSA II		**Grün and Beaumont, 2001**	Isotope analysis of eggshell	processes, spalling, erosion
Rose Cottage Cave	Platberg, near Ladybrand	LSA	Radiocarbon (^{14}C)	Wadley & Vogel 1991	Faunal: Macro & microfauna	
	Eastern Free State	ELSA: ~29-40ka	OSL	Jacobs, 2004; Pienaar *et al*., 2008	Botanical: charcoal, pollen	Orange Sand layer: sterile
		post-HP: 56ka	TL	Tribolo *et al*, 2005; Woodborne and Vogel 1993		aeolian sands: ~39-55ka
		Howiesons Poort: 65ka-63ka		**Jacobs and Roberts, 2008**		
Klasies River	Southern Cape coast	MSA III: ~>45-50ka	Radiocarbon (^{14}C)	Vogel, 2001	Faunal: Macro & microfauna	
	Overlooking Indian Ocean	**Howiesons Poort: 65ka-63ka**	AAR	Bada & Deems, 1975	Botanical: geophytes	
		Pre-HP: 72ka-71ka	OIS correlation	Deacon & Geleijnse, 1988; Shackleton, 1982	Sedimentology & geology	
		MSA II: ~75-94ka	Palaeoenviro-proxies	Butzer, 1978; Deacon, 1989	Lithostratigraphy	Long hiatus: 12.5-50ka when
		MSA I: ~90-115ka	Uranium series	Vogel, 2001		cave sealed by dune sands

Site	Location	Age range	Dating techniques	Dating references	Environmental proxies	Hiatus type
			OSL	Feathers, 2002; Tribolo *et al*., 2005		
			ESR	Grün *et al.,* 1990b		
				Jacobs and Roberts, 2008		
Boomplaas Cave	Foothills of the Swartberg	LSA	Radiocarbon (^{14}C)	Fairhall *et al*., 1976	Botanical: seeds, charcoal,	Numerous short hiatus periods
	in the Cango Valley	ELSA: ~21ka	Palaeoenviro-proxies	Deacon *et al*., 1984	pollen, macrobotanical remains	
	Southern Cape	post-HP: >40ka	U-Th	Vogel, 2001	Faunal: Macro & microfauna	with sterile deposits due to
		Howiesons Poort: ~55-65ka	AAR	**Brooks *et al*. 1993; Miller *et al,* 1999**	Sedimentology & geology	natural processes
		MSA 2				
Blombos Cave	On coast overlooking the	LSA: ~2ka	Radiocarbon (^{14}C)	d'Errico *et al*, 2001	Faunal: Marine fauna, shellfish	
	Indian Ocean	3 MSA phases, including	OSL	Henshilwood *et al*., 2001; Vogel *et al*., 1999	Sedimentology & geology	LSA and MSA separated by
	South-western Cape	**Still Bay: 85ka-76ka, 73ka**		**Jacobs, 2004, 2005;**		sterile aeolian dune sands
		MSA 2: ~99-143ka		**Jacobs *et al.* 2003a, 2003b, 2006**		dating to 67.8±4.2ka
			ESR	Jones, 2001		
			TL	**Tribolo *et al.,* 2005, 2006**		
Diepkloof	Lower section Verlorenvlei	LSA: ~1800 BP	Radiocarbon (^{14}C)	Parkington and Poggenpoel, 1987;	Botanical: charcoal	
	18km from Elands Bay	**Howiesons Poort: 63ka-58ka**	Radiocarbon (AMS)	Parkington, 1990	Faunal: Macro & microfauna	
	North-western Cape	**Still Bay: 73ka-71ka**	OSL	Parkington, 1999	Sedimentology & geology	Long hiatus from
			TL	Parkington *et al*, 2005		~55-2ka
				Tribolo, 2003, Tribolo *et al*., 2005		
				Jacobs and Roberts, 2008		
Wonderwerk Cave	Kuruman Hills, west of the	MSA (incld Howiesons Poort):	U-Th	Johnson *et al*, 1997	Faunal: Macro & microfauna	Long hiatus from 70-12.5ka
	Gaap Escarpment	~70-220ka	AAR	Johnson *et al*, 1997	Sedimentology & geology	layers of culturally sterile
	Northern Cape			Beaumont and Vogel, 2006		deposits due to natural
						processes

APPENDIX A:

Detailed pre-preparation methods for wholewood, α-cellulose and charcoal samples for stable carbon isotope analysis and high precision radiocarbon dating.

A.1. Collection and treatment of trunk disc, branch and core samples

A series of modern trunk discs, core and branch samples from three indigenous species were collected to provide a range of analogue data to create absolute annual chronological isotopic records of environmental responses to prevailing climatic conditions. Trunk discs from *Mimusops caffra* were taken from two specimens that had been cut down as part of urban development project in the Umhlanga region north of Durban. A single trunk disc from a *Podocarpus falcatus* was obtained from the Baviaans Kloof region in the Eastern Cape Province. Once the trees had been felled, suitable discs, 15cm to 25cm thick, were cut from the trunk using a chainsaw or bow saw.

Core samples from *Podocarpus latifolius* were removed from selected specimens growing in Seaton Park, north of Durban, using a 12mm increment borer. In all cases cores were removed from the main trunk at a height of 115cm to 125cm from the ground. The increment borer was driven in as far as possible and the core sample carefully extracted and stored in 12mm diameter copper piping to prevent breakage. The borer was then removed from the trunk. All the holes in the trunks were sealed with tree sealant to prevent further damage and infection. Branch samples were also collected from the same trees that were cored. The branches had a diameter of 30mm to 60mm and were 15cm to 20cm in length.

Table A.1. GPS co-ordinates for all sites from where samples were collected.

Location	Province	Species analysed	GPS co-ordinates
Sibudu Cave	KwaZulu-Natal	*Podocarpus* and *Celtis* archaeological charcoal	29° 31'21 34" S 31° 05'07 94" E
Seaton Park	KwaZulu-Natal	*Podocarpus latifolius*	29° 47'32 39" S 31° 01'20 62" E
Admiralty Beach	KwaZulu-Natal	*Mimusops caffra*	29° 45'06 26" S 31° 04'19 17" E
Umhlanga Rocks	KwaZulu-Natal	*Mimusops caffra*	29° 43'30 96" S 31° 05'14 11" E
Baviaans Kloof	Eastern Cape	*Podocarpus falcatus*	33° 40'09 69" S 24° 34'39 26" E

On return to the laboratory, the trunk discs were labelled, sectioned parallel to the growth axis, and the transverse sections sanded with a belt sander using progressively finer grades of sandpaper (grades P22, extra coarse (1200µm) to P240, extra fine (40µm)) until the growth ring sequences were clearly visible (Fig. A.1). Grades for the sandpaper used are reported in internationally standardised terminology (Orvis and Grissino-Mayer, 2002). Core samples were air dried for three weeks. They were mounted between recessed blocks using cold glue (Ponel) and then cut in half using a band saw (Fig. A.2). Core samples were sanded in the same manner as the discs. Samples for carbon isotope analysis were taken from one half and the other was retained as a witness section. Three sections, approximately 15mm in thickness were cut from each branch and sanded to reveal their growth rings.

The growth rings were traced around the circumference of each disc and branch section and across each core using a binocular microscope and an incident light source. The total number of growth increments was established for each disc/core and each ring numbered from the exterior to the centre of the disc/branch or length of the core. This was necessary to ensure the accurate allocation of each sample to their respective rings. Once the growth rings were traced in pencil, they were scored with a sharp blade along the longest transect from the intersection of the bark and cambium to the centre of the disc (Fig A.1). This was done in order to obtain the maximum number of samples for isotopic analysis during the growth period of the tree/branch. The core samples were marked in a similar fashion (Fig A.2). Every tenth ring was marked with a nick to aid in counts and to facilitate sampling for high precision radiocarbon dating. The discs, branches and cores were lightly sanded removing all pencil marks to avoid sample contamination.

Figure A.1. Sample transect across a sanded trunk disc of *Mimusops caffra* from Admiralty Beach, KwaZulu-Natal.

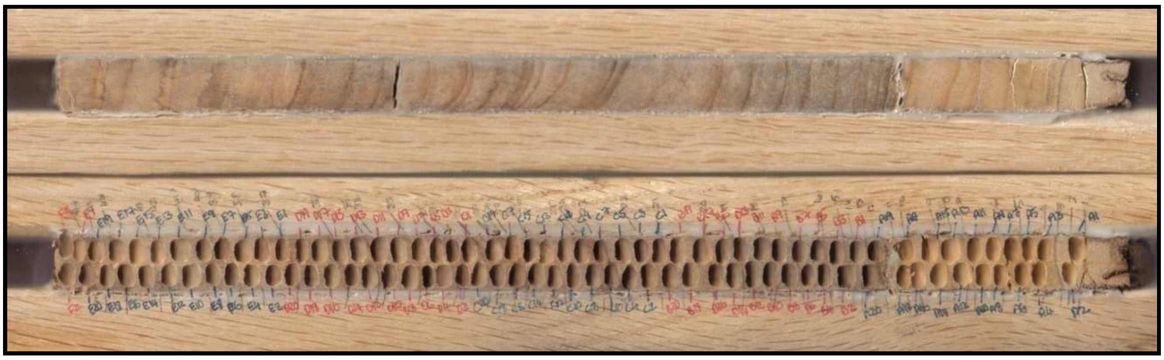

Figure A.2. A prepared core from *Podocarpus latifolius* from Seaton Park, showing the witness section (top) and the sampled section with sample and ring numbers.

Branch samples were used to compare carbon isotope values under reducing and oxidising conditions (Fig. A.3). Three adjacent discs were cut from each branch with each slice 15mm thick. The first disc was left un-burnt as a control to provide wholewood samples. A second disc was tightly wrapped in a double layer of heavy duty aluminium foil to exclude any oxygen. These discs were then placed in a muffle furnace, preheated to 450°C and left for two hours. This produced charcoal under reducing (O_2-free) conditions. The disc were removed from the furnace and allowed to cool. The third set of discs was placed on a foil covered grid over an open wood fire to simulate natural burning conditions and was left until completely charred (Fig. A.4). This method produced charcoal under oxidising (O_2-rich) conditions. This process took less than 15 minutes for the largest disc (60mm in diameter) and approximately five minutes for the smallest (30mm in diameter). Once the discs were completely carbonized, the combustion process was halted to prevent the discs becoming completely converted to ash.

Figure A.3. Three discs from a single *Podocarpus latifolius* branch. From left to right: Disc burnt under reducing conditions, un-burnt disc and disc burnt under oxidising conditions.

Figure A.4. Branch samples combusting under oxidising conditions.

Samples for isotope analysis were drilled out from the trunk and branch discs using a 2mm drill bit. The first sample was taken from the intersection of the bark and the most recent growth ring (Fig. A.5). The second sample was taken slightly offset from the first, but with some overlap to ensure that a continuous sample of wood tissue is taken across the entire growth sequence of each tree and to provide sub-annular samples from the wider growth rings. The samples were drilled out in batches of twenty. Each batch was assigned an alphabetic label and each sample numbered from one to twenty, e.g. A1 to A20, B1 to B20. Each sample was drilled out to a depth of approximately 10mm. The material removed by drilling was carefully collected using a paintbrush and a sheet of weighing paper. To ensure that sufficient material was available, 15mg to 25mg of wood tissue was removed from each drilling. Each sample was placed in a 15ml plastic container with a snap lid and carefully labelled e.g. Umhlanga 1 C17. Each batch of twenty samples was stored in a labelled zip-lock plastic bag, prior to further pre-treatment. Samples from the cores were removed using a woodworking burr, collected, labelled and stored in the same manner as the drilled samples. In the case of the core samples, the overall amount of wood tissue taken per drilling was more substantial due to the larger type of drill bit used and therefore the sub-annual resolution was not as fine as those taken from the discs.

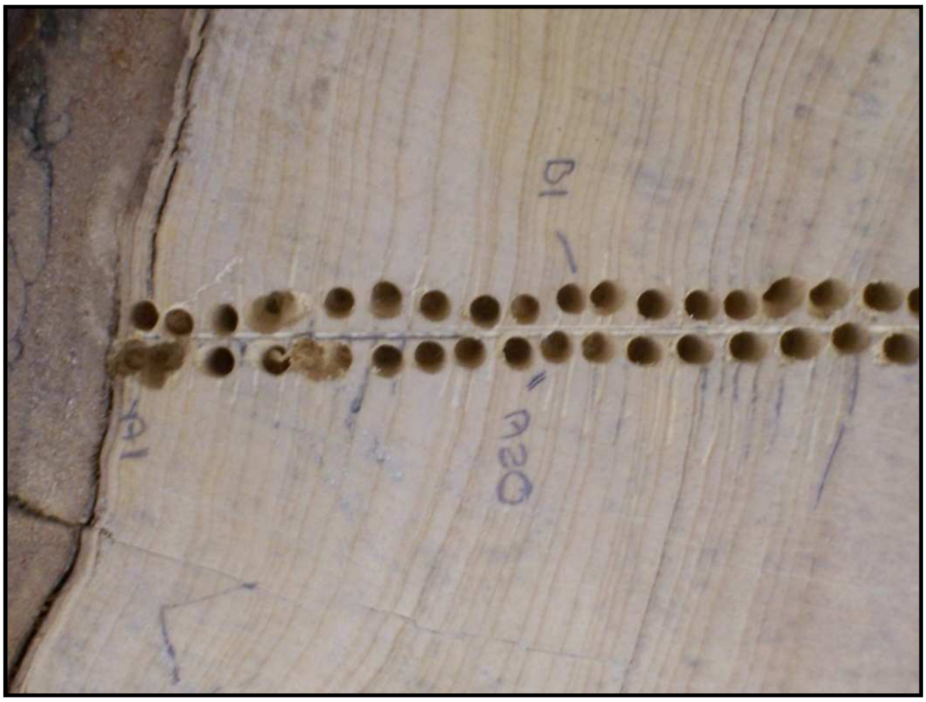

Figure A.5. Close-up view of samples drilled from *Podocarpus falcatus* from Baviaans Kloof, Eastern Cape. The first sample (A1) has been taken at the boundary between the bark and the first growth ring (left).

A.2. Pre-treatment of wood samples for radiocarbon dating

It was necessary to establish if the growth rings seen were representative of an annual growth cycle in order to allow the isotopic data to be compared with the climatic data on a sub-annual basis. Three samples were prepared for high precision radiocarbon dating from the Umhlanga 1 trunk disc using the acid-alkali-acid (AAA) treatment (Lerman *et al.*, 1970; Vogel and Waterbolk, 1967; Vogel and Marais, 1971).

The central core was carefully drilled out and the wood collected (Fig. A.6). In order to have sufficient material (20g to 25g) for a high precision date, approximately 10 rings were removed from the centre of the disc. Two additional rings were selected using the convention of counting backwards from the bark towards the centre of the tree in the anticipation that they would correlate with the years AD 1987 and AD 1979 respectively. Samples of 20g to 25g from each of these rings were shaved off, taking care to avoid contamination from adjacent rings. The samples each were split into small fragments and weighed. The samples were placed in clearly labelled Pyrex beakers and the following chemical treatment of the wood carried out.

The wood samples were covered with a 2% $HCl_{(aq)}$ solution and placed in an oven overnight at 70°C. The HCl solution was decanted and the samples washed with distilled H_2O until reaching a pH of 4. A solution of 2% $NaOH_{(aq)}$ was added to the samples and they were placed in an oven overnight at 70°C. The NaOH solution was decanted and the samples washed with distilled H_2O until reaching a pH of 8 and the wash water was clear. A second treatment of 2% $HCl_{(aq)}$ was added and the samples placed in an oven overnight at 70°C and then the samples were decanted and washed with distilled H_2O until reaching a pH of 4. The washed samples were placed back into the oven and allowed to dry out. They were then reweighed. A minimum of 8.5g of sample was required for high precision dating. The samples were then combusted and the carbon dioxide produced was collected and purified. Measurements were carried out on the samples at the Ecosystem Processes and Dynamics (EPD) laboratory at the CSIR in Pretoria.

Figure A.6. Trunk disc of *M. caffra* from Umhlanga Rocks, KwaZulu-Natal showing the removal of the central growth rings for high precision radiocarbon dating. Approximately 10 rings were sampled.

A.3. Chemical pre-treatment of wood and charcoal samples

The method used to pre-treat wood samples was initially developed by Green (1963) and adapted by Loader *et al.* (1997). This method allows for the rapid batch processing of numerous small wood samples for stable carbon isotope analysis. Originally this method was developed for processing wood samples to α-cellulose. However, recent research on wood cellulose preparation methods have shown that the Soxhlet extraction step is not necessary if α-cellulose is isolated (Boettger *et al.*, 2007; Rinne *et* al., 2005). The method has been adapted for this project with the pre-treatment proceeding to the end of the Soxhlet distillation and no further. An experiment was conducted to compare wholewood $\delta^{13}C$ values with α-cellulose $\delta^{13}C$ values and results indicate that suitable isotopic results can be obtained from wholewood samples (Chapter 4). Charcoal samples were pre-treated using a similar method used for radiocarbon samples.

A.3.1. Soxhlet distillation:

All the wood samples were run through a Soxhlet distillation process to remove all resins, oils and waxes present in the wood tissue. The removal of such components is particularly necessary for softwood species, such as *Podocarpus*. These mobile components move through wood tissue during tissue formation and have an effect on carbon isotope ratios. Their carbon isotope composition will not necessarily be reflective of the environmental conditions occurring during the formation of cellulose and lignin from a particular year and therefore give a mixed isotopic signal.

Each wood sample was placed in a clean and clearly labelled 70mm borosilicate Soxhlet extraction thimble with a No. 2 sintered glass filter in the base. A record was kept of which sample was placed in which thimble ensure that the sequence of wood samples was not altered. This was important as each wood sample from a particular tree is representative of a specific growth period in the tree's lifespan.

The thimbles with samples were placed in a Soxhlet apparatus and underwent a two-stage extraction process (Fig. A.6). All reagents used in this study were standard laboratory grade and were used without further purification. Each Soxhlet apparatus could hold twelve thimbles and for each extraction stage, two units were used, allowing 24 samples to be prepared at a time. During the first stage, samples were processed with a 2:1 toluene-ethanol azeotropic mixture for six hours. The thimbles were removed and dried overnight in an oven set to 100°C. The following day the samples were processed with 100% ethanol for six hours and dried. The wood samples were carefully removed from the thimbles and replaced in their original, cleaned containers prior to being analysed on the mass spectrometer. The toluene-ethanol and ethanol were replaced on a regular basis to avoid any sample contamination. After each two-stage processing, the extraction thimbles are carefully washed and cleaned to avoid contamination. The thimbles are placed in chromic acid (chromium (III) oxide, Cr_2O_3, in 80% sulphuric acid) for twelve hours and then washed repeatedly with distilled water and dried. The chromic acid ensures that any organic matter is removed from the thimbles.

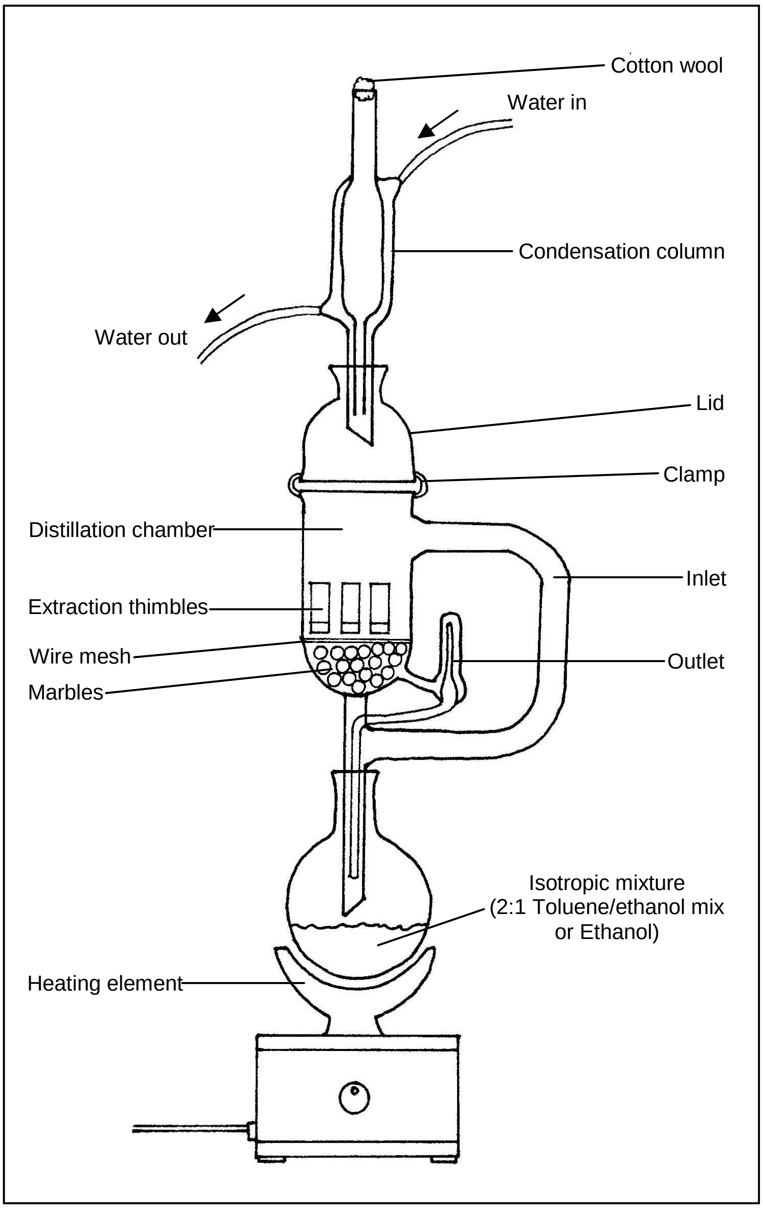

Figure A.7. Soxhlet distillation apparatus for extracting resins, oils and waxes from wood samples.

A.3.2. Isolation of α-cellulose:

At the start of the study an experiment was carried out to compare carbon isotope values of wholewood and α-cellulose from the same samples. This was done to determine the manner in which the remainder of the samples would be pre-treated. The results of this experiment are presented in Chapter 4. α-cellulose was isolated using the following method.

After Soxhlet distillation, the wood samples were left in the engraved Soxhlet thimbles. Two 400ml Pyrex beakers were filled with distilled water and heated to 70°C on a hot plate. A thermometer was used to ensure the temperature remained constant. Twelve thimbles were placed in each beaker and allowed to partially fill with water. A small amount of acidified sodium chlorite ($NaClO_{2\,(aq)}$) solution was added to each thimble and left to react for 60 minutes. This entire process must take place in a fume cupboard as potentially dangerous chlorine dioxide (ClO_2) gas is produced during the reaction.

After 60 minutes, each sample was filtered *in vacuo* and placed back in the beakers. A second amount of ($NaClO_{2\,(aq)}$) was added to the samples and allowed to react again. This process can be repeated up to eight times or until the samples appear completely white. In the case of this project, α-cellulose was isolated after two to three bleaching procedures. This was due to the fact that the samples were very small. Larger samples will take longer.

Once the samples were bleached, they are be washed with distilled water and filtered *in vacuo* for a minimum of five additions. The temperature of the water baths was increased to 80°C and the thimbles placed back in the water. The thimbles were then filled with 10% $NaOH_{(aq)}$ and allowed to react for 45 minutes. The samples were then filtered *in vacuo* and washed with distilled water (min. 5 additions). The water was drained off from the beakers and replaced with distilled water at room temperature. The samples were placed back in the water and the thimbles filled with a 17% $NaOH_{(aq)}$ solution and allowed to react for 45 minutes. They were then filtered *in vacuo*, washed with 17% $NaOH_{(aq)}$, with distilled water and then washed with 1% $HCl_{(aq)}$. After the acid wash, the samples were repeatedly washed with distilled water until pH neutral. The samples were dried in an oven at 60°C overnight.

A.4. Collection of archaeological charcoal samples

A.4.1. Charcoal analysis from Sibudu Cave

An analysis of charcoal from the MSA layers has been carried out by Allott (2004, 2005, 2006) characterising temporal changes in vegetation and wood use at the site. The identification of the various taxa was done using characteristic wood anatomy features visible under an incident light microscope and a scanning electron microscope and comparing these with a series of modern charcoal reference collections. The charcoal subjected to stable carbon isotope analysis in this project was derived from the material analysed by Allott (2004, 2005, 2006). For a detailed explanation of Allott's sampling and identification methodology, please refer to Allott (2005).

A.4.2. Selection of charcoal for isotopic analysis

Two genera, *Podocarpus* and *Celtis*, were selected for stable carbon isotope analysis. Both genera were been identified in three MSA periods (Howiesons Poort, post-Howiesons Poort and late MSA). Charcoal identified as either *Podocarpus* or *Celtis* by Allott was removed from the assemblages representing the three periods. Charcoal fragments identified as *Podocarpus* were taken from layer RSp (late MSA, ~48ka), SPCA (post-Howiesons Poort, ~58ka) and layers Grey Rocky (GR) and Grey Sand (GS) representing the Howiesons Poort (65ka-62ka). *Celtis* charcoal fragments were taken from layer OMOD (late MSA), SPCA (post-Howiesons Poort) and layer Grey Sand (GS) representing the Howiesons Poort.

A.4.3. Treatment of archaeological charcoal

Each charcoal fragment was initially manually cleaned to remove any contaminants on the surface. They were then sub-sampled. Using a razor blade, the fragments were carefully cut into smaller fragments and placed in labelled 15ml plastic containers with snap lids. Where possible, fragments were sub-sampled along visible growth ring sequences. The samples were then ready for chemical pre-treatment prior to isotopic analysis.

Charcoal samples were placed in clearly labelled Pyrex test tubes and covered with a 1% $HCl_{(aq)}$ solution. The test tubes were packed in to small beakers to prevent spillage and placed in an oven at 100°C overnight. The following day, the samples were removed and allowed to cool. They were repeatedly washed with distilled water until pH neutral. The samples were once again placed in an oven and allowed to dry. After drying they were replaced in their respective plastic containers to await isotopic analysis.

A subset of charcoal samples was subjected to additional pre-treatment to ensure that there were no post-depositional contaminants present, using the acid-alkali-acid (AAA) method. Charcoal samples were placed in clearly labelled Pyrex test tubes and covered with a 0.5% $NaOH_{(aq)}$ solution. Due to the fragile nature of the charcoal and potentially aggressive reactions to the $NaOH_{(aq)}$ solution, all the samples were placed in a refrigerator overnight. The following day the samples were repeatedly washed with distilled water until pH neutral. The samples were then again covered with a 1% $HCl_{(aq)}$ solution and placed in an oven at 100°C overnight. The following day, the samples were removed and allowed to cool. They were repeatedly washed with distilled water until pH neutral. The samples were once again placed in an oven and allowed to dry. After drying they were replaced in their respective plastic containers to await isotopic analysis.

APPENDIX B:

Botanical and environmental information on the selected tree species used in the analysis.

B.1. Mimusops caffra

Taxonomy:

Family: SAPOTACEAE

This is a large family occurring in predominantly tropical and sub-tropical areas. The family is characterised by the presence of a milky latex or sap present in the bark, branches, leaves and fruit. There are four species of *Mimusops* found in southern Africa.

Genus: *Mimusops caffra* E. Mey ex. A.DC.

South African tree no.: 583

Common name: Coastal Red Milkwood

Description:

This is a variable, evergreen species. The growth form is affected by the location in which the tree grows. It may occur as a small to medium-sized (4m-10m, up to 20m) tree in favourable, sheltered conditions or as a gnarled shrub in more exposed areas, such as the salt-spray zone. The bark is dark grey in colour and fissured. The leaves are hardy and leathery, arranged alternately with a blue-green upper colouration and paler with whitish hairs below (Fig.B.1a). The species produces small, creamy-white flowers between June and October and edible, red, oval fruits from June to January. The wood is reddish-pink in colour. Due to the hard and durable nature of the wood, it is used for general construction and boat-building.

Figure B.1a. Close up view of leaves and trunk of a *M. caffra* growing in the dune cordon along Admiralty Beach, North Coast of KwaZulu-Natal.

Figure B.1b. Distribution of *M. caffra* in South Africa.

Distribution:

The four species of *Mimusops* are concentrated in the warmer, moist regions of southern Africa. Two species are restricted to the eastern coastal belt and one has a wider range across the north-eastern portion of southern Africa. All the species grow at low altitudes. *M. caffra* is restricted in a narrow band, to the east coast of southern Africa, occurring from Mozambique, along the KwaZulu-Natal coastline, through the Transkei and into the Eastern Cape Province. It is a major component of Coastal and Dune forests and may comprise up to 75% of the actual tree cover. They are generally found on poor, sandy soils from the high-water mark into the dune cordon and beyond. This species plays an important role in dune stabilization. They may also occur along riverine fringes.

Sources:

Coates Palgrave (2002), Palmer and Pitman (1972), Pooley (2003), Van Wyk and Gericke (2000) and Van Wyk and Van Wyk (1997).

B.2. Podocarpus latifolius and P. falcatus

Taxonomy:

Family: PODOCARPACEAE

The family is widely distributed in the forests of southern Africa, as well as further northwards up to Ethiopia. Two of the three species found in southern Africa often comprise a significant proportion of forest communities.

Genus: *Podocarpus latifolius* (Thunb.) R.Br. ex Mirb.
Podocarpus falcatus (Thunb.) R.Br. ex Mirb.

South African tree no.: *P. latifolius*: 18
P. falcatus: 16

Common name: *P. latifolius*: Broad-leaved Yellowwood
P. falcatus: Outeniqua Yellowwood

Description:

P. latifolius is variable in appearance, depending on the locality in which it grows. It occurs as an evergreen, tall, straight small to medium-sized (10m to 30m) tree in sheltered and forested areas (Fig B.2a) or as a stunted evergreen shrub in exposed areas on mountainsides or at the coast. The bark is light to dark greyish-brown in colour, longitudinally fissured and peeling in strips on older specimens. The leaves are thick, leathery, dark green in colour and are spirally arranged, concentrated at the branch tips. They bear male and female cones. The male cones are produced from July to September and female cones develop seeds on a fleshy receptacle from December to February. The receptacles are edible. The fine-grained, yellow to white wood is highly utilised for furniture today.

Figure B.2a. A specimen of *P. latifolius* from Seaton Park, north of Durban in KwaZulu-Natal.

P. falcatus occurs as a tall (20m to 60m) medium to large evergreen tree in forests. This species is the tallest indigenous South African forest tree. The bark is dark purplish-brown and flakes off in rough round or rectangular flakes on older specimens. The leaves vary in colour from light yellowish to dark green and are arranged in a spiral pattern. Male cones develop from September to May and female cones form a yellow, fleshy seed from December to June. They are eaten by a variety of animals. The wood is fine-grained and is also highly prized for general construction and furniture.

Distribution:

P. latifolius is the most common species, widely distributed in the forests of South Africa. It occurs from the Western Cape in a broad band along the coast and escarpment, the Drakensberg, KwaZulu-Natal, Swaziland and further north into Mpumalanga (Fig B.2b). The species also occurs further northwards, extending up to Ethiopia. This species is found at a range of altitude, from sea-level up to 2150m in the eastern sections of the Drakensberg Mountains. *P. latifolius* often forms the major constituent of evergreen forest types. It can be found in evergreen forests, afromontagne forests, exposed mountainsides, coastal forests, as well as along river and stream banks, deep kloofs and gorges. *P. falcatus* has a more reduced range, occurring from the southern Cape northwards in a similar manner to *P. latifolius* (Fig B.2b). This species occurs as a medium to large tree in high, moist forests, but is generally lower growing in drier conditions. It is also found in sheltered woodland ravines, patches of mountain forest and in coastal swamp forests.

In southern Africa forests follow the line of highest rainfall, between 760mm to 1525mm per year. These conditions tend to prevail along the eastern and south-eastern slopes of mountain ranges and along the southern and eastern coasts of South Africa. However, in drier areas, if there is sufficient moisture available (e.g. groundwater), *P. latifolius* will be able to establish itself. The following factors play a role in the distribution of this genus, namely geographical position, climatic conditions, aspect, soil type, moisture availability, frequency of fires and degree of exposure. Both species favour southern and eastern-facing slopes which are more shaded, cooler, less exposed and wetter than warmer, drier northern and western-facing slopes.

Figure B.2a. Distribution of *P. falcatus* in South Africa.

Figure B.2b. Distribution of *P. latifolius* in South Africa.

Sources:

Coates Palgrave (2002), Grant and Thomas (2000), Killick (1990), Palmer and Pitman (1972), Pooley (2003), Schmidt et al. (2002b), Van Wyk and Gericke (2000) and Van Wyk and Van Wyk (1997).

Environmental control of $\delta^{13}C$ for *P. falcatus* from the Baviaans Kloof

As part of the analysis to demonstrate that the $\delta^{13}C$ values of stem samples recorded past environmental conditions presented in Chapter 5, a disc from a *Podocarpus falcatus* from the Baviaans Kloof was analysed. The results for this were not included in the paper. The carbon isotope sequence was compared with annual rainfall records for the region (Fig. B.2c). Unfortunately the rainfall records for the Baviaans Kloof region were incomplete (Appendix C) with data missing for the period 1944 to 1955. Interpretation of the tree's response to rainfall variability was further complicated by a number of missing rings at various points during its lifespan. A tentative interpretation of the environmental signal recorded in the $\delta^{13}C$ time series suggests that the tree had an annual response to rainfall, but this could not be verified statistically due to the missing rings and rainfall data. During periods of high rainfall $\delta^{13}C$ values became more negative and less negative during drier periods, suggesting a negative correlation between isotopic composition and rainfall. The Baviaans Kloof region receives low average annual rainfall and thus moisture availability will be a major constraint for trees growing in this environment as opposed to trees from the

KwaZulu-Natal region where humidity has a greater effect on stomatal opening and closing and therefore will have a greater influence on the carbon isotope composition of the tree.

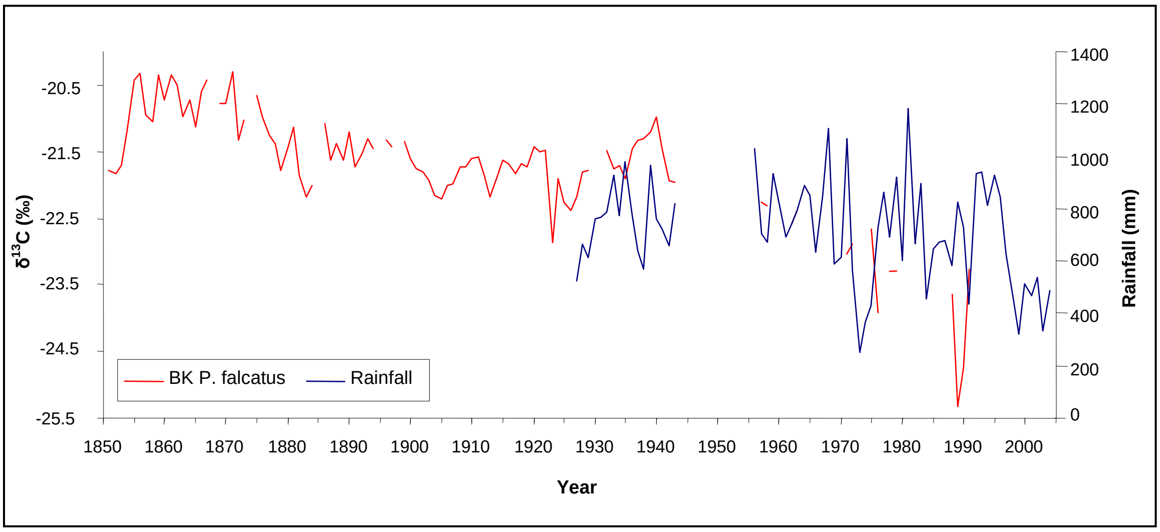

Figure B.2c. Modern δ^{13}C values for *Podocarpus falcatus* from the Baviaans Kloof plotted with corresponding annual rainfall for the region.

B.3. Celtis africana

Taxonomy:

Family: ULMACEAE (CELTIDACEAE)
This family is represented by five species in southern Africa.

Genus: *Celtis africana* Burm. f.

South African tree no.: 39

Common name: White-stinkwood

Description:

C. africana is a morphologically variable species. It generally occurs as a small to medium-sized (10m to 30m) deciduous tree (Fig B.3a), but can also be small and shrub-like under certain conditions. The growth form of this species will vary according to rainfall, with specimens smaller and stunted in areas of lower rainfall. It is generally deciduous, although along the coast the species will keep their old leaves until the appearance of new ones. The bark is pale grey to almost white in colour and smooth. Mature leaves are dark green, whilst young leaves are pale green. They are asymmetrically shaped with three prominent veins and serrated edges. *C. africana* produces separate male and female flowers on the same tree between August and October. Small yellow-brown fruits are present from October to December. The wood is white to yellow in colour, tough and although hard to work, used for a number of domestic purposes.

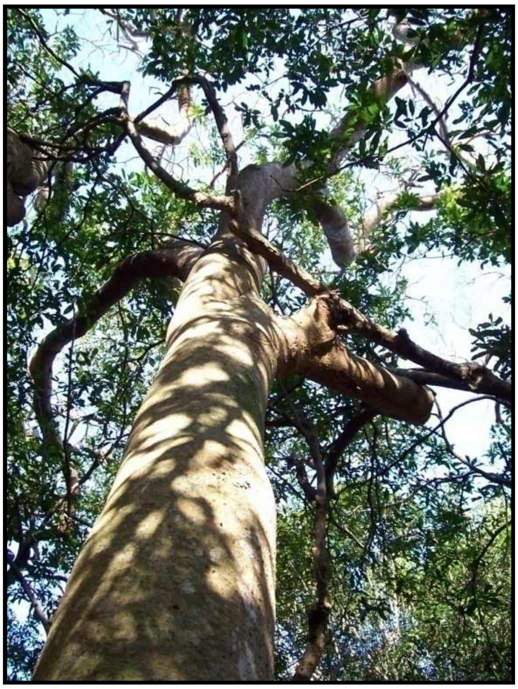

Figure B.3a. A large specimen of *C. africana* growing in the Hawaan Forest on the northern coast of KwaZulu-Natal.

Distribution:

This species is very widespread, occurring in a band from the Western Cape through to the majority of the eastern half of South Africa (Fig B.3b). The range extends further north as far as Ethiopia. *C. africana* grows from sea level up to an altitude of 2100m. It can be found in dense forest, rocky outcrops (particularly dolomite), in bushveld, open grassland, mountain slopes, kloofs, coastal dunes and along riverbanks. *C. africana* may also act as a pioneer species in forested areas undergoing succession. It prefers to grow on southern and eastern facing slopes.

Figure B.3b. Distribution of *C. afriana*.

Sources:

Coates Palgrave (2002), Palmer and Pitman (1972), Pooley (2003) and Van Wyk and Van Wyk (1997).

APPENDIX C:

Annualised rainfall, mean temperatures and relative humidity data from three weather stations in the vicinity of Sibudu Cave, KwaZulu-Natal and two weather stations in the vicinity of the Baviaans Kloof, Eastern Cape Province.

Summary table of global and regional palaeoclimatic records used in Chapter 6.

Table C.1. Annualised weather data (rainfall, temperature and relative humidity) from 2005 to 1928. The dataset is composed of weather data from three stations, Durban, Mount Edgecombe and Virginia Airport. Relative humidity data were only available until 1983 (South African Weather Service).

Year	Mean annual rainfall (mm)	Mean annual temperature (°C)	Mean annual humidity (%)	Year	Mean annual rainfall (mm)	Mean annual temperature (°C)
2005	453.37	20.88	70	1966	865.25	20.09
2004	710.43	20.40	68	1965	856.10	19.98
2003	775.60	21.32	68	1964	951.25	20.71
2002	1139.90	21.29	69	1963	972.20	20.58
2001	687.95	21.16	69	1962	736.10	20.27
2000	1495.43	21.49	71	1961	1214.35	21.00
1999	861.73	22.01	68	1960	773.55	20.20
1998	1194.67	20.72	71	1959	758.35	20.65
1997	1085.87	20.91	69	1958	1339.00	20.83
1996	1090.73	20.58	70	1957	1298.45	20.35
1995	986.32	20.59	66	1956	865.55	19.98
1994	888.90	21.48	63	1955	1084.80	20.16
1993	489.80	21.33	63	1954	839.90	20.47
1992	652.90	21.10	65	1953	1290.60	20.82
1991	1092.30	20.62	68	1952	2407.80	19.93
1990	1135.10	20.48	67	1951	1502.60	20.07
1989	983.00	20.45	67	1950	843.10	20.76
1988	1978.10	20.56	69	1949	864.70	20.59
1987	991.20	20.77	68	1948	931.50	20.31
1986	959.60	20.80	66	1947	861.50	20.73
1985	1032.20	20.60	67	1946	616.90	20.69
1984	1507.70	20.23	68	1945	903.70	20.72
1983	609.20	20.80	67	1944	1041.90	20.25
1982	926.90	19.77		1943	1309.80	20.33
1981	1163.90	20.34		1942	815.30	20.98
1980	646.50	20.34		1941	771.20	20.95
1979	712.50	20.67		1940	1018.50	20.55
1978	716.90	20.51		1939	1006.80	20.30
1977	1072.95	20.81		1938	978.10	20.13
1976	1365.75	20.29		1937	854.80	20.48
1975	887.50	20.46		1936	998.00	19.68
1974	1233.55	20.20		1935	1227.80	19.84
1973	670.35	20.23		1934	1006.40	20.48
1972	955.80	20.23		1933	640.80	20.68
1971	1222.95	20.38		1932	1014.90	20.40
1970	868.55	20.37		1931	837.30	20.23
1969	958.35	20.18		1930	837.20	19.90
1968	915.45	19.91		1929	1011.10	19.69
1967	832.80	20.28		1928	451.00	21.01

Table C.2. Annualised climatic data (rainfall, temperature and relative humidity) from 2004 to1927. The data set is composed of weather data from weather stations in Joubertina and Kareedouw in the Eastern Cape. Relative humidity and temperature data were only available until early 1997 (South African Weather Service).

Year	Mean annual rainfall (mm)	Mean annual temperature (°C)	Mean annual humidity (%)	Year	Mean annual rainfall (mm)
2004	483.4	14.50	51	1965	849.1
2003	330.1	15.70	53	1964	889.6
2002	537.9	16.20	54	1963	789.8
2001	469.25	16.40	55	1962	742.4
2000	514.25	16.60	57	1961	687.9
1999	319.8	16.60	55	1960	825.9
1998	459.1	16.30	57	1959	933.2
1997	629.05	13.60	60	1958	668.4
1996	840.9			1957	700.5
1995	927.3			1956	1026.7
1994	810.8			1955	NA
1993	937.8			1954	NA
1992	933.4			1953	NA
1991	434			1952	NA
1990	728.5			1951	NA
1989	826			1950	NA
1988	578.9			1949	NA
1987	675.7			1948	NA
1986	672.5			1947	NA
1985	647.6			1946	NA
1984	453.6			1945	NA
1983	896.7			1944	NA
1982	664.7			1943	818.4
1981	1179.8			1942	661.6
1980	602.6			1941	721
1979	918.8			1940	761.5
1978	689.7			1939	964.8
1977	864.5			1938	569.8
1976	725.8			1937	636.3
1975	429.7			1936	781.6
1974	363			1935	979.8
1973	252.2			1934	774
1972	559.7			1933	929.5
1971	1068.7			1932	786.7
1970	612.3			1931	764.7
1969	591.2			1930	758.8
1968	1108.5			1929	615.5
1967	850			1928	668
1966	633.1			1927	523

Table C.3. Summary table for all sources of palaeoenvironmental proxies cited. The type of site (e.g. archaeological, deep sea core), location, age model or dating methods, proxy data types, a brief indication of environmental changes for the period 70-50ka and references are provided for each site.

Site name	Sample	Location	Age model/Dating	Proxy data	Environmental changes 70-60ka	References
Sibudu Cave	archaeological site	KwaZulu-Natal, South Africa	OSL dating	Seeds, charcoal, pollen, fauna, phytoliths, sedimentology geology, magnetic susceptibility carbon isotopes	Shift from cooler, humid, moist, *Podocarpus* evergreen forest environment to colder, drier savanna grassland, very reduced forest	Refer to Wadley and Jacobs, 2006 for full listing
Tswaing Crater	borehole	Gauteng, South Africa	C^{14} and sedimentation rates Fission-track dating at base	Lithological data, soil texture to create rainfall proxy	Wetter between ~70-67ka and then drier from ~62-50ka	Partridge *et al.*, 1997
Lake Sibaya	coastal lake system	KwaZulu-Natal, South Africa	C^{14} and geology	sedimentology, geology diatomite deposits, aeolian sands	Coastal dune cordon re-established ~60ka with sediments formed under coastal wetland conditions	Wright *et al.*, 2000
Port Durnford	geological formation	KwaZulu-Natal, South Africa	Th/U disequilibrium dating Note: Dating not secure!	Peat, pollen, fauna sedimentology, geology	Formation of marshland (peat) at 70ka followed by development of *Podocarpus* forest under cooler conditions	Scott *et al.*, 1992 Maud and Botha, 2001 Oschadleus *et al.*, 1996
RC 17-69	deep-sea core	West Indian Ocean east of KwaZulu-Natal South Africa	$\delta^{18}O$ record of foraminifera correlated with data from other cores	$\delta^{18}O$ and foraminiferal assemblages indicate shifts between occurrence of cold and warm water masses in region	Isotopes and foraminifera indicate colder SST conditions in MIS 4 and slightly warmer in MIS 3	Hutson, 1980 Prell *et al.*, 1979, 1980
MD962080	deep-sea core	Western slope of Agulhas Bank, south of Africa	$\delta^{18}O$ record of benthic foraminifera correlated with SPECMAP record	Planktonic foraminifera assemblages, $\delta^{18}O$ benthic foraminifera record and sediment composition trace temporal behaviour of water masses	Warm water taxa low abundance, high sand content and low $\delta^{13}C$ during MIS 4 (H6) glacial due to pulse of cold subantarctic water	Rau *et al.*, 2002
PS2487-6	deep-sea piston core	Agulhas Current Retroflection	$\delta^{18}O$ record of planktonic foraminifera correlated with	Nannofossil and foraminifera fossil assemblages used to	During MIS 3 and 4 there is a reduction in tropical/subtropical	Flores *et al.*, 1999

Site name	Sample	Location	Age model/Dating	Proxy data	Environmental changes 70-60ka	References
		south of Cape Town	data from other cores	trace glacial-interglacial cyclicity	species and increase in cold species	
MD962094	deep-sea core	Walvis Ridge, SE Atlantic	$\delta^{18}O$ record of planktonic foraminifera correlated with SPECMAP record	$\delta^{18}O$ record and sediment grain-size as proxy for wind strength and aridity	Relatively humid conditions in glacial (MIS 4) shifting to relatively arid conditions in interglacial (MIS 3)	Stuut *et al*., 2002
MD962086	deep-sea core	Lower slope, Namibian coastline, near Lüderitz	$\delta^{18}O$ record of benthic foraminifera correlated with SPECMAP record	Alkenone measurements as proxy for SST	Near-shore SSTs are cooler during MIS 3 and 4 due to increased upwelling	Pichevin *et al*., 2005
MD962087	deep-sea core	Upper slope, Namibian coastline, near Lüderitz	C^{14} AMS dates of planktonic foraminifera and data correlation with other cores	Sediment grain-size as a proxy for wind strength	Windier conditions during MIS 4 and early MIS 3 resulting in increased upwelling	Pichevin *et al*., 2005
GeoB 1706 GeoB 1711	deep-sea gravity cores	Upper continental slope of Walvis Ridge	$\delta^{18}O$ record of benthic and planktonic foraminifera correlated to SPECMAP	Geochemical, micropalaeontological and $\delta^{18}O$ & $\delta^{13}C$ analyses	Eutrophic conditions between MIS 3 and MIS4, high abundance of cold water foraminifera, low $\delta^{13}C$ - high productivity due to upwelling, glacial	Little *et al.* 1997
WC03-1, 2, 5 WC03-10, 11, 18	aeolian dune cores	West coast of South Africa Elands Bay to Kleinsee	OSL dating of dune sand	Sedimentation changes related to variations in moisture, windiness and sediment supply	Increased phase of aeolian activity/deposition 63-73ka during glacial period of increased humidity and windiness, also wetter	Chase and Thomas, 2007
Lake Malawi & Lake Tanganyika	lacustrine deposit cores	Malawi & Tanzania East Africa, Rift Valley	C^{14} AMS dates of bulk organic matter & OSL	Ostracods, diatoms, pollen and sedimentological analyses used as proxies to reflect local & regional conditions	Region experienced extremely arid conditions prior to 70 ka and then became more humid	Cohen *et al*., 2007 Scholz *et al*., 2007
Bahia state caves	speleothems & travertine	North-eastern Brazil	U-series & U/Th dating	Dated speleothem growth phases associated with other high-resolution records such as Hulu Cave, GISP	Pluvial conditions between 60-74ka, correlates with H6 indicating a wet period	Wang *et al*., 2004
Botuvera Cave	speleothem	South-eastern Brazil	U/Th dating	High-resolution $\delta^{18}O$ record reflecting shifts in rainfall	$\delta^{18}O$ record indicates a wetter period at 70ka, followed by drier conditions until ~62ka when wetter conditions prevail	Cruz Jr. *et al*., 2005

Site name	Sample	Location	Age model/Dating	Proxy data	Environmental changes 70-60ka	References
Hulu Cave	speleothem	Nanjing, China	^{230}Th dating	High-resolution $\delta^{18}O$ record of the Late Pleistocene East Asian Monsoon	$\delta^{18}O$ record indicates a drier period between 70-60ka, followed by wetter conditions from 58-55ka shows shift from dry to wet during H6	Wang *et al*., 2001
Vostok	ice core	Antarctica	GT4 timescale	High-resolution records of δD, CH_4, dust flux and CO_2	δD record indicates a slow period of warming during H6 The dust flux and CH_4 records show increasing aridity and the CO_2 concentration rises, indicating lower marine productivity	Barnalo *et al*., 1987 Chappellaz *et al*., 1990 Jouzel *et al*., 1987 Leuschner and Sirocko, 2000 Petit *et al*, 1990, 1999 Schmittner *et al*., 2003 Stocker, 2000
EPICA	ice core	Antarctica	Ages are given on ECD2 timescale	High-resolution records of δD Fe, nssCa, ssNa and SO_4 fluxes	δD record indicates a slow period of warming during H6 The Fe and Ca records show increasing aridity and the SO_4 flux is reduced, indicating lower marine productivity ssNa flux slowly decreases, extent of sea ice reduced	Jouzel *et al*., 2005 Wolff *et al*., 2006
Byrd	ice core	Antarctica	See file gisp2age.dat for further information on the timescale.	High-resolution $\delta^{18}O$ record	$\delta^{18}O$ record indicates a slow period of warming during H6	Blunier and Brook, 2001 Stocker, 2000
GRIP	ice cores	Greenland	glaciological timescale given in the file gripage.dat	High-resolution $\delta^{18}O$ and δD records	$\delta^{18}O$ and δD records indicate an abrupt cooling during H6, between D/O 18 and 17	Blunier and Brook, 2001 Grootes *et al*., 1993 Jouzel *et al*., 2005, 2007 Landais *et al*., 2007 Schmittner *et al*., 2003 Stocker, 2000
GISP2	ice core	Greenland	See file gisp2age.dat for further information on the timescale.	High-resolution $\delta^{18}O$ and δD records	$\delta^{18}O$ and δD records indicate an abrupt cooling during H6, between D/O 18 and 17	Blunier and Brook, 2001 Grootes *et al*., 1993 Jouzel *et al*., 2005 Landais *et al*., 2007

Site name	Sample	Location	Age model/Dating	Proxy data	Environmental changes 70-60ka	References
						Leuschner and Sirocko, 2000 Schmittner *et al*., 2003